# RELAXATIONS IN POLYMER BLENDS WITH LCP'S

**afstudeerverslag**

June, 1992

Gerard C. Poolman

Delft University of Technology
Laboratory of Polymer Technology

begeleider: ir. Casper Willems
afstudeerhoogleraar: prof.dr.ir. J. van Turnhout

*Maar de wijsheid- waar wordt zij gevonden,*
*en waar toch is de verblijfplaats van het inzicht?*

**Job 28:13**

## Preface

This thesis is written in the scope of my graduation as a Materials Science Engineer. It reflects the results of my experimental work carried out from september 1991 till may 1992 in the Laboratory of Polymer Technology at Delft University of Technology, the Netherlands.

I sincerely want to thank my supervisor, ir. Casper Willems, who greatly contributed to this thesis and whom I am very much obliged. I would like to express my appreciation to my professor, dr.ir. J. van Turnhout, for his guidance, encouragement and patience throughout the coarse of the work.

The reader of this report is supposed to possess a general knowledge of materials science at an undergraduate level. For an introduction to this thesis I refer to my literature study (1991) completed at the Laboratory of Polymer Technology at Delft University of Technology.

Gerard C. Poolman

CONTENTS

## SUMMARY

Melt blending of Liquid Crystalline Polymers (LCP's) with thermoplastic polymers often results in fiber forming of the minor LCP component during processing and hence gives an "in situ" improvement of the mechanical properties. The molecular processes like the miscibility between the two components play an important role both in the fiber formation and the self-reinforcement.
These processes are often studied with DSC or Dynamic Mechanical Thermal Analysis (DMTA). Dielectric spectroscopy however has the clear advantage of the wide frequency and temperature range covered. Furthermore, this technique makes it also possible to evaluate processes which take place on the interfaces of a blend.

Two of these systems (Vectra, the LCP, with polycarbonate resp. Noryl) have been studied owing to their difference in fibril break-up. The analysis has been carried out using mainly dielectric spectroscopy. DSC and DMTA measurements as well as electron microscopy have been carried out for the purpose of comparison.

In blends of Vectra and polycarbonate partial miscibility as well as interactions between the components occur. In Vectra/Noryl blends phase separation in the Noryl takes place. No interactions between the components occur. The thermal treatment of the sample appears to determine largely the phase behaviour.

## SAMENVATTING

Het in de smelt verwerken van vloeibaar kristallijne polymeren (LCP's) met thermoplasten resulteert dikwijls in vezelvorming van de in lage concentratie aanwezig zijnde LCP. De LCP geeft als het ware in dezelfde processtap een verbetering van de mechanische eigenschappen. De moleculaire processen zoals de mengbaarheid van de twee componenten spelen een belangrijke rol in zowel de vezelvorming als de zelfversterking.
Deze processen worden vaak bestudeerd met DSC of dynamisch-mechanische (DMTA) meetmethoden. Diëlektrische spectroscopie heeft evenwel het duidelijke voordeel dat een breed frequentie- en temperatuursgebied bestreken wordt. Deze techniek maakt het ook nog eens mogelijk om processen te beschrijven die op de grensvlakken tussen twee componenten van een mengsel plaatsvinden.

Twee van deze zelfversterkende systemen (Vectra, het LCP, met respectievelijk polycarbonaat en Noryl) zijn bestudeerd omdat zij verschillend opbreekgedrag vertonen. Als analysemethode is voornamelijk diëlektrische spectroscopie gebruikt. De DSC en DMTA metingen zijn samen met elektronenmicroscopie gebruikt als vergelijkingsmateriaal.

In mengsels van Vectra en polycarbonaat blijken zowel gedeeltelijke mengbaarheid als interacties tussen de componenten op te treden. In Vectra/Noryl mengsels treedt fasescheiding in Noryl op. Hier treden geen interacties tussen de componenten op. De warmtebehandeling van het proefstuk bepaalt grotendeels het fasegedrag.

# 1 INTRODUCTION

Polymer blends with Liquid Crystalline Polymers (LCP's) enjoy a considerable amount of today's attention. Melt blending of LCP's with thermoplastic polymers often results in fiber forming of the minor LCP component during processing and hence gives an "in situ" improvement of the mechanical properties. These so-called self-reinforcing blends might in the future even replace glass reinforced polymers. The molecular processes like the miscibility between the two components play an important role both in the fiber formation and the self-reinforcement.
These processes are often studied with DSC or Dynamic Mechanical Thermal Analysis (DMTA). Dielectric spectroscopy however has the clear advantage of the wide frequency and temperature range covered. Furthermore, this technique makes it also possible to evaluate processes which take place on the interfaces of a blend.

The aim of this research was to study the processes which take place at a molecular level of polycarbonate (Makrolon 2805) containing 0 to 23 vol.% Vectra (a random copolyester of 73 % 4-hydroxy benzoic acid (HBA) and 27 % 2-hydroxy 6-naphtoic acid (HNA)) as well as blends of a homogeneous mixture of 50 wt.% polystyrene and 50 wt.% polyphenyleneether (Noryl MX 4717) and Vectra. These systems have been chosen owing to their difference in fibril break-up. The analysis has been carried out using mainly dielectric spectroscopy. DSC and DMTA measurements as well as electron microscopy have been carried out for the purpose of comparison.

Chapter 2 highlights the principles of relaxation and calorimetric measurements. Also a small introduction to polymer blends with LCP's is given. In chapter 3 the preparation of the samples and the set-ups are explained. Chapter 4 gives the results which are discussed in chapter 5. In the sixth chapter conclusions are drawn whereas chapter 7 gives recommendations for further research.

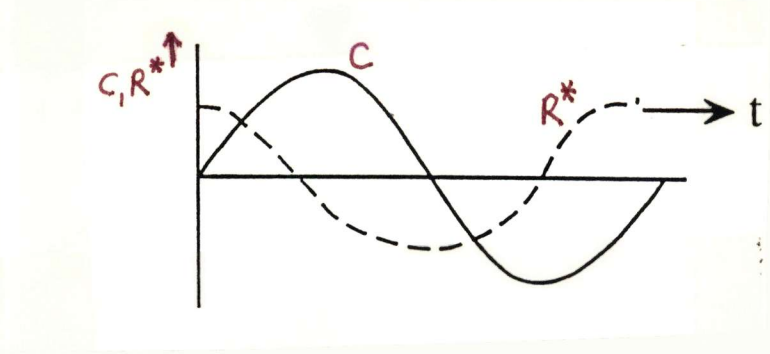


Fig. 2.1. The observed response, $R^*$, lags behind the imposed constraint C.

# 2 THEORY

## 2.1 Relaxation measurements

Kauzmann (1942) defined relaxation as the delay in the response of a system to a change in the forces to which it is subjected. Often the velocity with which a disturbed system returns to its equilibrium is proportional to the rate the system is removed from equilibrium.

In experimental situations the force is often varied sinusoidally. The observed response lags behind the imposed constraint because of the time the molecules need to rearrange themselves, as shown in fig. 2.1. The observed response $R^*$ is described with complex numbers. In this case it is easier to account for the phase differences.

Hence,

$$R^* = R' - iR''. \tag{2.1}$$

where R' is the real response, i the imaginary unit and R" the imaginary response.

When we call $R_0$ the response at angular fequency $\omega = 0$ and $R_\infty$ the response at angular frequency $\omega = \infty$, it can be proved (Bailey, North and Pethrick, 1981) that:

$$\frac{R'-R\infty}{Ro-R\infty} = \frac{1}{1+\omega^2\tau^2}, \tag{2.2}$$

$$\frac{R''}{Ro-R\infty} = \frac{\omega\tau}{1+\omega^2\tau^2}, \tag{2.3}$$

where $\tau$ is the relaxation time.

This implies that all sorts of relaxations can be described mathematically in the same way. If the constraint is a deformation the relaxation is called mechanical. If the electrical field is

varied and the polarisation is measured then the relaxation is called dielectric.

If R" is plotted as a function of the temperature T, one can observe maxima. These maxima are called transitions and they belong to a discrete motion of molecules since any motion needs its own time to contribute to the relaxation (Te Nijenhuis, 1986). On the proposal of Deutsch et al. (1954) the transition at the highest temperature is called the $\alpha$-transition. In amorphous polymers the $\alpha$-transition at low frequencies corresponds to the glass-transition. With decreasing temperature the $\beta$-, $\gamma$-, $\delta$- etc. transitions follow.

The glass-transition depends differently on temperature than the other transitions. This is because a large-scale rearrangement of the long-chain molecules involves a co-operative mechanism, i.e. the displacement of one molecule is not independent of its neighbours. One way of describing this process is the free-volume theory. (Ward, 1971)

Free volume is the volume which is not occupied by molecules or parts of molecules. Above the glass-transition temperature, $T_g$, the free volume increases rapidly with temperature. Below $T_g$ the free volume changes barely. Thus, when decreasing the temperature from a temperature above $T_g$, the free volume decreases. At $T_g$, the molecules move so slowly that the decrease in free volume does not remain in thermodynamical equilibrium. Using this theory, Williams, Landel and Ferry (1955) derived the following equation for $\tau$, for temperatures above $T_g$:

$$\log \frac{\tau_T}{\tau_{T_g}} = \frac{-C_1(T-T_g)}{C_2 + T-T_g} \qquad (2.4)$$

in which $\tau_T$ is the relaxation time at temperature T, $\tau_{T_g}$ the relaxation time at temperature $T_g$ and $C_1$ and $C_2$ are universal constants.

For the other transitions such a drastic rearrangement of the main chains is not required. In this case side group rotations or rotations around the main chain are involved (Shatzki, 1962). These transitions satisfy Arrhenius' law (Bailey, North and

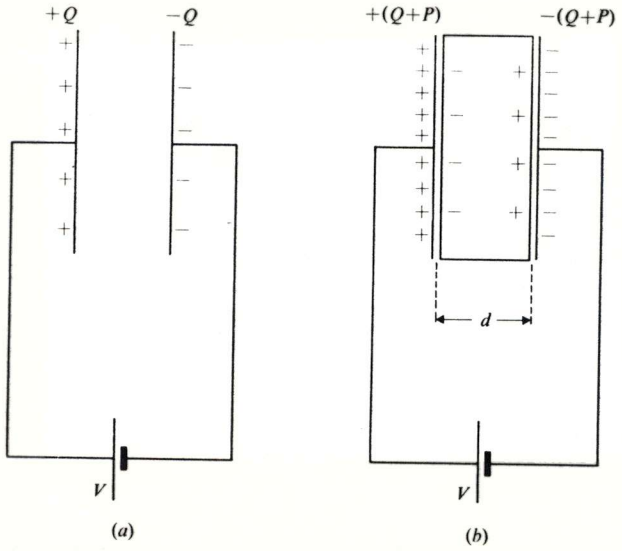


Fig. 2.2. Charges on a parallel plate capacitor with (a) a vacuum between the plates, and (b) a dielectric between the plates.

Pethrick, 1981):

$$\tau = \tau_o \exp(A/kT) \qquad (2.5)$$

where A is the activation energy, k Boltzmann's constant, T the absolute temperature, $\tau$ the relaxation time and $\tau_o$ the relaxation time at infinite temperature.

### 2.1.1 Dielectric relaxations

Dielectric relaxation is the exponential decay with time of the polarisation in a dielectric when an externally applied field is removed (Ku and Liepins, 1987). The degree to which a material responds to an applied electric field can be most easily appreciated for a parallel-plate capacitor. The charges +Q and -Q per unit area stored on the plates are directly proportional to the magnitude of the field, i.e.:

$$Q = \varepsilon_o E \qquad (2.6)$$

The constant of proportionality $\varepsilon_o$ is called the permittivity of vacuum and has the value of 8.85 $pFm^{-1}$. E is the strength of the electric field. The capacitance per unit area of the electrodes in vacuum, $C_o$, is defined as the ratio of the stored charge per unit electrode area to the applied voltage, hence:

$$C_o = Q/V \qquad (2.7)$$

Polarisation (symbol P) occurs when a dielectric is placed between the plates of the capacitor, as shown in fig. 2.2. The material will respond to the applied electric field by redistributing its charges in the molecules to some extent, positive charges being attracted to the negative electrode and vice-versa. The capacitance of the capacitor increases.

The relative permittivity is the relation between the capacitance of the capacitor with a dielectric, C, and the capacitance in vacuum:

$$\varepsilon = \frac{C}{C_o} = \frac{Q+P}{Q} \qquad (2.8)$$

By substituting (2.6) in (2.8), we obtain:

$$\varepsilon = \frac{\varepsilon_o E+P}{\varepsilon_o E} \text{ or} \qquad (2.9)$$

$$P = \varepsilon_o(\varepsilon-1)E$$

The quantity $\varepsilon_o\varepsilon E$, called the electric displacement D in the material, can be obtained by rearranging equation (2.9):

$$D = \varepsilon_o\varepsilon E = \varepsilon_o E+P \qquad (2.10)$$

Dielectric relaxations are generally examined in an alternating field. Our examination starts by considering the application of an alternating electric field E with amplitude $E_o$ and angular frequency $\omega$, across a dielectric material

$$E = E_o\cos\ \omega t. \qquad (2.11)$$

This will cause a polarisation and, if the frequency is sufficiently high enough, the orientation of any dipoles which are present will inevitably lag behind the applied field. Mathematically this can be expressed as a phase lag $\delta$ in the electric displacement:

$$D = D_o\cos(\omega t-\delta), \qquad (2.12)$$

which may be written:

$$D = D_1 \cos\ \omega t + D_2 \sin\ \omega t \qquad (2.13)$$

in which $D_1 = D_o \cos\delta$ and $D_2 = D_o \sin\delta$.

This leads to the definition of two dielectric constants

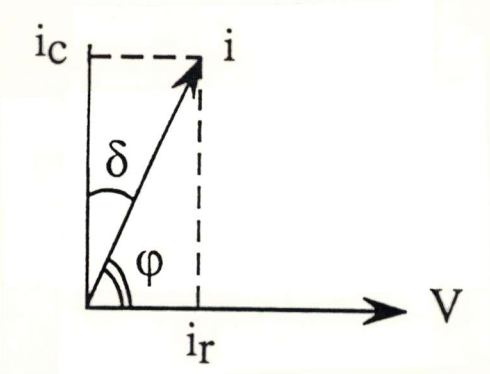


Fig. 2.3. Vector diagram of the applied voltage, V, and the resulting current, i.

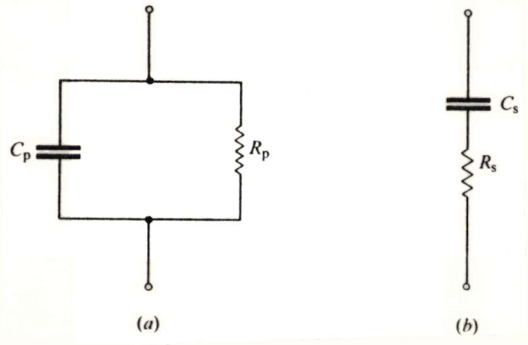


Fig. 2.4. Equivalent electrical circuits of dielectric specimens: (a) parallel, (b) series.

$$\varepsilon' = \frac{D_1}{\varepsilon_o E_o} \text{ and } \varepsilon'' = \frac{D_2}{\varepsilon_o E_o} \qquad (2.14)$$

linked by the relation:

$$\tan\delta = \frac{\varepsilon''}{\varepsilon'} \qquad (2.15)$$

It is convenient to combine these two quantities into a complex dielectric constant or relative permittivity:

$$\varepsilon^* = \varepsilon' - i\varepsilon'' \qquad (2.16)$$

The meaning of the real and the imaginary parts may be readily appreciated by considering the material in a capacitor. Due to the alternating field, the dipoles have to rearrange themselves. This takes time and makes the current lag behind the applied field. If the dipoles would react instantaneously on the applied field, the current would be 90 $^{o}$ in phase ahead of the voltage, since:

$$I = dQ/dt = C\ dV/dt \qquad (2.17)$$

However, the dipoles don't react instantaneously and because of this the phase angle is an amount $\delta$ less than 90 $^{o}$, see fig. 2.3. This implies that we have a capacitive component of the current which leads the voltage by 90 $^{o}$, and a resistive component which is in phase with the voltage. Work can only be done by the latter component and the physical meaning of tan $\delta$ becomes apparent now:

$$\tan\delta = \frac{\varepsilon''}{\varepsilon'} = \frac{\text{energy dissipated per cycle}}{\text{energy stored per cycle}} \qquad (2.18)$$

It goes without saying that the capacitive and the resistive component of the current can be replaced by respectively a capacitor and a resistor. By doing so, a polymer can be modelled by a parallel circuit of these components. This model assumes that the capacitive and resistive component behave independently of each other. If a dependence is assumed, a series model is used. The models are represented schematically in fig. 2.4.

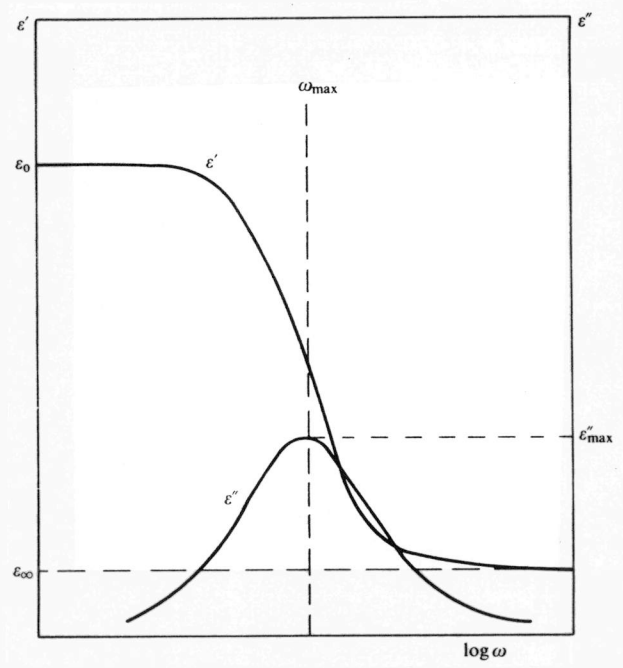


Fig. 2.5. Debije dielectric dispersion curves.

When $\varepsilon_s$ is the dielectric constant which corresponds to the maximum polarisation in the material, the so-called static dielectric constant ($\omega \rightarrow 0$) and $\varepsilon_\infty$ is the observed instantaneous dielectric constant ($\omega \rightarrow \infty$), then the two following equations, derived by Debije (1929), are valid:

$$\varepsilon' = \varepsilon_\infty + \frac{\varepsilon_s - \varepsilon_\infty}{1+\omega^2\tau^2} \tag{2.19}$$

$$\varepsilon'' = \frac{\varepsilon_s - \varepsilon_\infty}{1+\omega^2\tau^2}\omega\tau \tag{2.20}$$

Note the similarity with equations (2.2) and (2.3). The graphs of $\varepsilon'$ and $\varepsilon''$ versus the frequency of the applied field through the dispersion region are shown in fig. 2.5. The maximum loss value occurs when $\omega\tau = 1$, corresponding to a critical frequency $\omega_{max} = 1/\tau$ and the location of this peak provides the easiest way of obtaining the relaxation time from experimental results. The difference in dielectric constant measured at high and low frequencies is called the strength of the relaxation and it is related to the area under the absorption curve:

$$\Delta\varepsilon = \varepsilon_s - \varepsilon_\infty = \frac{2}{\pi}\int_{-\infty}^{\infty}\varepsilon''(\omega)\,d(\ln\omega) \tag{2.21}$$

The subject of dielectric relaxation is further and in more detail discussed by Blythe (1977) and Hedvig (1977). It is important to keep in mind, however, that the above description is valid for an ideal relaxation with one relaxation time. In polymers there will not be one relaxation time but a distribution of relaxation times.
Besides, in a polymer there will always be a small conductivity current as a result of ions, impurities etc. This conductivity will show up in the relaxation spectrum at high temperatures and low frequencies.

The advantage of dielectric spectroscopy is the wide frequency and temperature range covered. The shift and broadening of relaxation

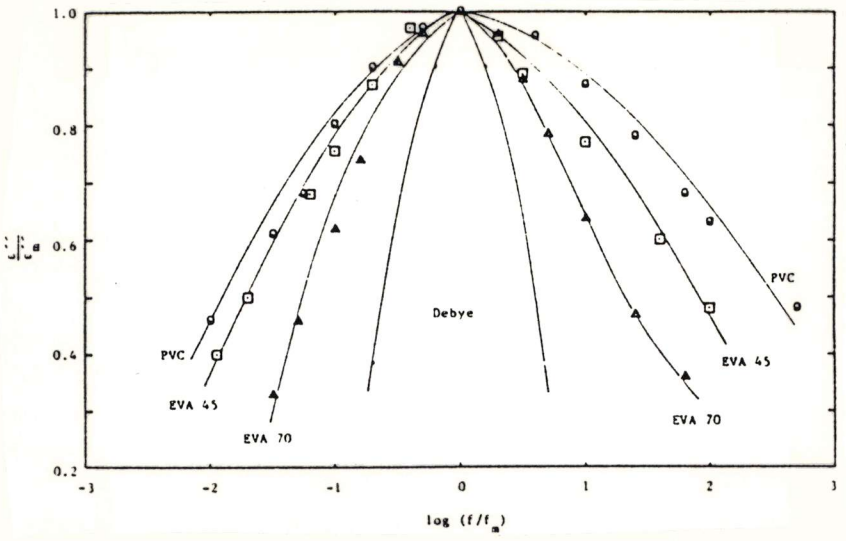


Fig. 2.6. Normalized loss factor curves for unblended polymers. A Debije curve for a single relaxation time is included for comparison. (from Rellick and Runt, 1986)

peaks can therefore be detected both in the temperature and in the frequency domain (Willems, 1992). Rellick and Runt (1986) discuss the subject of peak broadening in the frequency domain further. The broadness of a loss curve can only be measured properly in the frequency plane using the loss factor $\varepsilon''$. The broadness of the loss curves is usually taken as a measure of the range of local molecular environments the moving units experience.

The broadness of different peaks can be most easily compared by normalising the peaks. All values of $\varepsilon''$ are divided by the maximum value of $\varepsilon''$, $\varepsilon''_{max}$. All values of the frequency are divided by the frequency at $\varepsilon''_{max}$, $f_{max}$. A plot is made of $(\varepsilon''/\varepsilon''_{max})$ as a function of $(f/f_{max})$. This way of representation has the advantage that all curve maxima lie on the same point, namely (0,1) and that broadnesses can be compared directly as seen in fig 2.6. It was stated earlier that conductivity shows up in the relaxation spectrum at high temperatures and low frequencies. In the temperature domain, the conductivity contribution can be subtracted using e.g. the method Rellick and Runt use (1988). In the frequency domain it is easier to subtract the conductivity contribution since it manifests itself as a straight line at low frequencies when using a normalised frequency plot as described earlier. A formula for the loss due to conductivity is given by Schlosser and Schönhals (1989):

$$\varepsilon''(\omega) = A\omega^{-\sigma} \qquad (2.22)$$

In which $\sigma$ is a constant. In the case of pure ohmic conductivity, $\sigma$ has the value 1. Due to interfacial polarisation (Maxwell-Wagner effects) $\sigma$ can in practice be lower than 1.

When $\sigma = 1$, the total loss can be equalled to the conductivity loss and the conductivity contribution to the total loss can be represented as a straight line. Now the dc conductivity can be calculated at all frequencies and be used to calculate the net loss effectively due to dipole relaxation.

Moreover, dielectric measurements show other practical advantages, such as ease of handling and processing (Van Turnhout, 1990).

A lot of mixing formulas which predict the $\varepsilon'$ or $\varepsilon''$ for a blend have been derived. In this report four of them will be discussed in more detail.

When is assumed that the components behave independently of each other, a parallel model can be used (fig. 2.4a). The formula for the calculated $\varepsilon^*$ is:

$$\varepsilon^* = v_1\varepsilon_1^* + v_2\varepsilon_2^* \tag{2.23}$$

where $v_1$ and $v_2$ are the volume fractions and $\varepsilon_1^*$ and $\varepsilon_2^*$ are the complex permittivities of component 1 and 2 respectively. Separating $\varepsilon^*$ in real and imaginary parts leaves unaffected the shape of the formula.

When is assumed that the components are dependent of each other, a series model can be used (fig. 2.4b). For $\varepsilon'$ and $\varepsilon''$ a simplified formula has been used:

$$\frac{1}{\varepsilon} = \frac{v_1}{\varepsilon_1} + \frac{v_2}{\varepsilon_2} \tag{2.24}$$

where $\varepsilon$ applies both for $\varepsilon'$ and $\varepsilon''$.

From a theoretical point of view, the $\varepsilon^{1/3}$ formula of Landau, Lifshitz and Looijenga (Van Turnhout, 1990) is interesting. This formula has the following form:

$$(\varepsilon^*)^{1/3} = v_1(\varepsilon_1^*)^{1/3} + v_2(\varepsilon_2^*)^{1/3} \tag{2.25}$$

The shape of this formula remains unaltered when $\varepsilon'$ is applied. When $\varepsilon''$ is applied the formula changes to:

$$\frac{\varepsilon''}{(\varepsilon')^{2/3}} = \frac{v_1\varepsilon_1''}{(\varepsilon_1')^{2/3}} + \frac{v_2\varepsilon_2''}{(\varepsilon_2')^{2/3}} \tag{2.26}$$

This approximation can be made when the losses are small (Van Turnhout, 1992).

### 2.1.2 Mechanical relaxations

In this case, the relaxation is often measured by means of sinusoidal deformations in the shear (or bending or extension) mode. Let $\sigma$ be the stress and $\gamma$ be the shear, then this is represented as follows:

$$\gamma = \gamma_o \sin\omega t \tag{2.27}$$

where $\gamma_o$ is the amplitude of the shear. The corresponding stress is ahead in phase with an angle $\delta$. Hence:

$$\begin{aligned}\sigma &= \sigma_o \sin(\omega t+\delta)\\ &= \sigma_o(\sin\omega t \cos\delta+\cos\omega t \sin\delta)\\ &= \gamma_o(G'\sin\omega t + G''\cos\omega t)\end{aligned} \tag{2.28}$$

in which

$$G' = \frac{\sigma_o}{\gamma_o} \cos\delta \text{ is the storage-modulus} \tag{2.29}$$

$$G'' = \frac{\sigma_o}{\gamma_o} \sin\delta \text{ is the loss-modulus.} \tag{2.30}$$

This yields immediately

$$\tan\delta = \frac{G''}{G'}, \tag{2.31}$$

For the mathematical description it is more convenient to use the complex notation:

$$G^* = G'+ iG''. \tag{2.32}$$

We define the complex compliance as (Murayama, 1978):

$$J^* = (G^*)^{-1}. \tag{2.33}$$

This leads to:

$$J^* = J'- iJ''. \tag{2.34}$$

The response of a visco-elastic material to a periodic mechanical

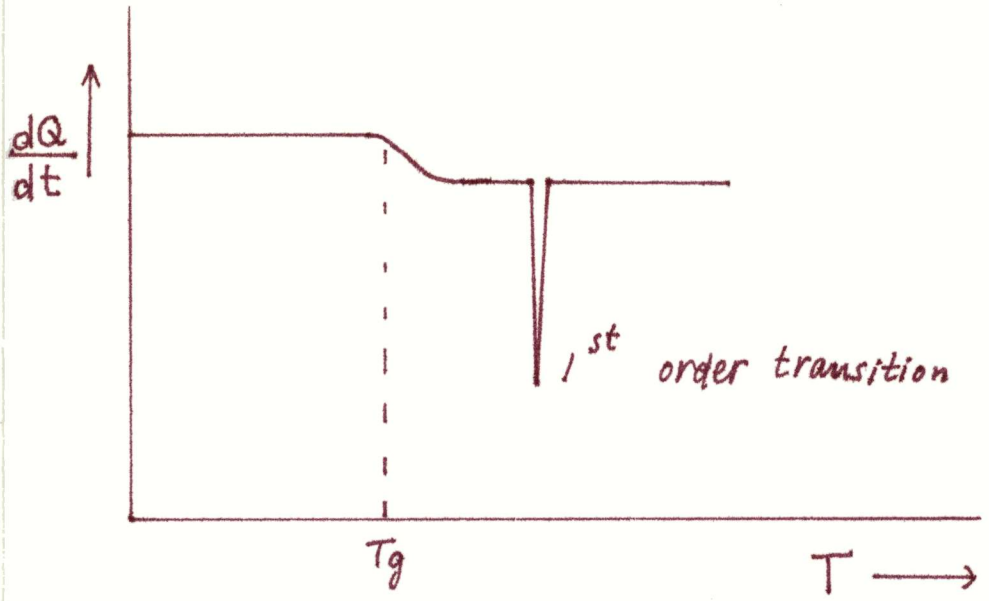


Fig. 2.7. A schematic DSC curve in which a glass-transition and a $1^{st}$ order transition can be discerned.

force is analogous to the response to an electric field when $J^*$ is used instead of $\varepsilon^*$ (Hedvig, 1977). This yields:

$$J' = J_\infty + \frac{J_o - J_\infty}{1+ \omega^2\tau^2} \qquad (2.35)$$

$$J'' = \frac{J_o - J_\infty}{1+ \omega^2\tau^2}\omega\tau \qquad (2.36)$$

Here $J_o$ and $J_\infty$ are the relaxed ($\omega \rightarrow 0$) and unrelaxed ($\omega \rightarrow \infty$) compliances respectively. Notice the analogy with the Debije equations. In practice the modulus G is most often used.
Just as dielectric measurements, dynamic mechanical measurements can be applied in a large range of frequencies. Moreover, the molecules need not to be electrically active or polar, which is an advantage. In practice, these measurements are carried out in a broad range of temperatures. In this report the name DMTA will be used which means Dynamic Mechanical Thermal Analysis.

## 2.2 Differential Scanning Calorimetry (DSC)

DSC measures the differences in energy input into a substance and a reference material when both are subjected to a controlled temperature program. For this purpose two identical sample holders one empty and the other filled with the material under study are heated at the same rate. A DSC measurement gives the rate of change in enthalpy, so that the area between a DSC curve and its extrapolated baseline indicates the total heat of reaction. Fig. 2.7 shows a DSC trace for a polymer at constant heating rates. If the polymer contains amorphous material, it passes through a glass-transition. Because the abscissa of a DSC trace at constant heating rate is proportional to the change in $d\Delta H/dT$ a second-order transition (such as $T_g$) manifests itself by an endothermic amplitude change and so the glass transition temperature $T_g$ can be approximated. The glass transition temperature is often empirically defined as the temperature at which the amplitude of the DSC reaches the midpoint of its

extrapolated initial and final values. Another definition is the temperature of the intersection of the glassy and the supercooled liquid enthalpy curves extrapolated through the glass transition region (Flynn, 1990).

## 2.3 Polymer blends with LCP's

The α-relaxation in polymer blends is mainly determined by the mutual solubility of the components (Ward, 1971). If two polymers are miscible on a molecular level one glass transition appears which lies in between the two glass transitions of the pure components. In blends where the components are immiscible, the glass transitions of the separate components remain visible. The glass transition as a means of determining the miscibility on a molecular level has become an accepted criterion (Wetton and Corish, 1989).

The blends investigated, which consist of a liquid crystalline polymer and a thermoplastic, are not miscible on a molecular level. Therefore it can't be expected that experimental formulas which predict the glass transition of miscible polymer blends do also apply for polymer blends with LCP's.

For an introduction to Liquid Crystalline Polymers one is referred to Ciferri (1991).

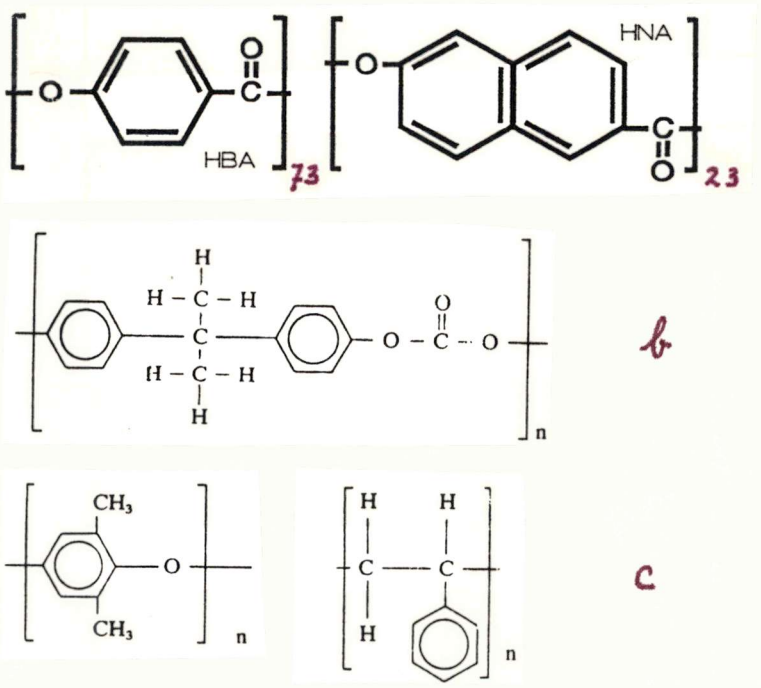


Fig. 3.1. Structure formulas of the polymers used: (a) Vectra, (b) polycarbonate, (c) Noryl (PPE/PS).

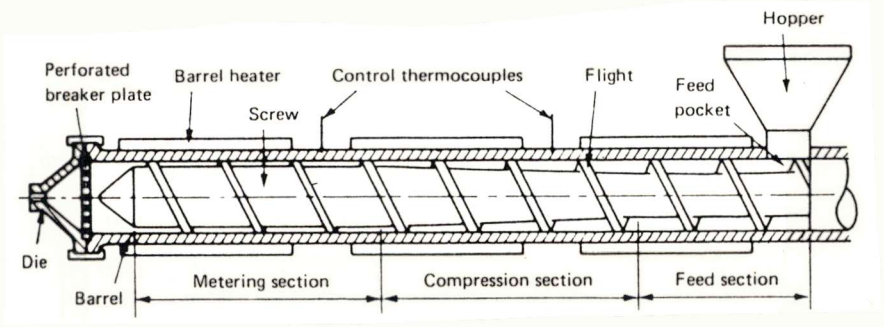


Fig. 3.2. Illustration of a single-screw plasticating extruder.

# 3 EXPERIMENTAL

## 3.1 Materials used

The LCP used is Vectra A 900, produced by the Hoechst Celanese company. Used is a grade the properties of which are listed in table 3.1. Noryl, one of the thermoplastics used, is a totally miscible blend of PPE and PS (C. Verbraak, personal communication). Noryl is produced by General Electric Plastics. The grade used (MX 4717) is non-commercial and contains equal (weight)amounts of PPE and PS. The polycarbonate used is Makrolon 2805, produced by Bayer. Table 3.1 lists some properties of the three polymers. The molecular structures of these three components are shown in fig. 3.1.

Table 3.1 Density ($\rho$), glass transition temperature ($T_g$), melting temperature ($T_m$) and extrusion temperature ($T_e$) of Vectra A 900, Noryl and Makrolon 2805.

| | $\rho$ ($g/cm^3$) | $T_g$ ($^\circ C$) | $T_m$ ($^\circ C$) | $T_e$ ($^\circ C$) |
|---|---|---|---|---|
| Vectra A 900 | 1.4 | 107 | 280 | 290 |
| Noryl MX 4717 | 1.06 | 160 | - | 270 |
| Makrolon 2805 | 1.2 | 150 | - | 250 |

## 3.2 Preparation of the samples

### 3.2.1 Extrusion

For dielectric measurements thin films are the most suitable. In order to obtain these films and also a good degree of mixing between the two components it was tried to extrudate the mixed granulate. Used is a film extruder head in order to obtain thin films. The used extruder is a Collin single screw extruder. Fig. 3.2 gives a schematic view of the extruder. Fig. 3.3 gives a view

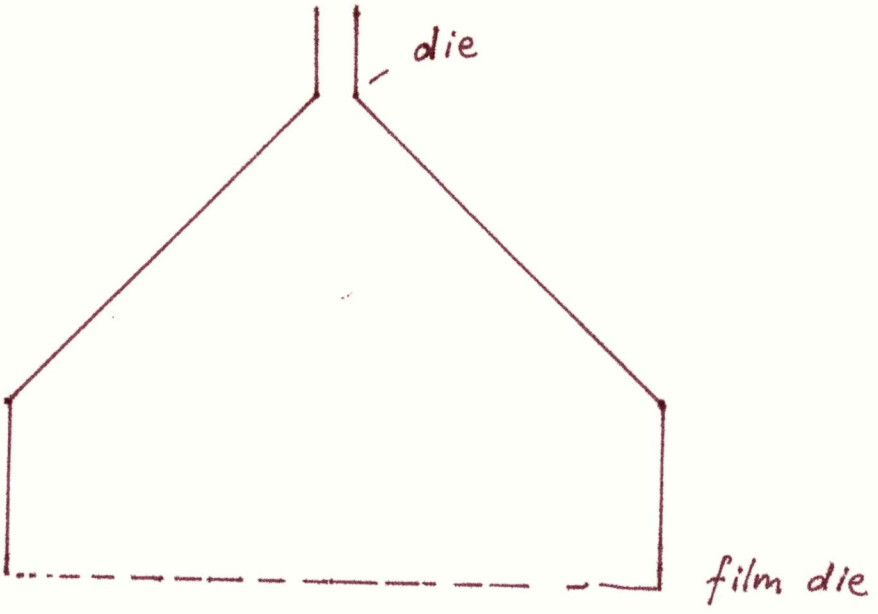


Fig. 3.3. Schematic drawing of the film extrusion head.

of the extruder head. To obtain various thicknesses of the films, the extrudate was drawn at various ratios. The following composition ratios were extruded.

Table 3.2. Weight fractions and volume fractions of the Vectra in polycarbonate and the codes used.

| $w_v$ | $vol\%_v$ | code |
|---|---|---|
| 0 | 0 | PC |
| 0.04 | 3.5 | 5V/PC |
| 0.08 | 6.8 | 10V/PC |
| 0.15 | 12.7 | 20V/PC |
| 0.20 | 18.0 | 30V/PC |
| 0.26 | 22.7 | 40V/PC |
| 1 | 100 | V |

Table 3.3. Weight fractions and volume fractions of the Vectra in Noryl and the codes used.

| $w_v$ | $vol\%_v$ | code |
|---|---|---|
| 0 | 0 | N |
| 0.05 | 4.1 | 5V/N |
| 0.10 | 7.9 | 10V/N |
| 0.18 | 14.6 | 20V/N |
| 0.25 | 20.4 | 30V/N |
| 0.30 | 25.5 | 40V/N |
| 1 | 100 | V |

Before extrusion the PC was dried in a vacuum of less than 10 mbar at a temperature of 80 $^{o}$C during at least 24 hours. The Vectra was dried in a stove at 175 $^{o}$C during four hours using nitrogen as a purge gas. Afterwards the Vectra was stored in a vacuum of 10 mbar at a temperature of 80 $^{o}$C. Noryl was also dried in a vacuum of 10

mbar at a temperature of 80 °C.

It turned out that extrusion of Vectra and PC was not successful. Large particles of Vectra remain visible in the film. Furthermore, the surface of the films was unsmooth. It was tried therefore, to cool the extrudate immediately in water because it was supposed that large particles of Vectra may be formed and that these eventually break up when the films are drawn. The reason might be that Vectra becomes already solid again when coming out of the extruder while PC still has a very low viscosity. So, the PC is still drawn whereas the Vectra is not. For this reason granules of PC and Vectra were extruded and regranulated. The resulting granules were extruded to a film. In table 3.4 the temperature program of the extruder for the different blends is listed.

Table 3.4. Temperature program of the Collin extruder. $T_1$ to $T_5$ are the temperatures of the different heating zones. $T_1$ = 170 °C. $T_2$ = 240 °C. $T_{eh}$ is the temperature of the extrusion head.

| code | $T_3$ (°C) | $T_4$ (°C) | $T_5$ (°C) | $T_{eh}$ (°C) |
|---|---|---|---|---|
| N | 260 | 260 | 260 | 240 |
| 5V/N | 320 | 320 | 320 | 290 |
| 10V/N | 320 | 320 | 320 | 290 |
| 20V/N | 320 | 320 | 320 | 290 |
| 30V/N | 320 | 320 | 320 | 295 |
| 40V/N | 320 | 320 | 320 | 300 |
| PC | 265 | 275 | 275 | 270 |
| 5V/PC | 320 | 320 | 320 | 260 |
| 10V/PC | 320 | 320 | 320 | 265 |
| 20V/PC | 320 | 320 | 320 | 275 |
| 30V/PC | 330 | 330 | 330 | 285 |
| 40V/PC | 330 | 330 | 330 | 290 |
| V | 340 | 340 | 340 | 300 |

It should be noted that the following blends: 20, 30 and 40 V/PC still are not sufficiently disperged after this second extrusion.

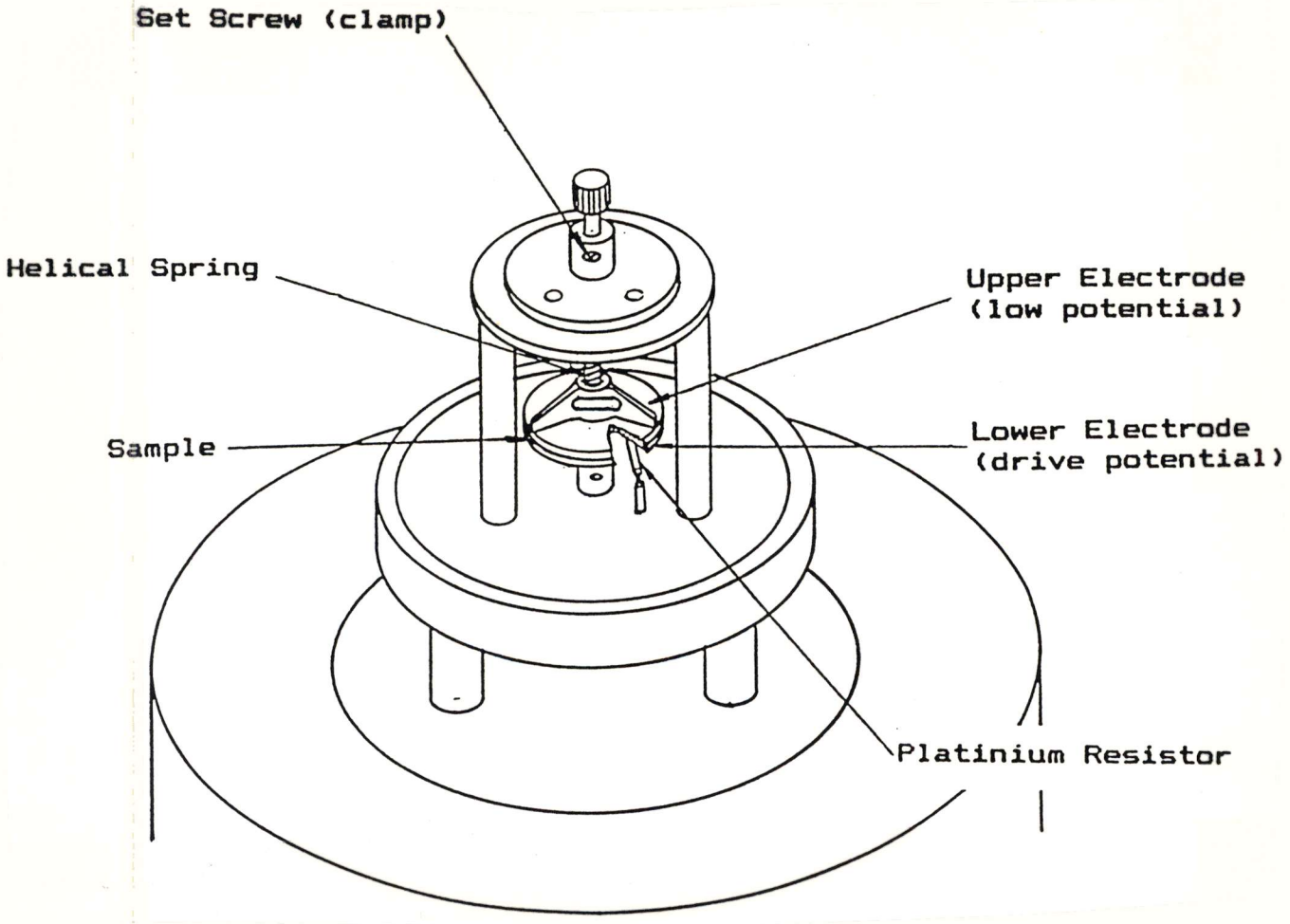


Fig. 3.4. Illustration of the DETA sample holder.

### 3.2.2 Hot pressing

The dynamic mechanical measurements require thicker samples than the dielectric measurements. For this purpose use is made of a press. To enable comparison between dielectric and mechanical measurements also samples for dielectric measurements have been pressed. More important considerations for this are however the fact that in this way smooth films are obtained and secondly that pressing diminishes the tensions which might have been introduced in the sample because of the extrusion. A Fontijne TP 200 hydraulic press has been used.

To obtain different thicknesses use can be made of various moulds. It is also possible to press without a mould. This process is primarily used for the blends 20, 30 and 40V/PC because extrusion of these blends didn't turn out successfully. Other compositions were pressed as well to enable a comparison between extruded and pressed films. It should be noted that extruded films were pressed. The temperature is raised up to 240 °C. The polymer is heated two minutes. After this interval of time it is pressed with a force of 200 kN for another two minutes. In all cases the polymer samples have been pressed between two layers of polyimide-foil. This was done to obtain smooth films.

## 3.3 Dielectric relaxation experiments

The dielectric relaxation measurements have been carried out by two measuring set-ups which will be described below.

### 3.3.1 Polymer Laboratories equipment

The Polymer Laboratories Dielectric Thermal Analyser (DETA) is an instrument capable of measuring the damping factor (tan $\delta$) and the relative permittivity ($\varepsilon'$) of polymers. It contains a General Radio RLC digibridge. Measurements were performed over the range from 20 Hz to 100 kHz using 9 preset frequencies. The voltage applied to the sample can be controlled in 5 mV steps from 5 mV to 1.275 V. A voltage of 1 V has been used. The instrument performs and stores in its memory the capacitance values from the connecting leads between the sensing circuit and the sample. No

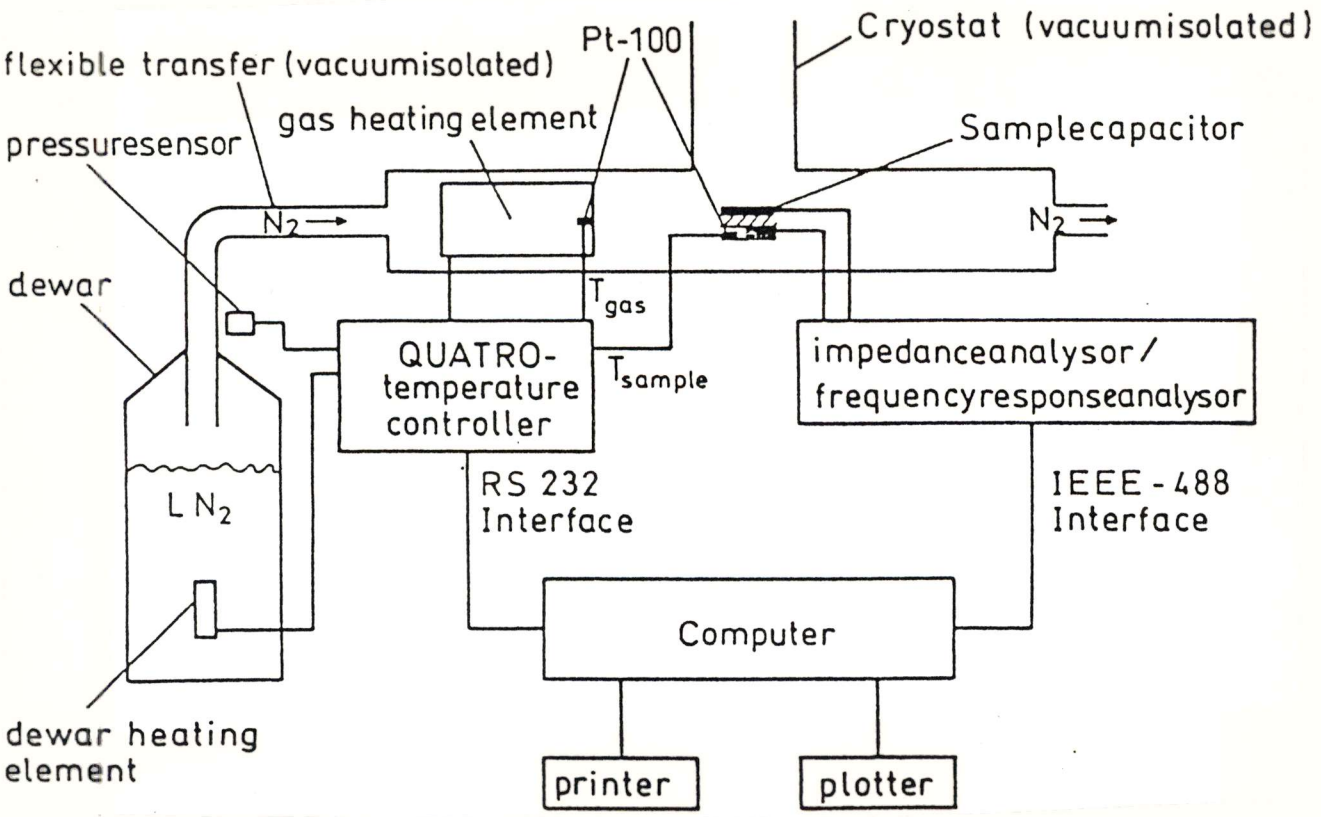


Fig. 3.5. Schematic view of the Novocontrol dielectric system.

corrections on the measured data have been carried out.

The environment within the temperature enclosure is controllable. The coolant circulates in a separate jacket and nitrogen is introduced from pipes in the upper bulkhead. The temperature is sensed and controlled by a blackened platinum resistor lying immediately under the sample. The sample temperature is scanned over the range from -100 °C to 250 °C at a rate of 1 °C per minute. It is imperative that the samples be smooth without holes or inclusions. Used were circular samples with a thickness between 20 and 100 μm and a diameter of 33 mm. The maximum variance in thickness per sample amounted 5%. The complete surface of the foil should make contact with the electrodes in order to obtain a homogeneously distributed electrical field. For better contact a conductive layer should be deposited on the foil. The first temperature scans were carried out with platinum electrodes. They were applied with an Edwards sputter coater 300. The measurements often delivered unuseful results. In a later stadium it was recognised that the surface impedance of the sputtered platinum layer was too high. Measurements showed that the surface impedance of platinum layers sometimes was more than 200 Ω, measured over the diameter of the sputtered electrode. Ideally, the maximum value of the surface impedance should be less than 20 Ω. For this reason gold was deposited with an Edwards sputter coater S150 A. A schematic view of the set-up is drawn in fig. 3.4. More details can be found in the operators manual of the PL-DETA.

### 3.3.2 Novocontrol equipment

The Novocontrol dielectric system has been developed at the Max Planck Institute for Polymer Research in Mainz, Germany (Kremer et. al., 1989). Automatic measurements in the frequency range from $10^{-4}$ Hz to $10^{7}$ Hz can be carried out. The system consists of a Frequency Response Analyser (Solartron Schlumberger 1260), a buffer amplifier (Chelsea Dielectric Interface) and a Quattro temperature controller as shown in fig. 3.5. Use has been made of a reference method (i.c. a reference capacitor) which corrects for deviations caused by the measuring circuit.

The cryostat is designed for temperatures from 100 to 600 K. It is

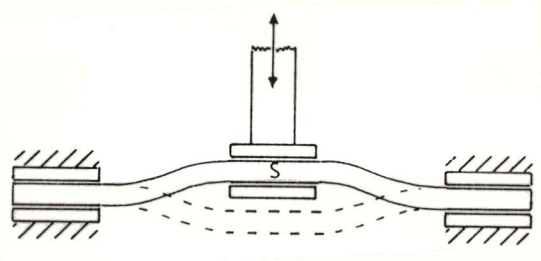

Fig. 3.6. The dual cantilever mode.

vacuum isolated. The sample temperature is controlled via a stream of temperature controlled nitrogen gas. The sample temperature is measured separately to an accuracy of 1 °C. The sample is held between the two plates of a parallel plate capacitor. As was the case with the DETA measurements, the samples need to be sputtered with gold. Thicknesses of the samples were comparable to the DETA samples. The diameters of the samples amount 20 mm. Temperature measurements of pressed V, N, PC, 40V/PC and 40V/N have been carried out with this equipment. Also frequency measurements of the above mentioned compositions have been carried out. A further description is given in the manual of the Novocontrol dielectric analyser.

### 3.4 Mechanical relaxation experiments

The Polymer Laboratories Dynamic Mechanical Thermal Analyser (DMTA) imposes a sinusoidal stress on a sample in the bending, shear or tensile mode. In our case, the samples have been measured in the bending mode. In this mode, the sample is in the form of a rectangular bar clamped rigidly at both ends and with its central point vibrated sinusoidally by the driver clamp. This is called the dual cantilever mode, see fig. 3.6. Used were samples with an average thickness of 1.0 mm and a width of 10 mm. The variance in thickness was not more than 5%.

The environment within the temperature enclosure is controllable. The coolant circulates in a separate jacket and nitrogen is introduced from pipes in the rear bulkhead. The temperature is sensed and controlled by a blackened platinum resistor lying immediately behind the sample. Measurements have been carried out over the range -100 to 250 °C. at a rate of 1 °C per minute. Three frequencies have been used: 3, 10 and 30 Hz. The strain level is $1/\sqrt{2}$. This means that the displacement signal is multiplied by $\sqrt{2}$. The clamps have been tightened at room temperature. A more thorough description gives the manual of the PL DMTA.

In most of the cases it was not possible to carry out the analysis over the entire temperature range. It appeared that the measurement stopped when the polymer was at the glass transition

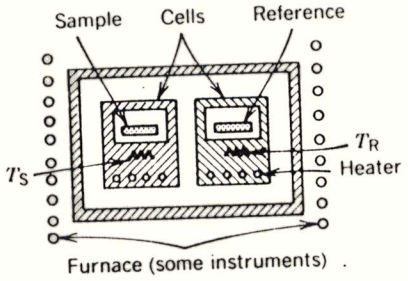


Fig. 3.7. Power-compensated DSC. $T_S$ = sample temperature, $T_R$ = reference temperature.

temperature of the matrix polymer. Most likely this is due to the fact that the modulus of the polymer decreases with a few decades. This assumption is supported by the fact that in cases where the modulus decreased only by one decade the measurement remained stable. In all other cases a second measurement was carried out with the starting point just below the glass transition temperature of the thermoplastic.

### 3.5 Differential Scanning Calorimetry (DSC)

The calorimeter used is a Perkin-Elmer DSC 7 differential scanning calorimeter. It belongs to the group of so-called power compensated DSC's, see fig. 3.7. It consists of a twin of micro calorimeters kept in a stable environment. Each calorimeter contains a temperature sensor, a heater and a container for the sample and reference material. The sample and reference calorimeters are each maintained at approximately the same programmed temperature by electric power. The difference in power supplied to the two heaters measures the rate of energy change in the sample. The DSC 7 is controlled by a personal computer. Two aluminum alloy cups function as sample holders in the DSC 7. These cups are mounted in a solid aluminum block which contains a heater and sensor.

As the system heats up in temperature, transitions such as melting, boiling, dehydration or crystallisation may occur in the sample material, resulting in endothermic or exothermic reactions. The amount of power required to maintain the sample holder at the same temperature as the reference holder during the transition is recorded as a trace. The values are read directly in millicalories per second, and this value is at all times equivalent to the rate of energy absorption or energy release of the sample. Argon is used as a purge gas which is circulated through the calorimeter chamber. A temperature calibration was carried out by using indium metal. A heating rate of 20 $^{o}$C per minute has been applied. The standard cooling rate is 200 $^{o}$C per minute. In practice this will tend to be 150 $^{o}$C per minute. For further details one is referred to the operators manual.

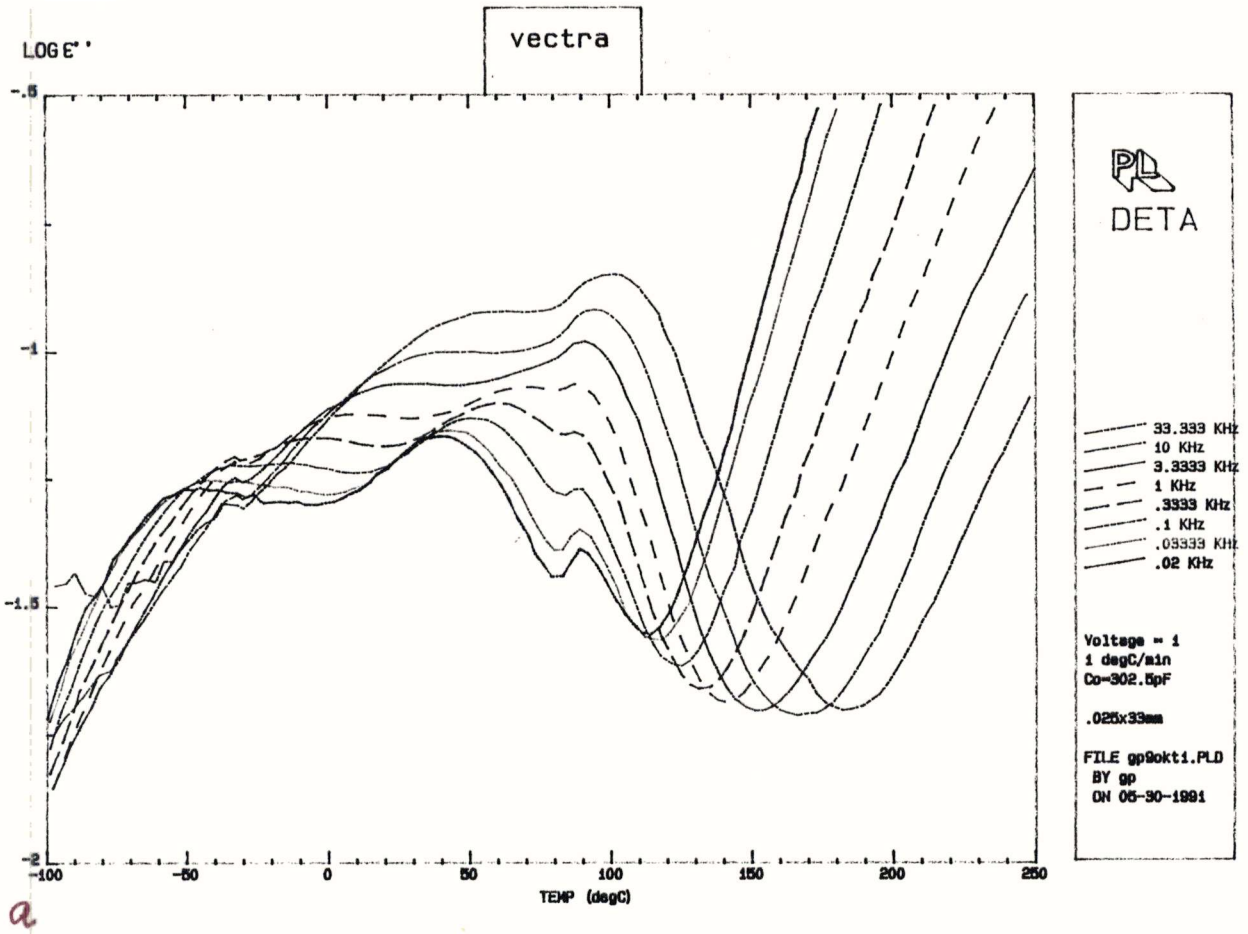


Fig. 4.1 Dielectric loss (a) and storage (b) spectrum of Vectra.

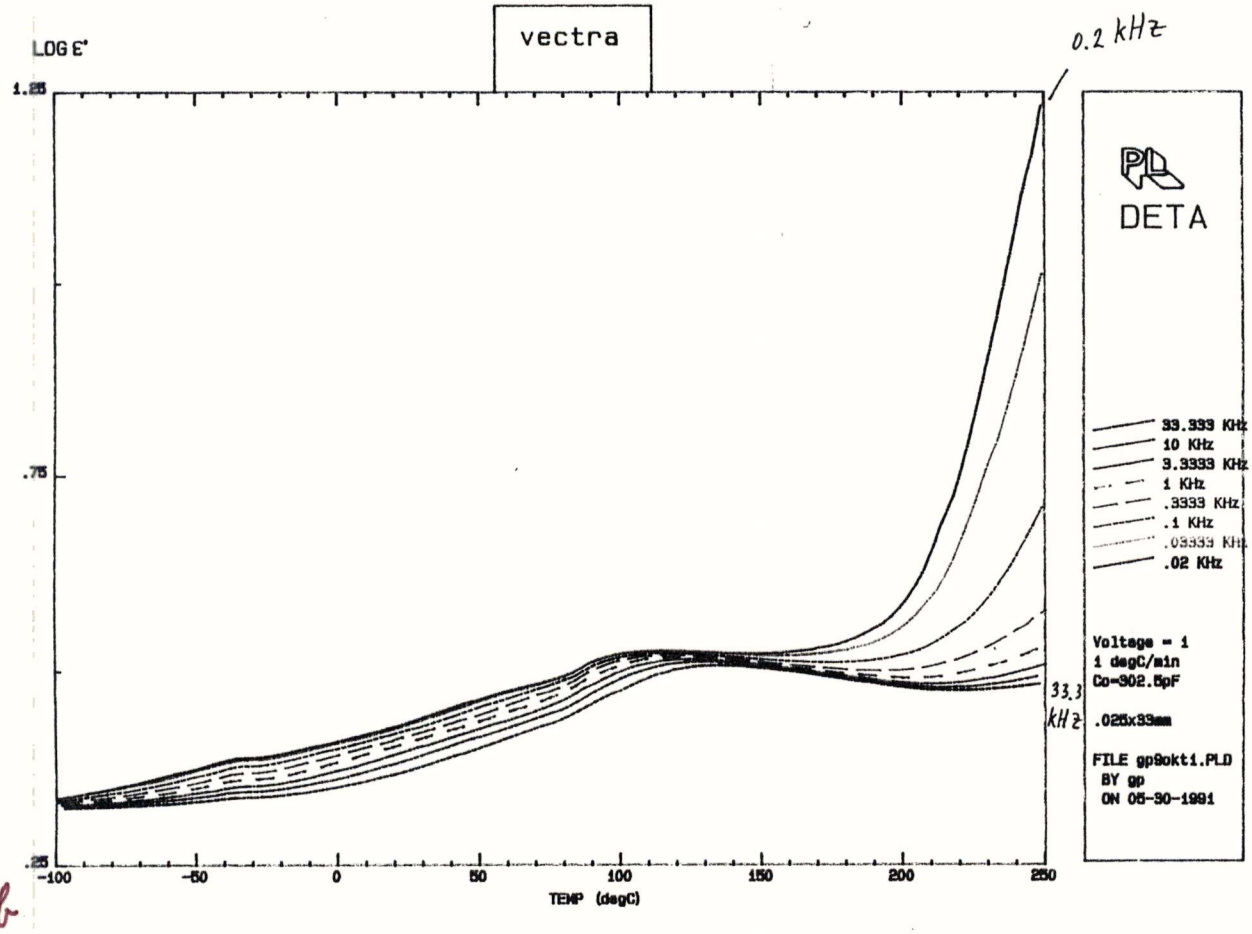

### 3.6 Scanning Electron Microscopy (SEM)

In order to evaluate better the structures of the blends on a microscale, SEM photographs have been made using a Philips XL 20 Scanning Electron Microscope. The photos are used to support and to elucidate the results found with the thermal analysis methods.

The samples were prepared as follows. Extruded and pressed samples of the compositions 10V/N, 10V/PC, 40V/N and 40V/PC have been cooled in liquid nitrogen. After having been cooled down sufficiently they were broken parallel and perpendicular to the extrusion direction. This was done to ensure that a brittle fracture had occurred. The samples were subsequently sputtered with gold using an Edwards sputter coater 300. This was done because the samples have to be conductive.

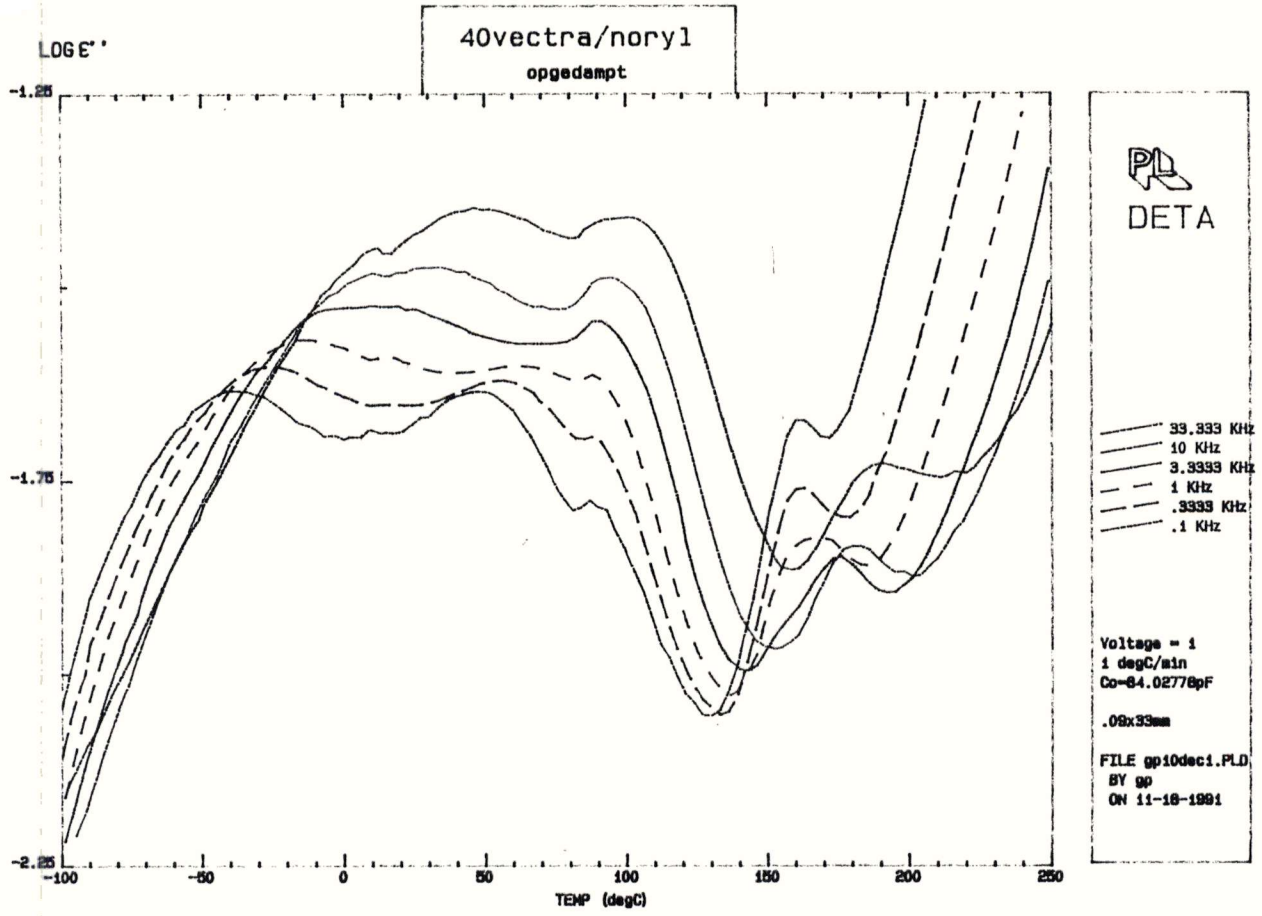


a

Fig. 4.2. Dielectric loss (a) and storage (b) spectrum of 40V/N.

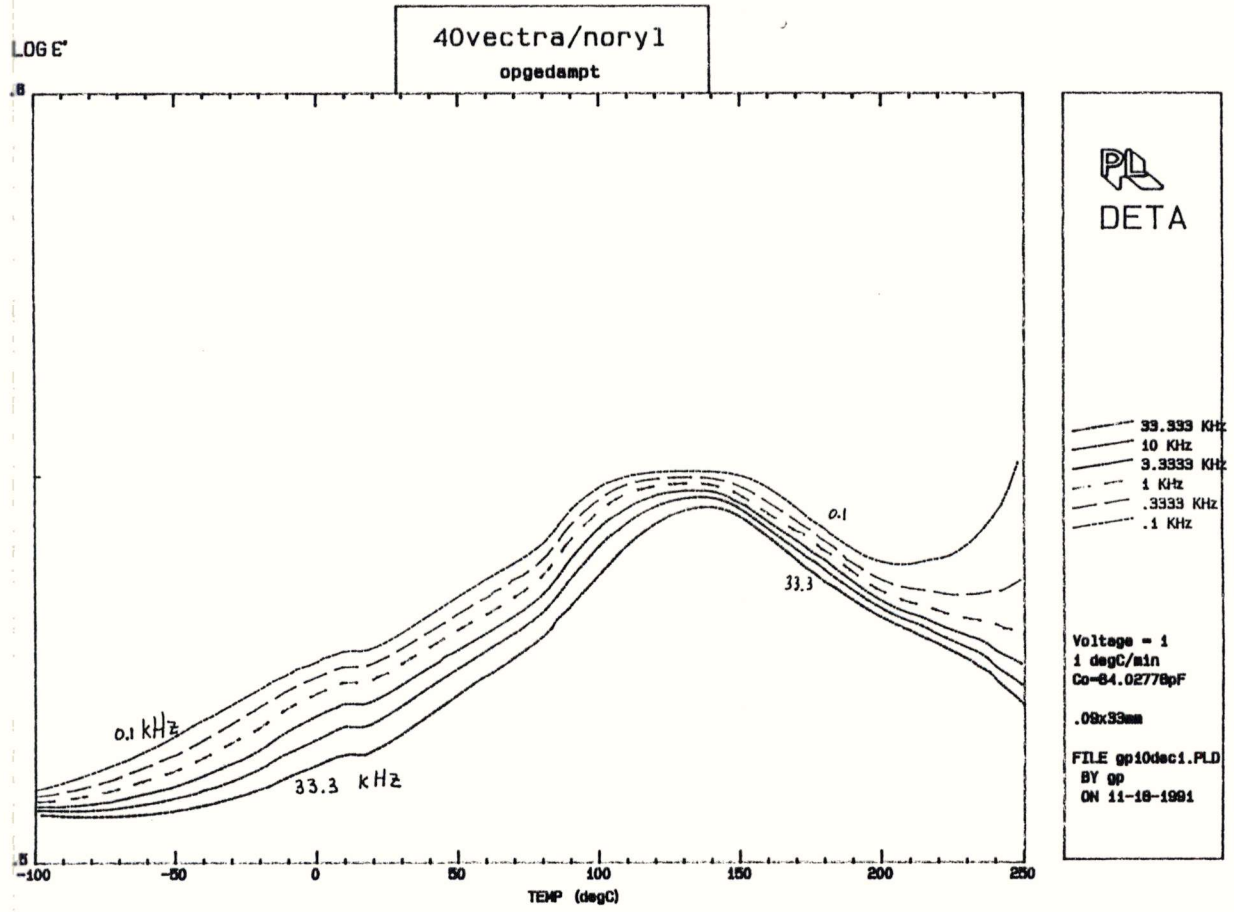


b

# 4 RESULTS

## 4.1 Dielectric relaxation experiments

### 4.1.1 Temperature scans

As was indicated in subsection 3.3.1, measurements have been carried out on both platinum and gold sputtered samples. More important, however, is the difference between pressed and extruded samples. In the following table all temperature scans are summed up conveniently.

Table 4.1. Survey of DETA measurements.

| | extruded | pressed |
|---|---|---|
| Pt | PC<br>5V/PC<br>10V/PC | 20V/PC<br>30V/PC *<br>40V/PC |
| Au | PC | PC *<br>5V/PC *<br>10V/PC *<br>20V/PC *<br>40V/PC * |
| Pt | N<br>5V/N *<br>10V/N *<br>20V/N<br>30V/N *<br>40V/N<br>V * | N |
| Au | N *<br>20V/N *<br>40V/N * | |

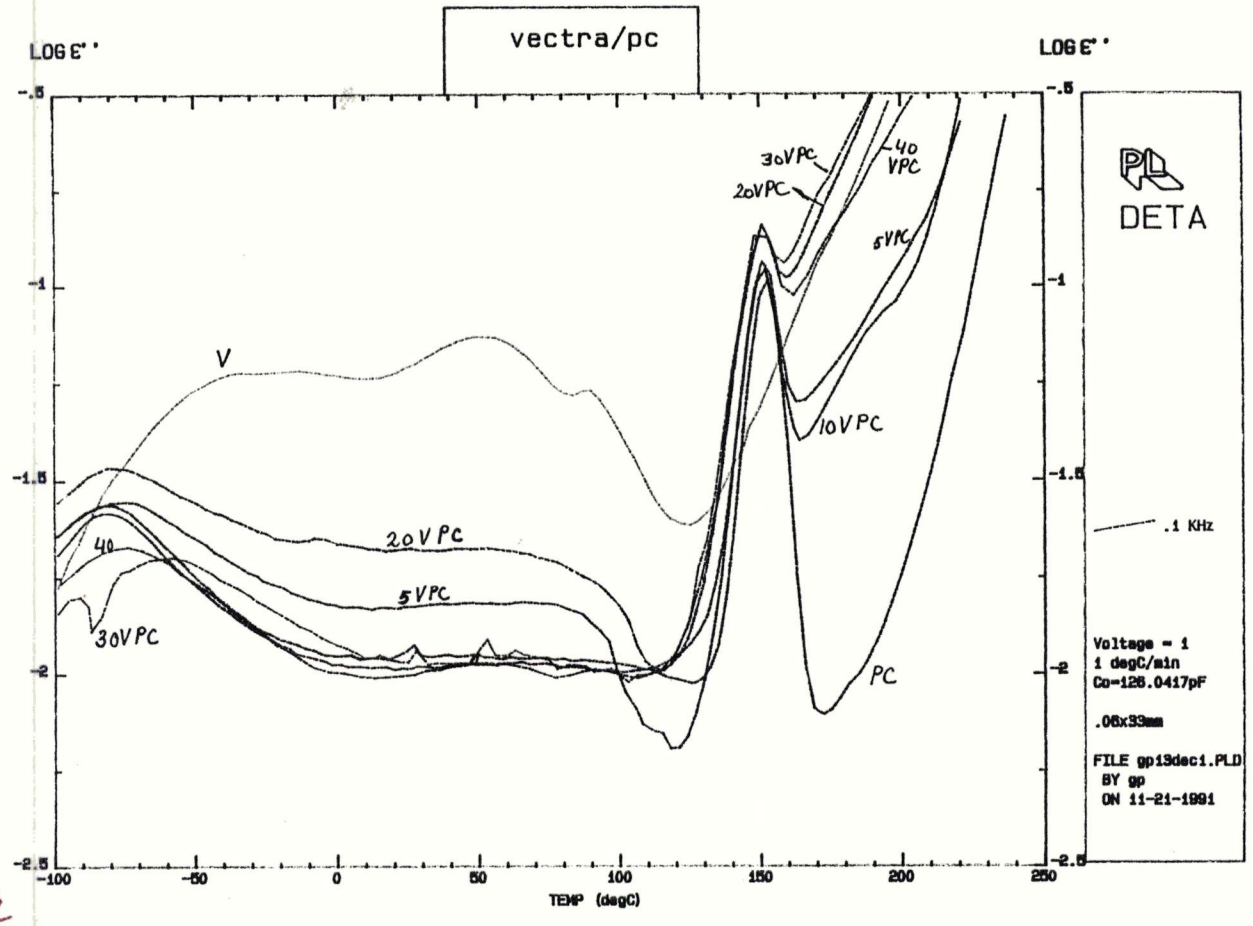


a

Fig. 4.3. Dielectric loss (a) and storage (b) spectra of V/PC blends at different composition ratios at a frequency of 0.1 kHz.

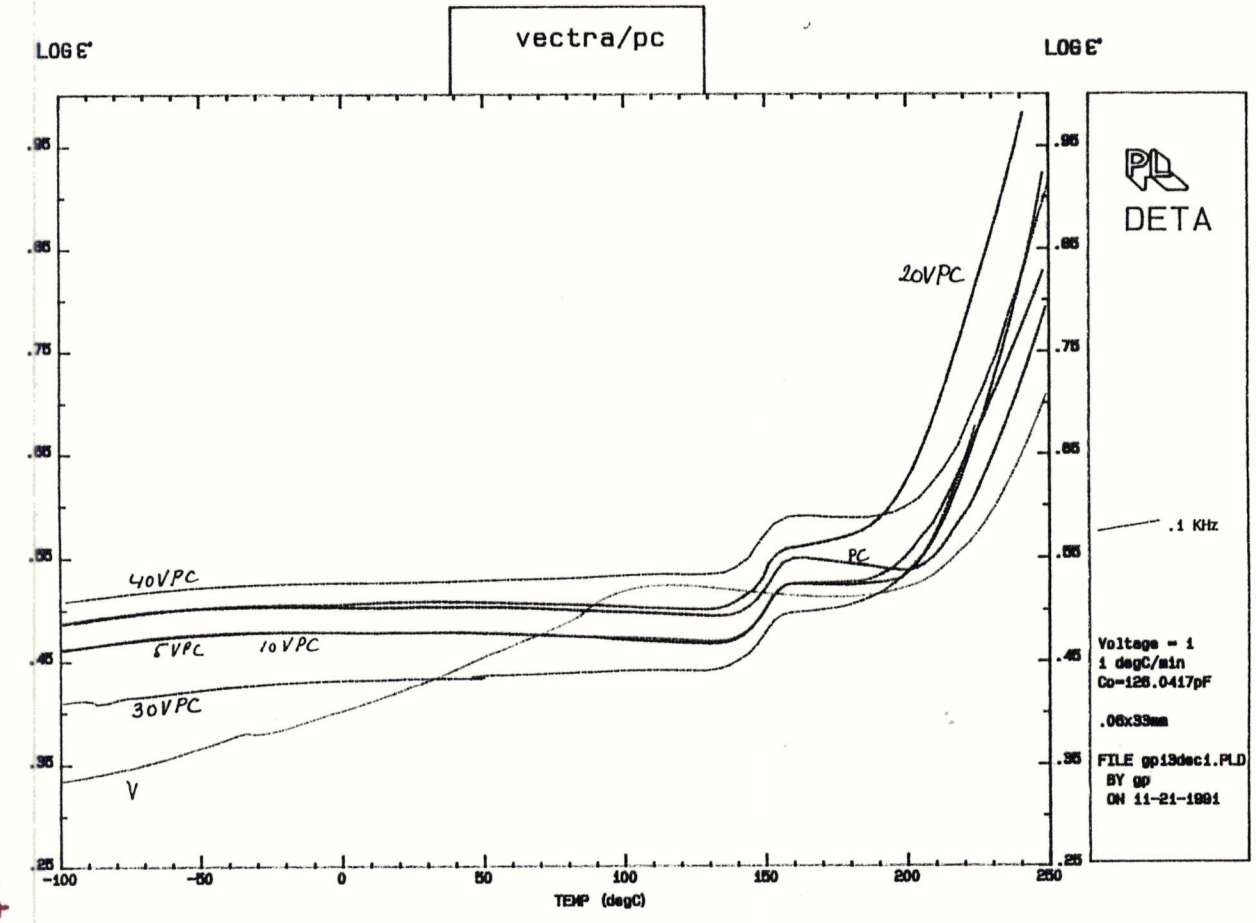


b

As an example, plots of ε" and ε' versus temperature for Vectra and 40 V/N are given in figs. 4.1 and 4.2. These figures were chosen because they neatly demonstrate the shift of transitions with frequency. The measurements marked with an asterisk have been compared in the following four figures.

Two frequencies of the series of (V/PC) have been selected for the purpose of comparison. Use has been made of a relatively low frequency and a relatively high frequency. So, in one figure the complete range from 0 vol.% Vectra till 22.7 vol.% Vectra can be seen at one frequency. Fig. 4.3 pertains to 0.1 kHz, whilst fig. 4.4 pertains to 10 kHz. It was tried to detect all transitions in the blend. Often this caused difficulties with transitions below the α-transition of the matrix polymer. In the following table the transitions of V/PC blends at a frequency of 33 Hz are represented. This frequency was chosen because it was the lowest possible frequency at which transitions could be measured with the equipment.

Table 4.2. ε" Transitions of V/PC blends at a frequency of 33 Hz.

| | $T_{\beta_{PC}}$ (°C) | $T_{\beta_{V}}$ (°C) | $T_{\alpha_{V}}$ (°C) | $T_{\alpha_{PC}}$ (°C) |
|---|---|---|---|---|
| PC | -83 | - | - | 150 |
| 5V/PC | -77 | - | - | 151 |
| 10V/PC | -86 | - | - | 149 |
| 20V/PC | -81 | - | - | 148 |
| 30V/PC | -60 | - | 90 | 148 |
| 40V/PC | -79 | 49 | 91 | 147 |
| V | - | 43 | 91 | - |

The measurements were reproducible within two degrees. A statistical estimation of the inaccuracy using a 95 % interval of reliability shows an error (δT) of 2 degrees. Three measurements on one sample have been carried out.

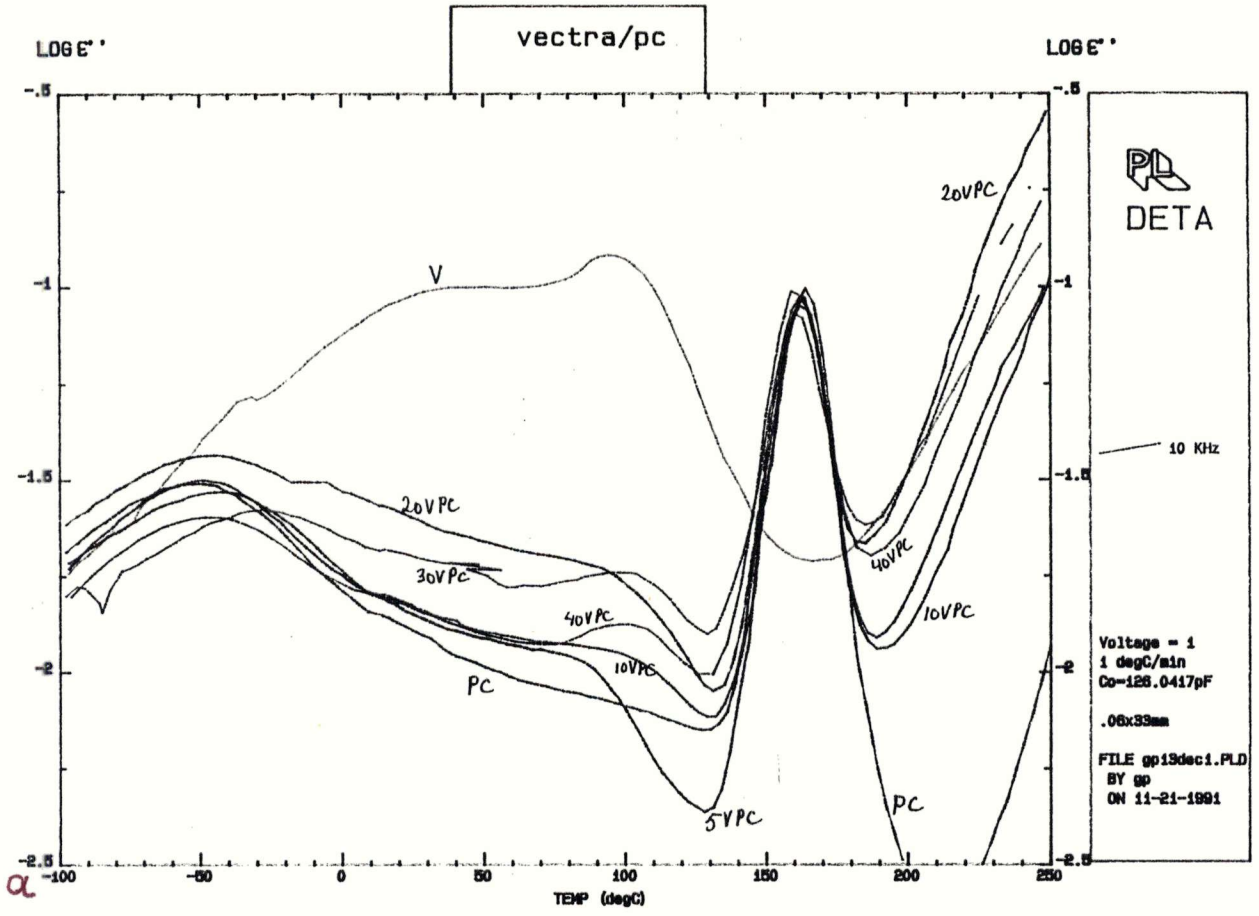


Fig. 4.4. Dielectric loss (a) and storage (b) spectra of V/PC blends at different composition ratios at a frequency of 10 kHz.

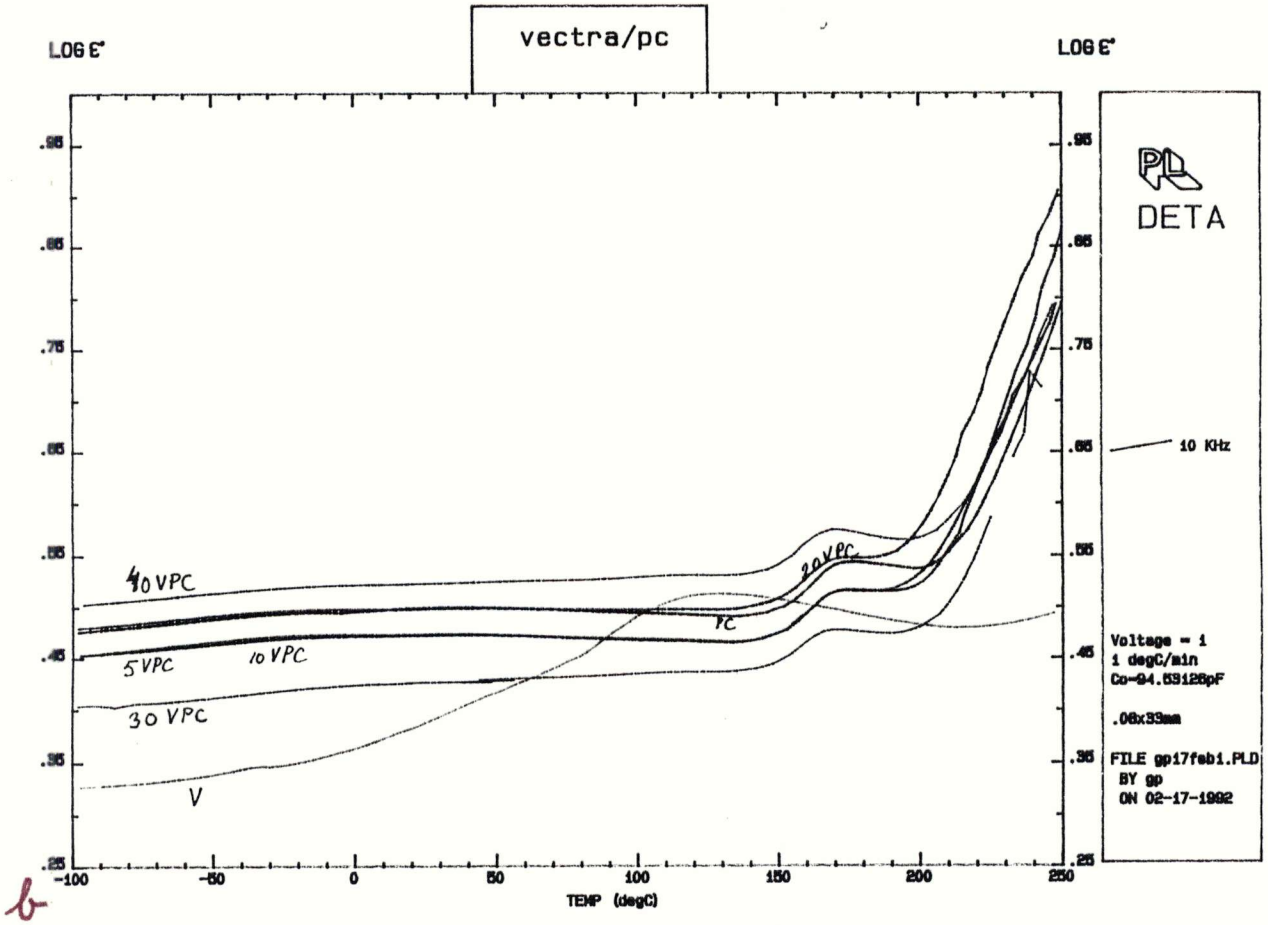

A similar sort of study has been carried out for the series of (V/N). Fig. 4.5 holds for 0.1 kHz, whilst fig. 4.6 holds for 10 kHz. Also in this case the ε" transitions have been located at a frequency of 33 Hz. These are represented in the following table.

Table 4.3. ε" Transitions of V/N blends at a frequency of 33 Hz.

| | $T_{\gamma_V}$ (°C) | $T_{\beta_V}$ (°C) | $T_{\alpha_V}$ (°C) | $T_{\alpha_N}$ (°C) |
|---|---|---|---|---|
| N | - | - | - | 143 |
| 5V/N | - | - | - | 158 |
| 10V/N | - | - | - | 159 |
| 20V/N | - | - | - | 162 |
| 30V/N | -28 | 38 | 90 | 162 |
| 40V/N | -34 | 35 | 87 | 161 |
| V | - | 43 | 89 | - |

Also in this case the 95 % error in the temperature measurement using three measurements is two degrees.

More measurements have been carried out than described above. This was done to enable comparisons between pressed and extruded samples and to compare platinum coated samples and gold coated samples. All PC measurements have been compared at two frequencies. Fig. 4.7 shows ε" data at 0.1 kHz, while fig. 4.8 shows these data at 10 kHz. Another comparison has been made between the measurements of 20V/PC. Fig. 4.9 gives the results at 0.1 kHz. No comparison has been made of the different Noryl measurements because of the poor quality of these measurements. Also the 40V/N measurements have been compared. Fig. 4.10 depicts the results at 0.1 kHz, while fig. 4.11 gives the results for 10 kHz.

A possible relation between the loss and storage permittivities of the pure components and the blends was investigated using the mixing formulas (2.23) till (2.26). The pressed blends of 40V/N

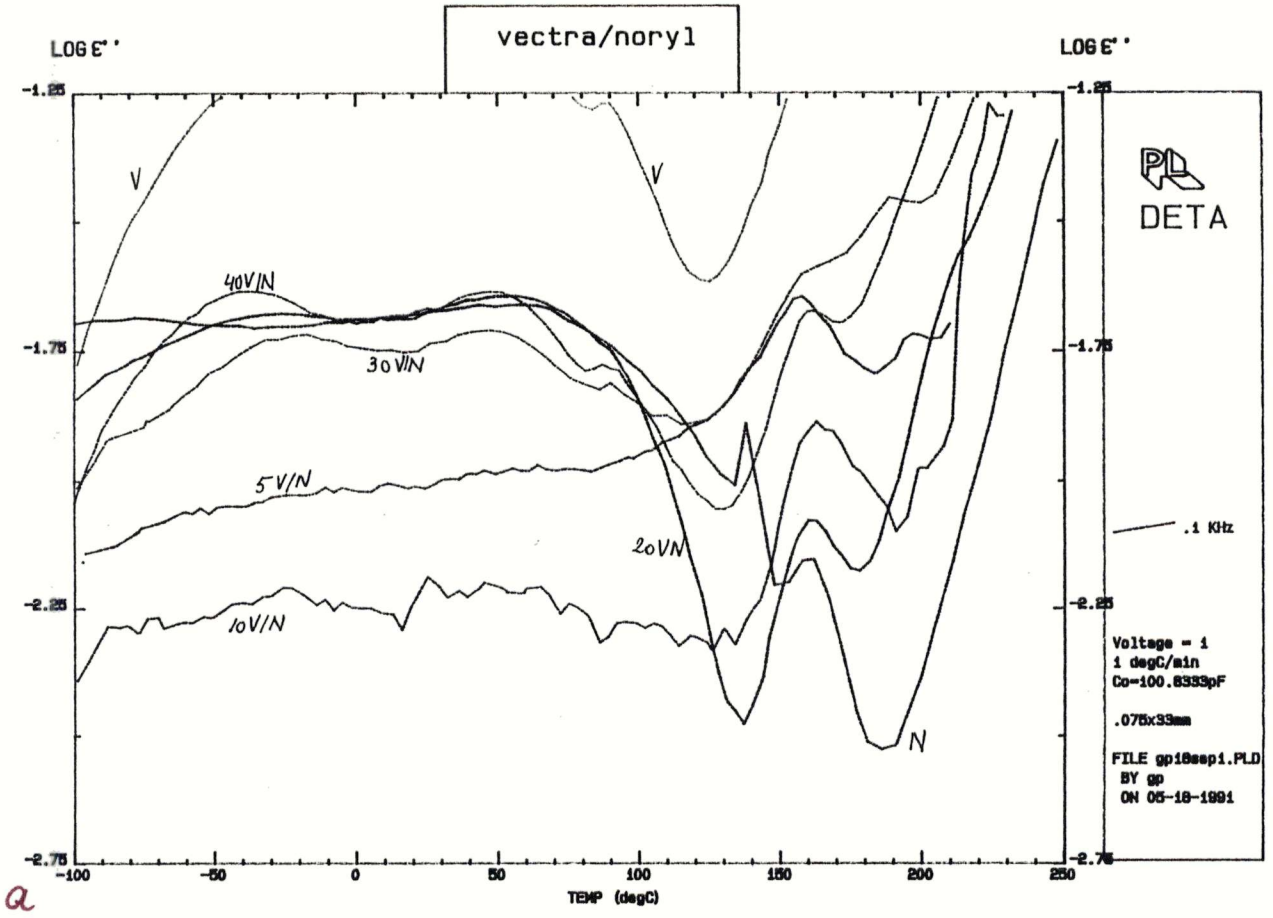


a

Fig. 4.5. Dielectric loss (a) and storage (b) spectra of V/N blends at different composition ratios at a frequency of 0.1 kHz.

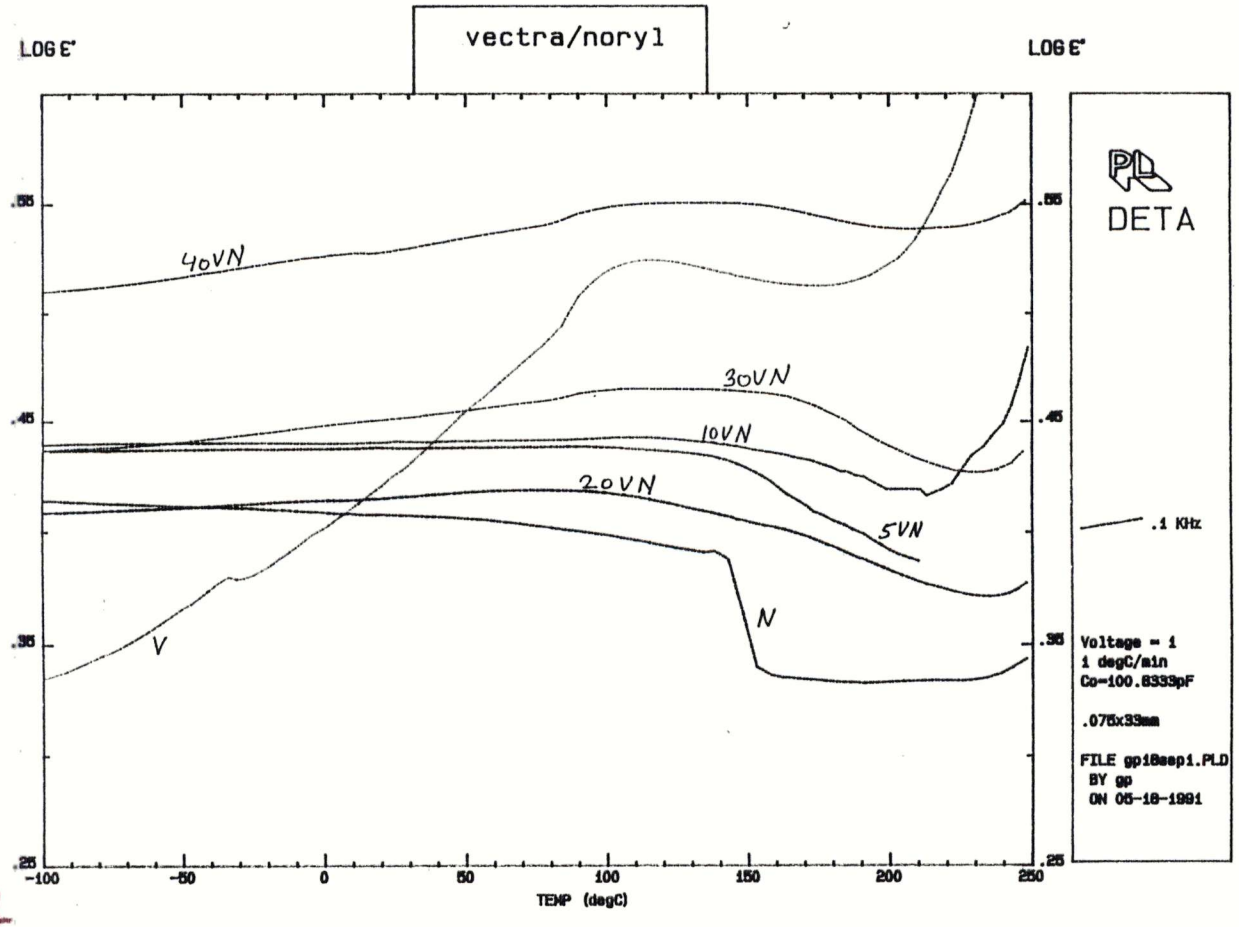


b

and 40V/PC are considered. In this way calculated and measured ε values are compared. The following table gives a survey of the comparisons.

Table 4.4. Comparison of calculated DETA curves with measured DETA curves.

| | fig. number | |
|---|---|---|
| quantity | 40V/N | 40V/PC |
| ε' | 4.12 | 4.14 |
| ε" | 4.13 | 4.15 |

### 4.1.2 Frequency scans

Frequency scans have only been carried out using pressed samples. As was indicated in chapter 2, frequency scans have been carried out to investigate peak broadening.

Fig. 4.16 shows the log(ε") as function of the frequency for polycarbonate. For the normalisation the most pronounced peak was chosen. In this case, this was the peak at 438.15 K. In the case of 40V/PC also the most pronounced peak (coincidently at the same temperature) was chosen. Both normalized peaks have been put together in one graph in fig. 4.17. Now we can see whether peak broadening occurs. At a first glance it does, but at the same time we see that the conductivity contributes significantly to the values at low frequencies of 40V/PC. The conductivity contribution should be represented as a straight line (slope -1). The slope of the line appears to be less than -1. This means that at the frequencies considered there is no pure dc conductance. In chapter 5 we elaborate on this phenomenon. In the meanwhile it will be referred to as conductivity. For a better comparison the contribution of the conductivity was subtracted from the curve of 40V/PC. This can be done when log(ε") is plotted as function of log(freq.) as has been shown in chapter 2. Fig 4.18 depicts the results of the subtraction. In the case of pure conductivity the corresponding ε' remains constant. This is not exactly the case as can be seen in fig. 4.18a. Nevertheless the subtraction was carried out. The resulting curve is again put together with the

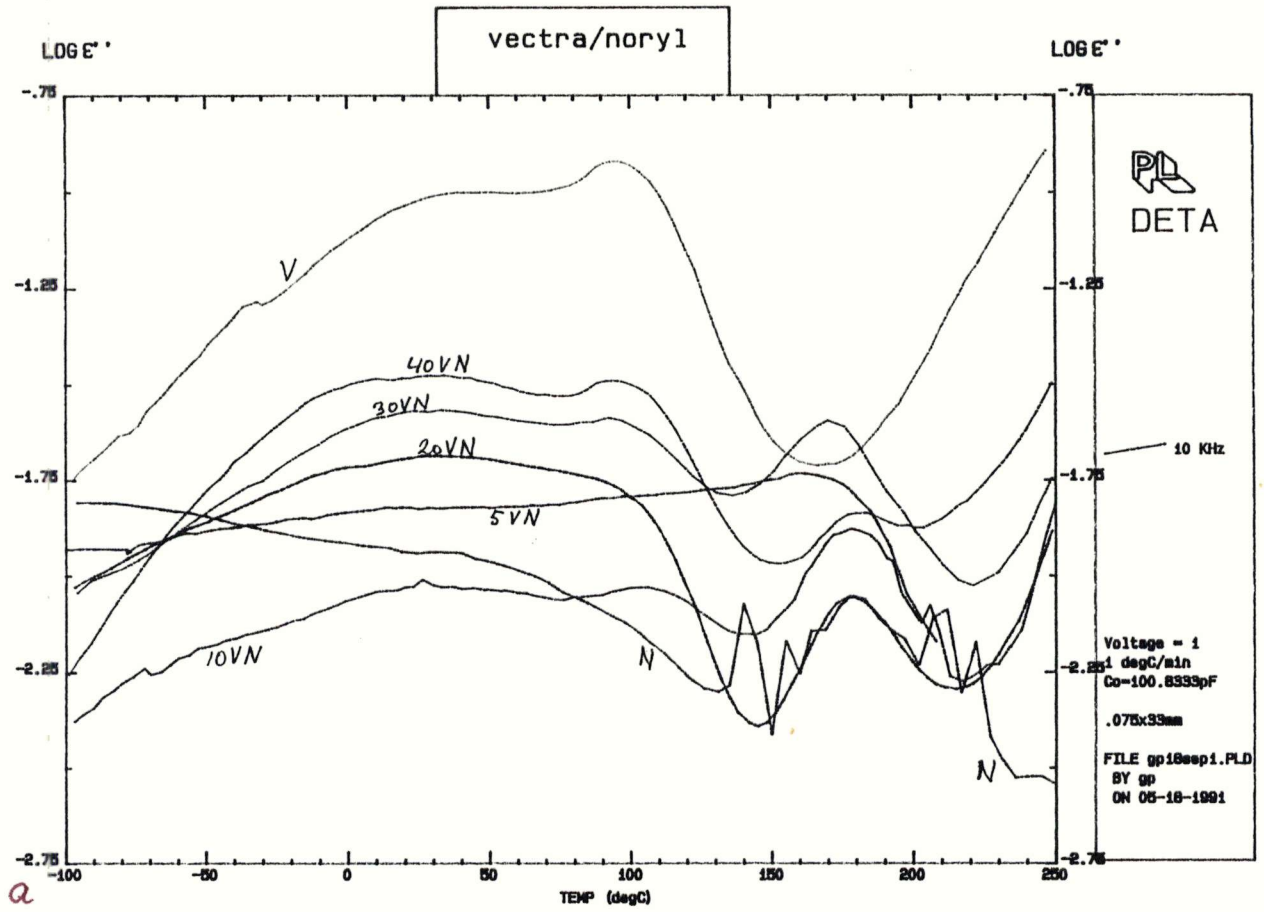


Fig. 4.6. Dielectric loss (a) and storage (b) spectra of V/N blends at different composition ratios at a frequency of 10 kHz.

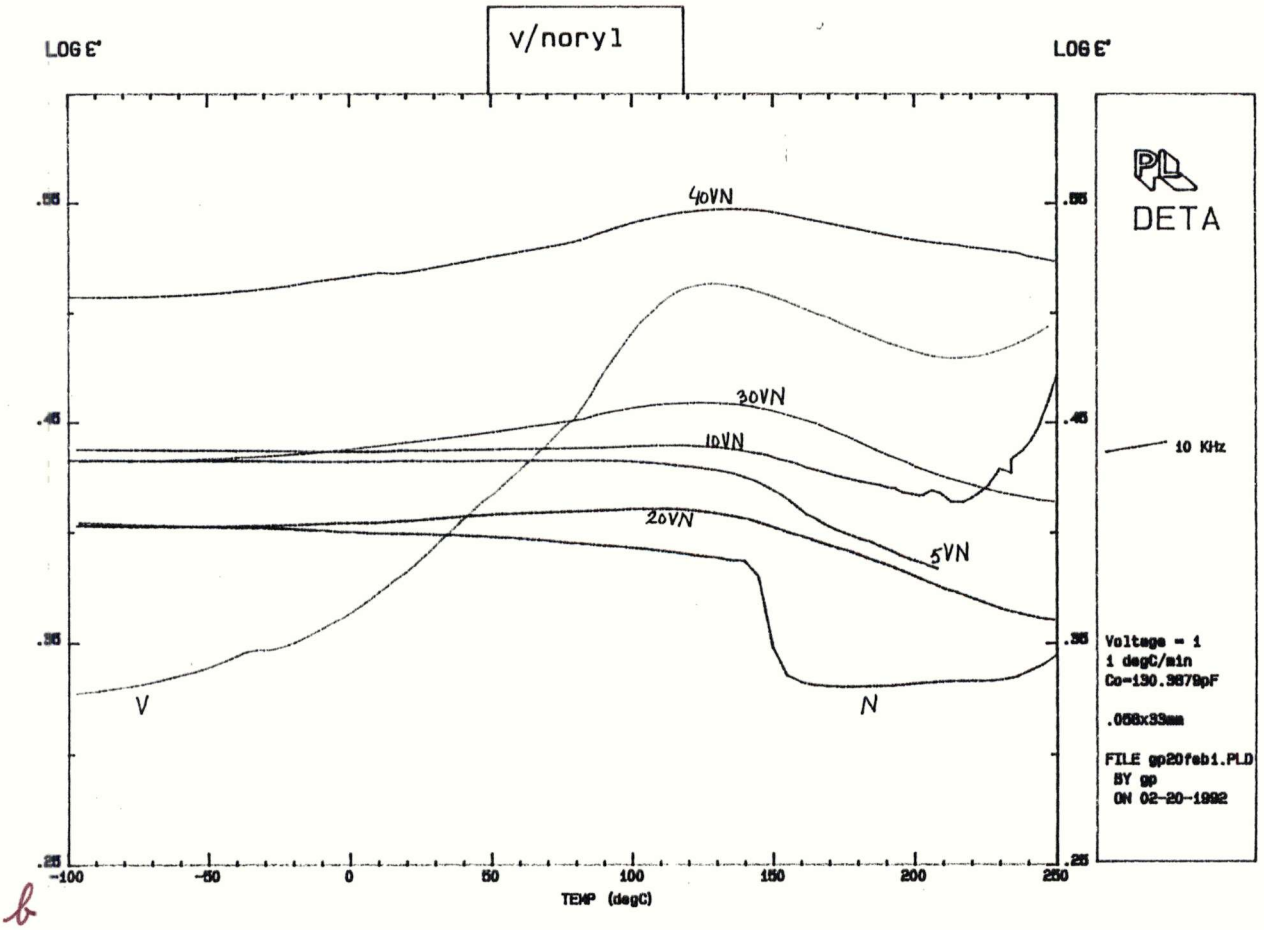

normalised curve of PC in fig. 4.19. Hardly any broadening can be seen now.

In the plot of log(ε") of Vectra as function of the frequency (at temperatures from 85 to 105°C) no maxima can be seen. Only a slight shoulder can be detected. For this reason no further analysis has been carried out on these data.

The process of selecting one temperature to make a normalised curve has also been carried out for Noryl and 40V/N. The result is shown in fig. 4.20. In fig. 4.20a the storage moduli for these two samples are represented.

### 4.2 Mechanical relaxation experiments

Just as was the case with the dielectric measurements comparisons have been made between the different compositions of V/PC and V/N. Two frequencies of the series of V/PC have been selected. Use has been made of the lowest (3 Hz) and the highest (30 Hz) frequency which are depicted in figs. 4.21 and 4.22. In this way the complete range from 0 vol.% Vectra till 22.7 vol.% Vectra can be seen at one frequency. The following table shows the transitions of V/PC at a frequency of 30 Hz. Just as was the case with the dielectric measurements not all transitions could be detected. The frequency of 30 Hz was chosen to enable comparison with the DETA measurements.

Table 4.5. E" transitions of V/PC at a frequency of 30 Hz.

| | $T_{\beta_{PC}}$ (°C) | $T_{\beta_V}$ (°C) | $T_{\alpha_V}$ (°C) | $T_{\alpha_{PC}}$ (°C) |
|---|---|---|---|---|
| PC | -72 | - | - | 144 |
| 5V/PC | -70 | - | - | 141 |
| 10V/PC | -58 | 43 | 97 | 140 |
| 20V/PC | -63 | 49 | - | 142 |
| 30V/PC | -63 | - | - | 140 |
| 40V/PC | -50 | 45 | 99 | 139 |
| V | - | 43 | 85 | - |

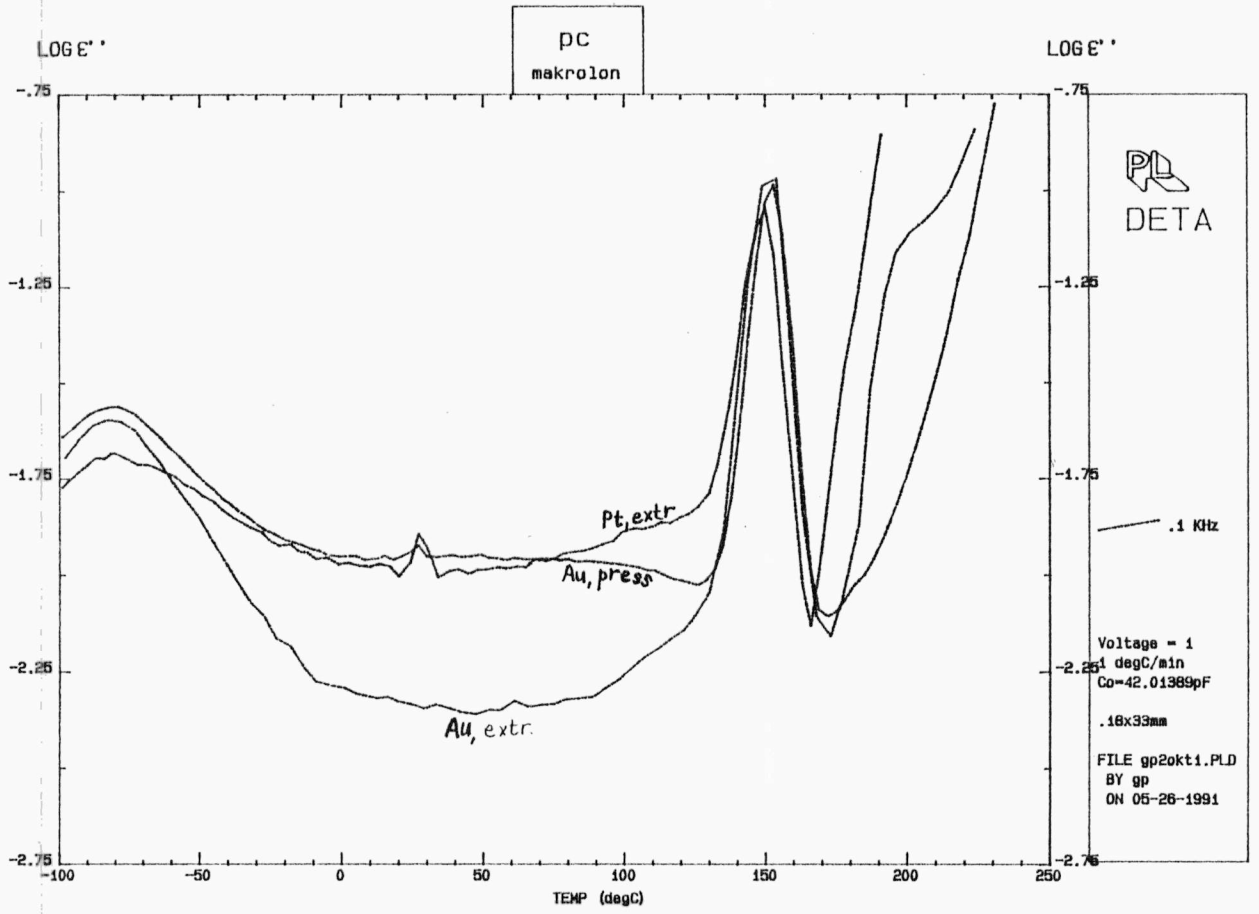


Fig. 4.7. Dielectric loss spectra of PC that underwent three different treatments at a frequency of 0.1 kHz.

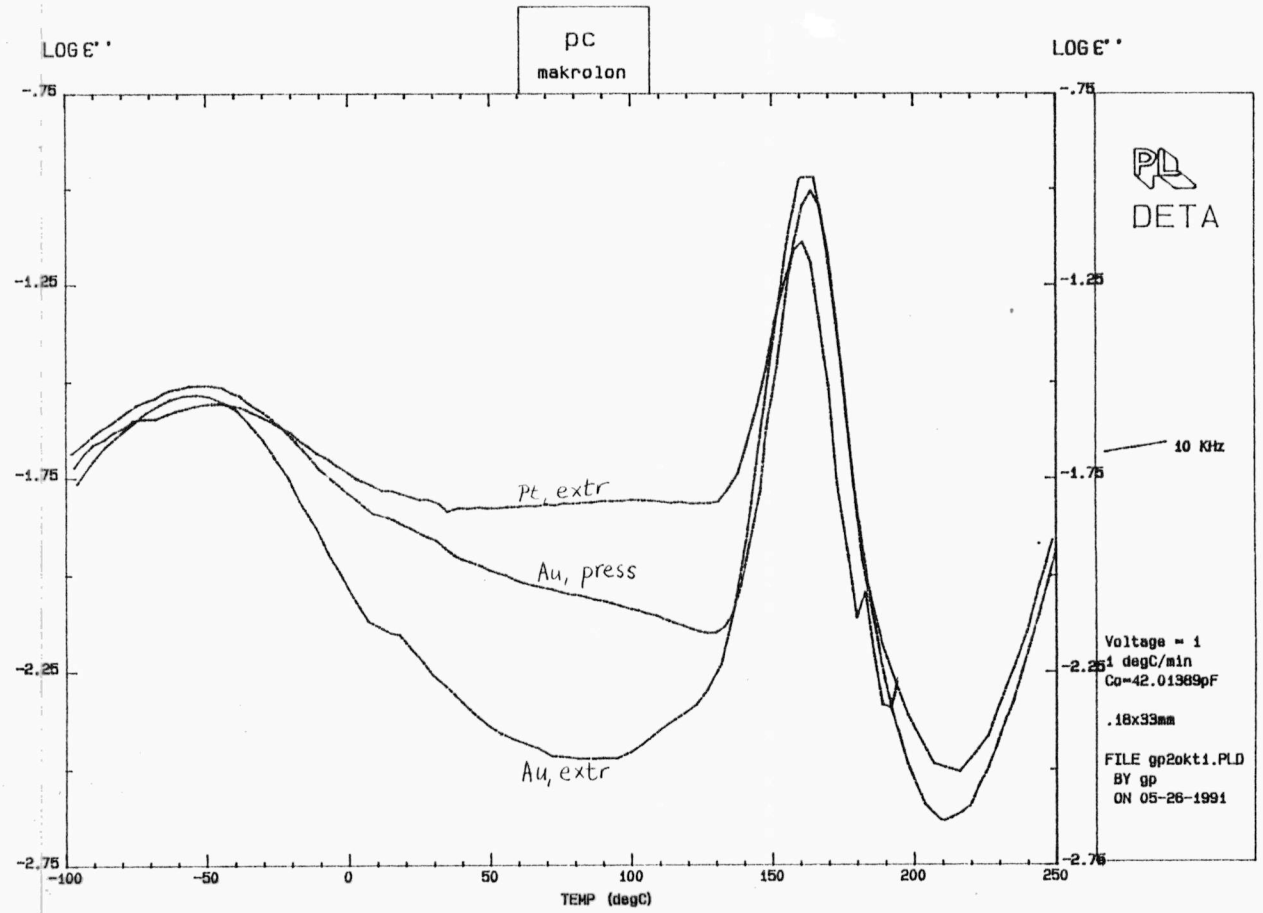


Fig. 4.8. Dielectric loss spectra of PC that underwent three different treatments at a frequency of 10 kHz.

The $\gamma$-transition of Vectra cannot be detected separately in this case. A statistical estimation of the inaccuracy using a 95 % interval of reliability shows an error in the temperature measurement ($\delta T$) of two degrees. Two measurements have been carried out on one sample.

In the same way the complete composition range of the V/N series is represented, in fig. 4.23 at 3 Hz and in fig. 4.24 at 30 Hz. The following table shows the transitions in these blends in the same way as seen before.

Table 4.6. E" transitions in V/N at a frequency of 30 Hz. $\delta T$ = 2 $^{o}C$.

| | $T_{\beta_V}$ ($^{o}C$) | $T_{\alpha_V}$ ($^{o}C$) | $T_{\alpha_N}$ ($^{o}C$) |
|---|---|---|---|
| N | - | - | 147 |
| 5V/N | 54 | 100 | 148 |
| 10V/N | 56 | - | 145 |
| 20V/N | 46 | 100 | 154 |
| 30V/N | 52 | 101 | 154 |
| 40V/N | 50 | 95 | 154 |
| V | 43 | 85 | - |

Because of the fact that the measured curves were rather unsmooth and are composed of two measurement runs no comparisons of the calculated with the experimental curves have been made.

### 4.3 Differential Scanning Calorimetry (DSC)

An example of a DSC scan is given in fig. 4.25. From the DSC scans only the glass transitions of the matrix polymers can be detected. In the following table the transitions of the various compositions are shown. During the first run (extruded samples) in N and 40V/N several glass-transitions were found. The accuracy in determining the $T_g$ amounts some 4 $^{o}C$. This is because of the fact that the $T_g$ in DSC can only be estimated.

Table 4.7. Glass transitions as measured with the DSC for two runs

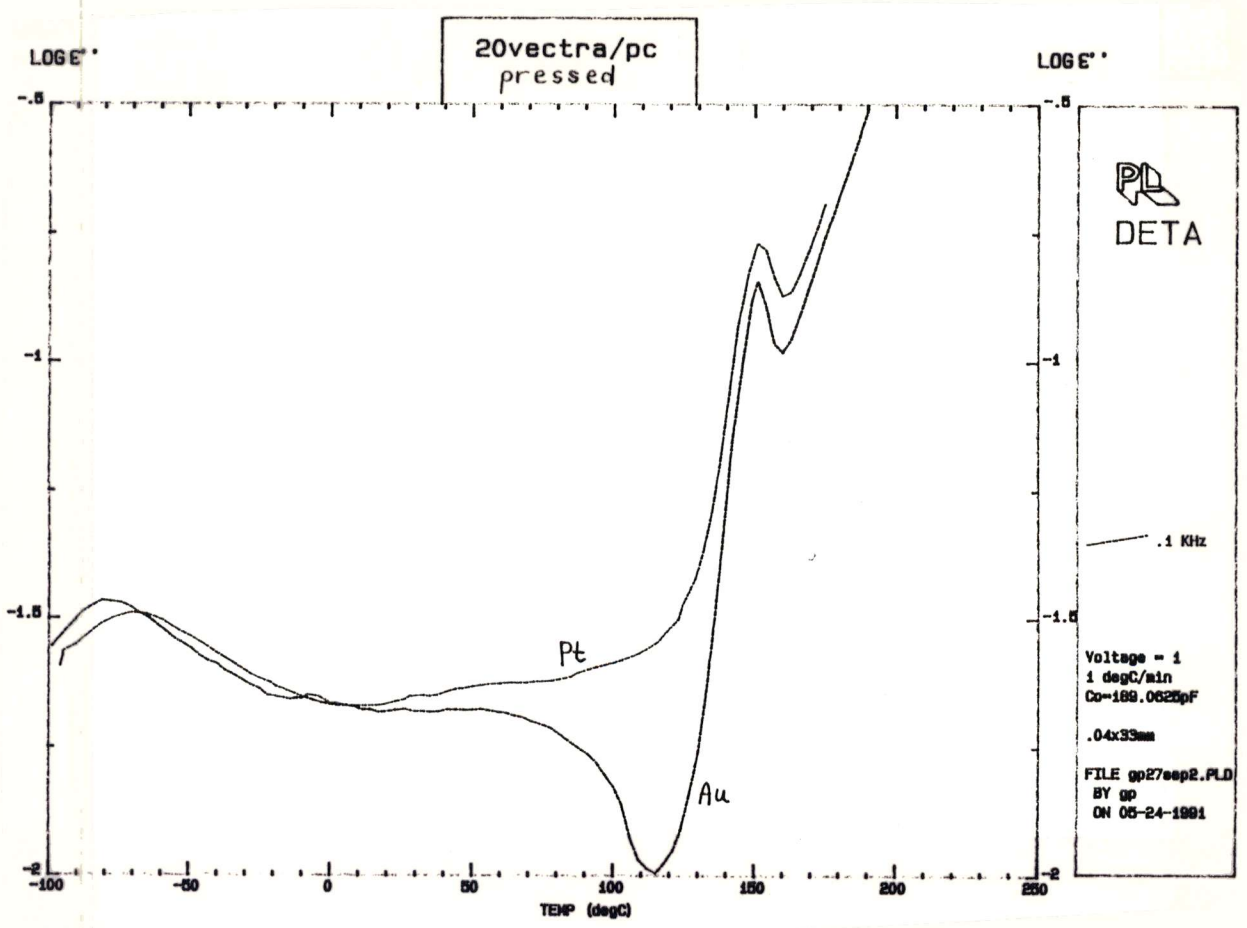


Fig. 4.9. Dielectric loss spectra of pressed 20V/PC either sputtered with platinum or using gold at a frequency of 0.1 kHz.

and the difference between the first and second run.

| code | $T_{g_1}$ (°C) | $T_{g_2}$ (°C) |
|---|---|---|
| PC | 147 | 147 |
| 5V/PC | 147 | 145 |
| 10V/PC | 146 | 148 |
| 20V/PC | 148 | 145 |
| 30V/PC | 147 | 145 |
| 40V/PC | 146 | 144 |
| | | |
| | 124 | |
| N | 154 | 151 |
| | 200 | |
| 5V/N | 151 | 148 |
| 10V/N | 153 | 147 |
| 20V/N | 150 | 147 |
| 30V/N | 152 | 149 |
| | 96 | |
| 40V/N | 118 | |
| | 149 | 145 |
| V | 100 | |

Fig 4.26 shows the glass transition temperatures for the first and second run as function of the vol.% Vectra in PC and N.

### 4.4 Scanning Electron Microscopy (SEM)

Photo 1 shows an extruded sample of 40V/PC that was broken parallel to the extrusion direction. It can be seen that Vectra appears as hairy, rather smooth spheres. The Vectra particles cluster whereas in the case of 10V/PC they do not. Samples broken perpendicular to the extrusion direction show the same effects. Moreover, no differences between pressed and extruded samples are seen.

This is in sharp contrast to photos 2, 3 and 4, showing

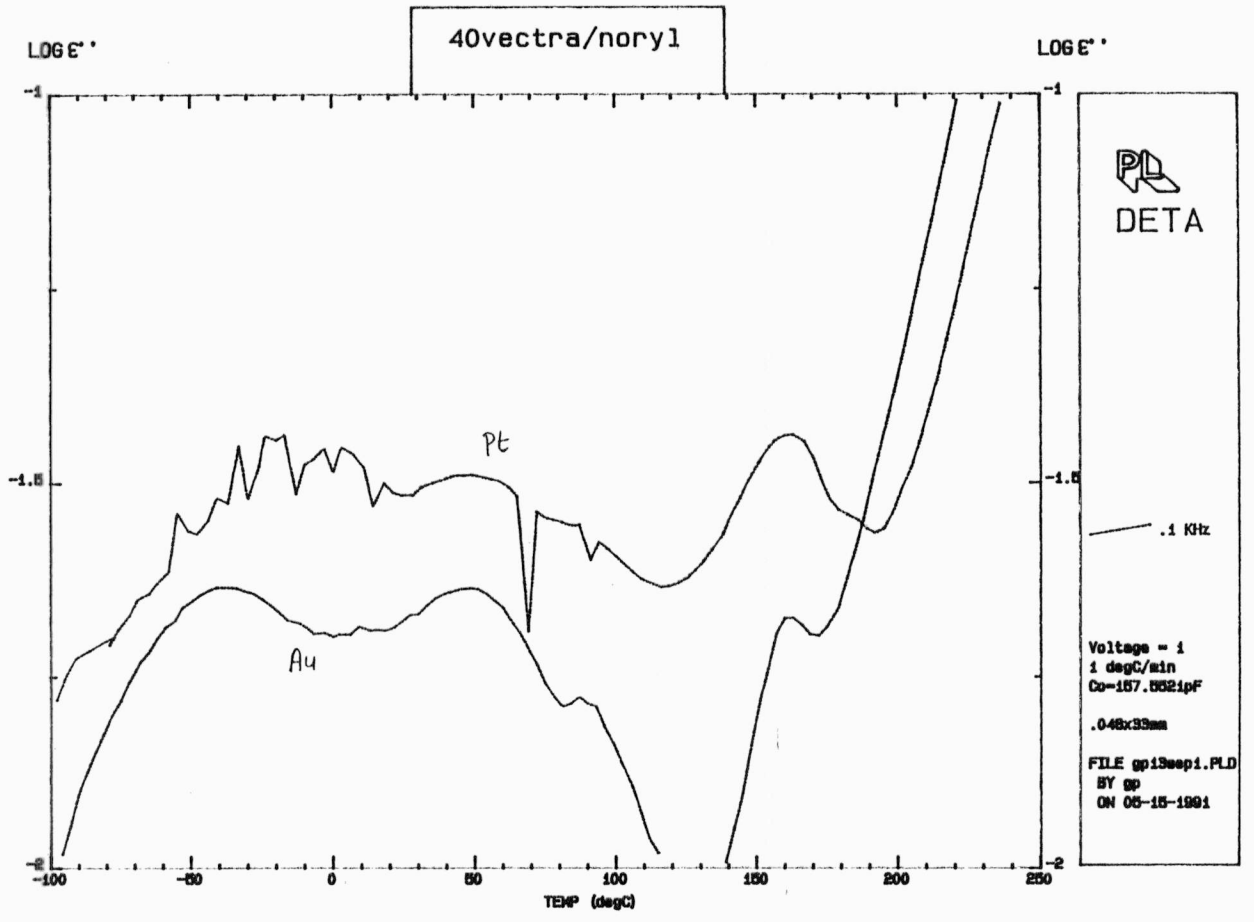


Fig. 4.10. Dielectric loss spectra of pressed 40V/N either sputtered with platinum or using gold at a frequency of 0.1 kHz.

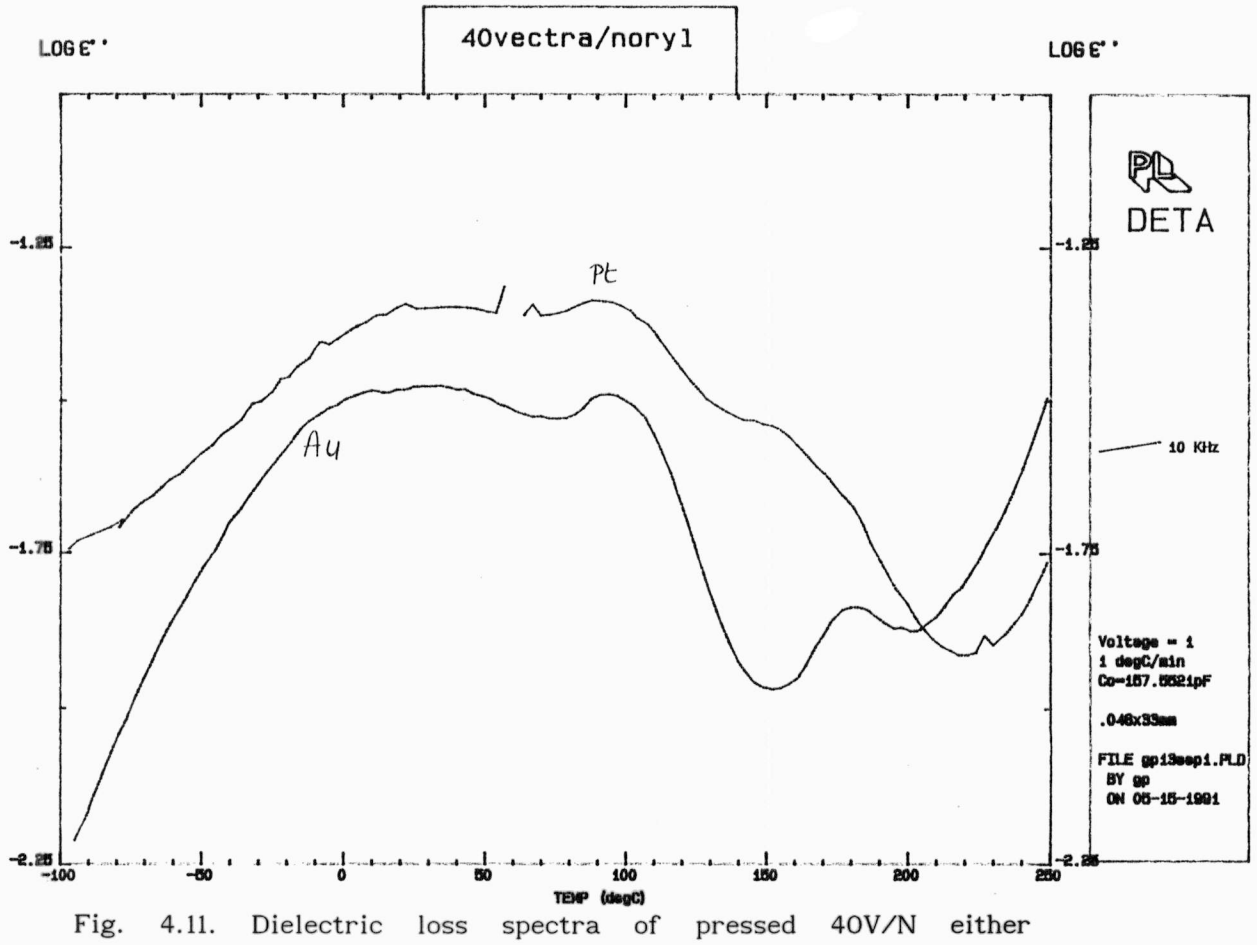


Fig. 4.11. Dielectric loss spectra of pressed 40V/N either sputtered with platinum or using gold at a frequency of 10 kHz.

respectively 10V/N perpendicular and parallel to the extrusion direction and 40V/N perpendicular to the extrusion direction. Photo 3 has been pressed after extrusion. Also in the case of V/N, no differences between pressed and extruded samples can be observed. It can be seen that fibers are formed, the surfaces of which are smooth. The fibers are all pulled out of the matrix. In photos 2 and 3 the fibers at the edge are smaller than those in the centre of the sample. This can be explained by the fact that the shear stress to which the extrudate is subjected is larger at the surface of the extrudate than in the middle.

In photo 2 also the break-up of Vectra threads is nicely demonstrated. Since this phenomenon is not a subject of this study, one is referred to Elmendorp (1986) for details. From photo 3 it becomes clear that the Vectra fibers are quite long. In some cases they can even be seen with the bare eye.

At higher concentrations of Vectra in Noryl lamellae instead of fibers are formed (photo 4).

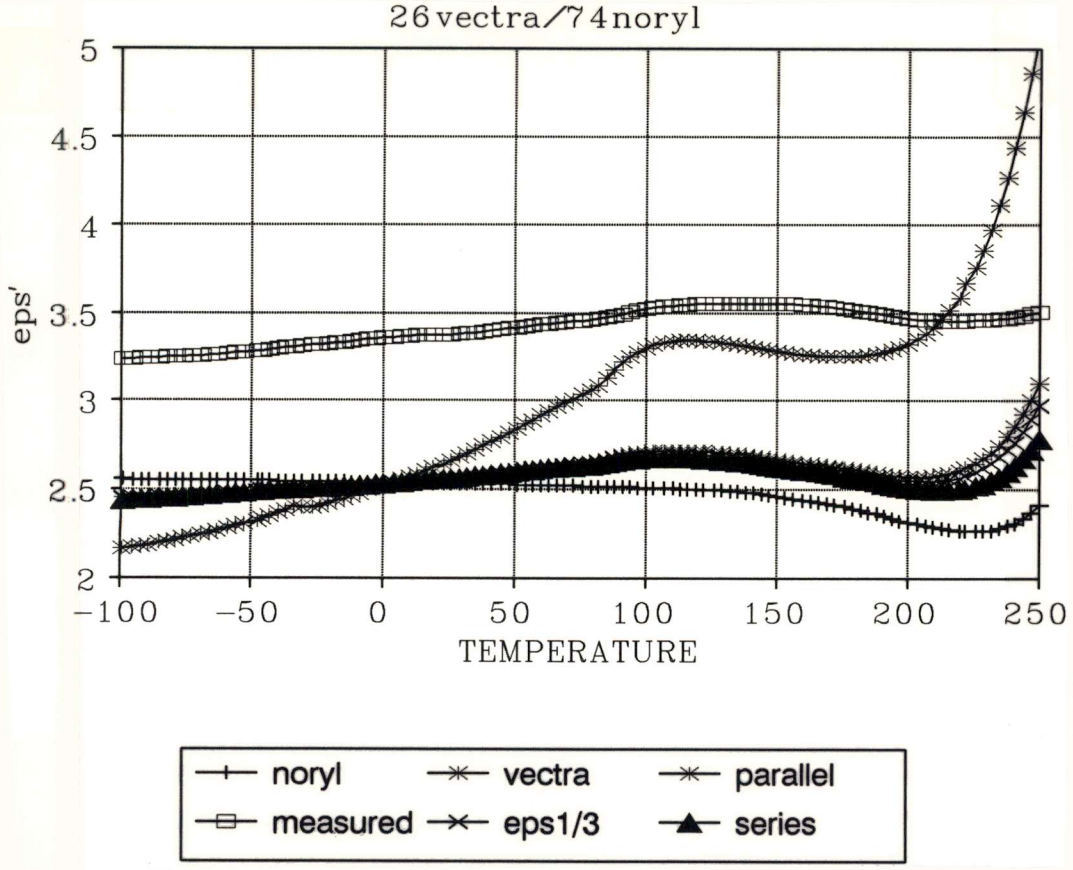


Fig. 4.12. Measured and calculated dielectric storage of 40V/N. For comparison, V and N are added. (f = 0.1 kHz.)

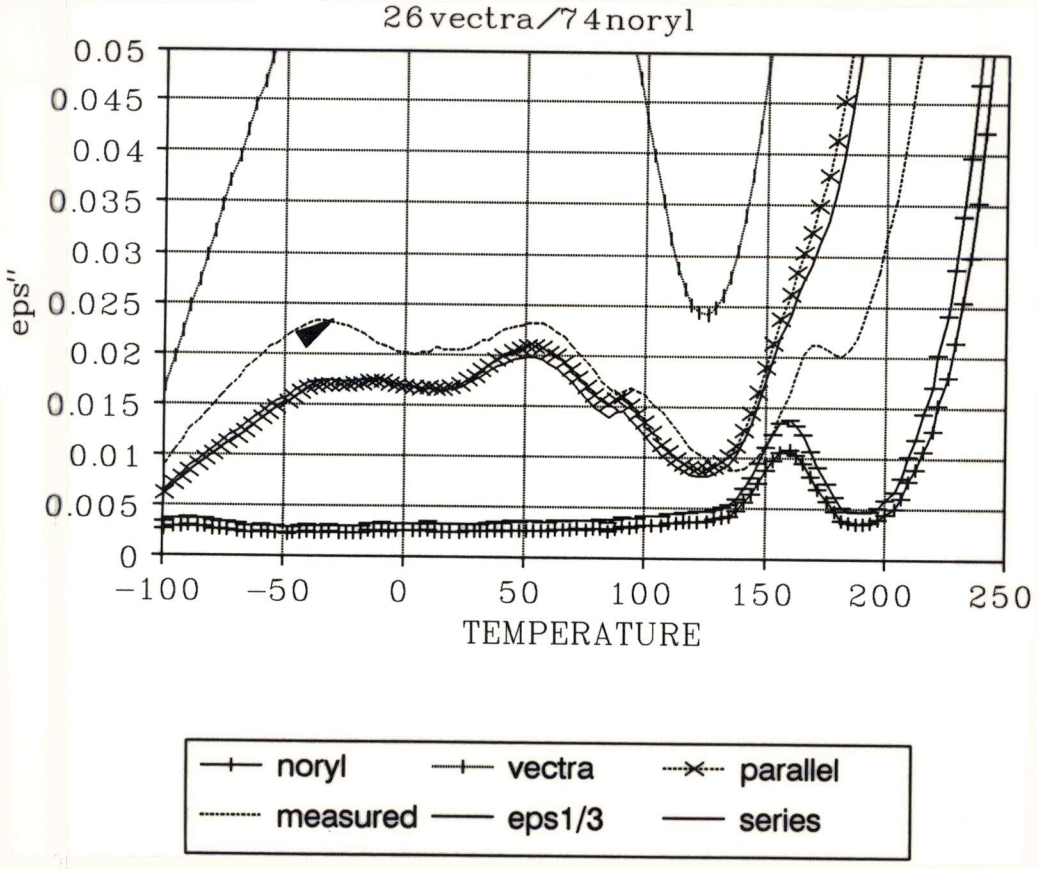


Fig. 4.13. Measured and calculated dielectric loss of 40V/N. For comparison, V and N are added. (f = 0.1 kHz.) The black triangle indicates the measured value.

# 5 DISCUSSION

## 5.1 Dielectric relaxation experiments

### 5.1.1 Temperature scans

In all temperature scans certain common characteristics can be seen.

* With increasing frequency all transition temperatures increase as well. This behaviour is not surprising. It is predicted by equation (2.4) for the $\alpha$-transitions and by (2.5) for the lower temperature transitions.

* With increasing frequency not only the temperatures of the $\beta$ and lower relaxation peaks increase, but also the loss increases. The peaks overlap each other and tend to become one at very high frequencies.

* At higher temperatures (above $T_g$ in most cases) the loss increases rapidly. This effect is generally attributed to the presence of conducting particles, impurities say. In the theory of dielectrics, conducting particles are generally referred to as free charges. Above the glass transition temperature the free charges become much more mobile (because the free volume is much higher) and thus get the possibility to migrate from one to the other electrode. This occurs more easily when a low frequency is applied since in that case the charges is given more time to migrate. This behaviour was also predicted in chapter 2.

In some measurements more particular phenomena occur.

* The height of the $\alpha$-peaks of the matrix polymer decreases with increasing frequency. This phenomenon can be explained as follows. At these temperatures the gross loss value consists both of the $\alpha$ loss peak and the conductivity. With increasing frequency the conductivity contribution begins at higher temperatures. Combining these two facts, it is not hard to understand that the height of the $\alpha$-peak diminishes with decreasing conductivity. What makes the explanation tougher, however, is the fact that this phenomenon

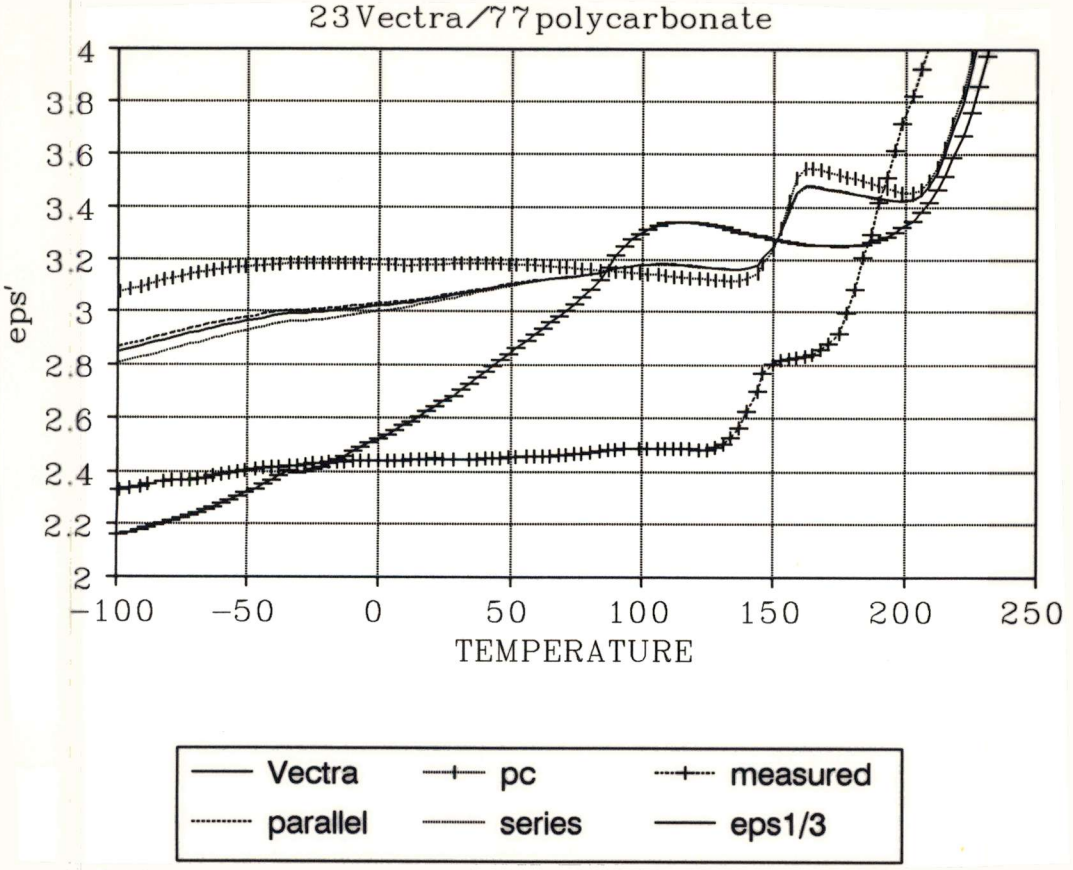


Fig. 4.14. Measured and calculated dielectric storage of 40V/PC. For comparison, V and PC are added. (f = 0.1 kHz.)

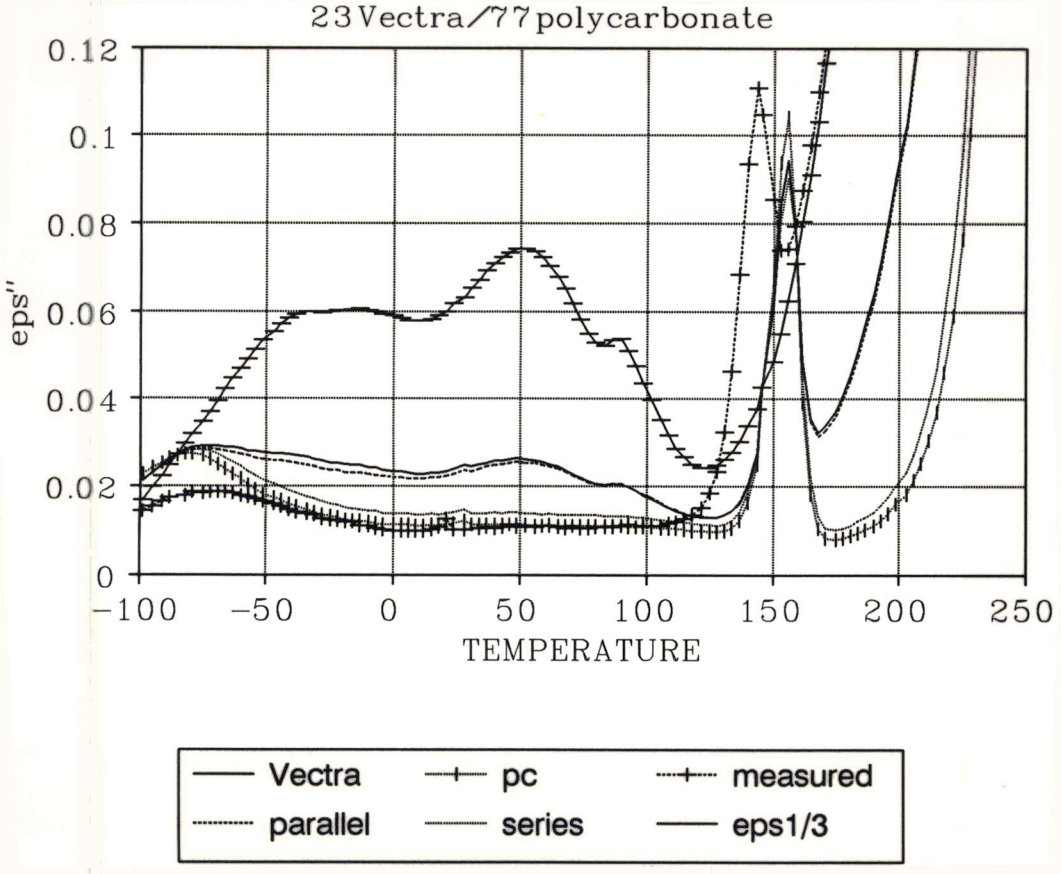


Fig. 4.15. Measured and calculated dielectric loss of 40V/PC. For comparison, V and PC are added. (f = 0.1 kHz.)

does not occur in PC, 10V/N and 20V/N. In these cases the conductivity shows up at more elevated temperatures. An explanation for this delayed appearance was not found.

* At the beginning of the temperature measurements at -100 °C all loss values are more or less equal.

In some cases however at high frequencies the loss has a higher value (confer fig. 4.1). The combination of low temperatures and high frequencies is exactly the opposite of the combination required for conductivity. This effect may be due to an extra impedance layer which might have been caused by bad contact between the electrode and the sample. This can be represented schematically by the following model, see fig. 5.1.

In many cases the V/N measurements show a very high loss at low and intermediate temperatures and high frequencies. The Noryl and Noryl blends may suffer from high internal stresses which cause these high losses. When a polymer is subjected to internal stresses, the main chains and side chains lack the space to rearrange themselves. They cannot follow the alternating frequency as fast as a relaxed polymer. This leads to greater phase differences and thus to higher losses, see fig. 2.3. This assumption will be discussed with the help of other results later. The V/N scans are of less quality than those of the V/PC blends.

In both cases the presence of the Vectra becomes clearly visible in the 30V/N or 30V/PC blends. It could be that in the case of DETA measurements a volume percentage of about 20 % is needed to distinguish the LCP in the thermoplastic matrix clearly. Nonetheless, the presence of Vectra is more pronounced in the V/N data than in the V/PC data. This is likely because $\varepsilon''$ of N is lower in this temperature region.

When figs. 4.1 and 4.2 are reconsidered now many of the above described phenomena can be recognized. What becomes clear in fig. 4.1 is that Vectra possesses two sub-$T_g$ relaxations, referred to as the $\beta$ and the $\gamma$ relaxation of Vectra. What can also be seen is that the $\alpha$ dispersion peak is very small. For the rearrangement of

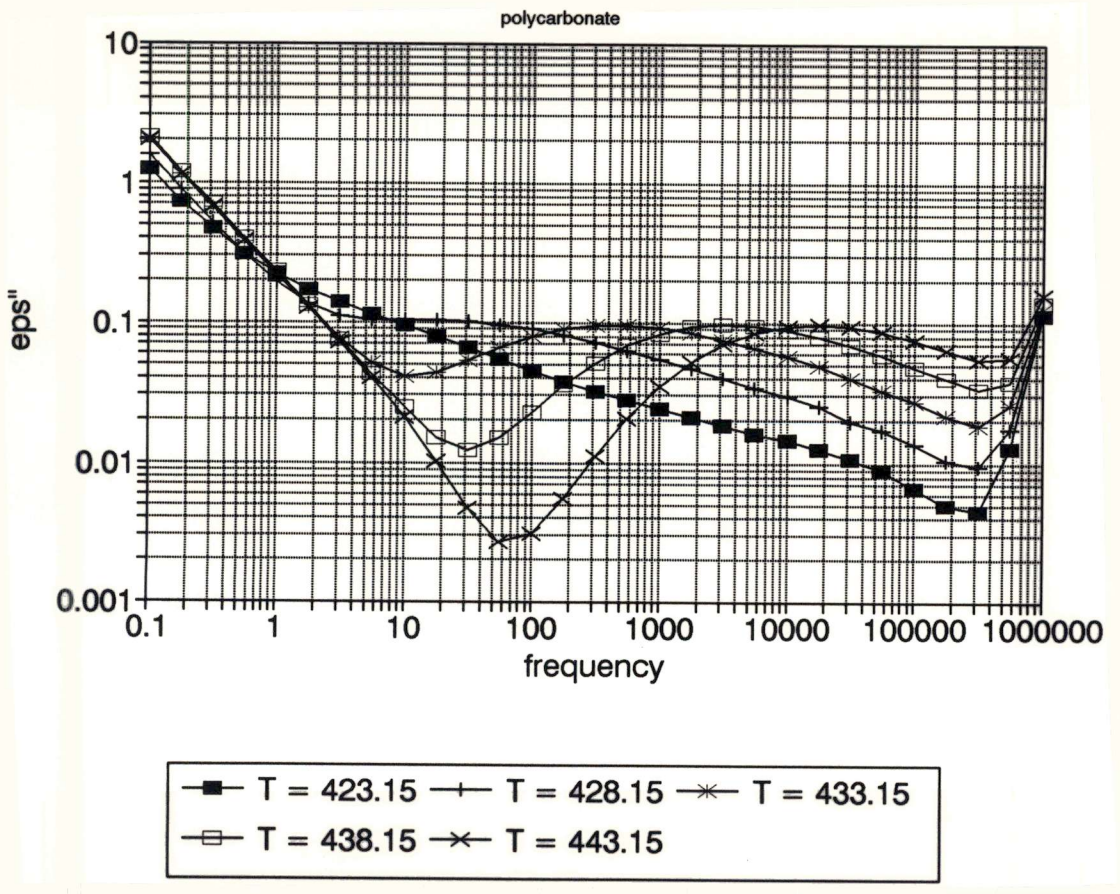


Fig. 4.16. Dielectric loss vs. frequency at various temperatures for PC.

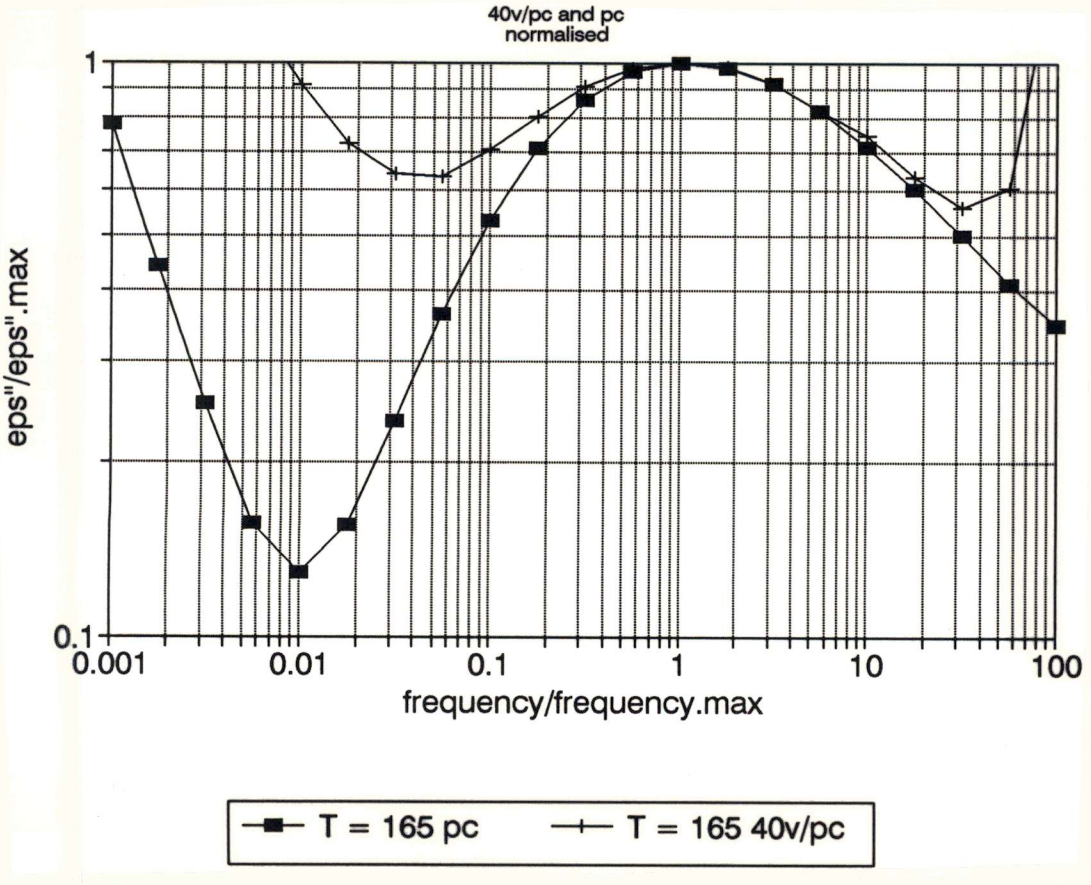


Fig. 4.17. Normalized loss curves of 40V/PC and PC at a temperature of 165 °C.

the main chain (Vectra is a main chain LCP!) only minor motions are necessary. In literature it is not yet clear which motion induces the glass-transition of Vectra. Moreover, Vectra is a semicrystalline polymer with a small amorphous fraction. In this graph is also nicely demonstrated that the β-peak "overtakes" the α-peak at high frequencies because of the much greater temperature shift of the β-peak. We also see that the α-peak almost remains at the same temperature when the frequency varies. This can be explained as follows. The α-peak lies in fact "in the domain" of the β-peak, see fig 5.2. The β-peak has already passed its maximum, so it is a descending curve. Because of this, the resulting α-peak will have a maximum which lies at a lower temperature. At higher frequencies, both the α- and β-peaks shift towards higher temperatures. But, since the temperature dependence of the β-peak is greater, this will only result in a minor shift of the gross α-peak towards higher temperatures.

In fig. 4.1b it appears that the storage increases rapidly at high temperatures and low frequencies. Under these conditions it is very easy for the dipoles to follow the alternating field. The phase angle will be small and the storage will be higher, see fig. 2.3.

All the observations made with respect to the Vectra results can be found back in literature. The measurements of Alhaj- Mohammed et al. (1988) reveal three relaxation processes at frequencies below 0.1 kHz, the values of which correspond very well to the values found in this report, e.g. $T_{\beta}$ = 53 °C in literature and 51 °C measured at a frequency of 100 Hz. At the same frequency the α-temperature corresponds exactly to the literature value. It is the view of these authors that the dielectric activity arises from the dipole moment of the ester linkage between the aromatic rings. Hummel and Flory (1980) pointed out that the motion of the ester group is dominated by motion of one of the aromatic groups to which it is attached. It is found by several authors that the β- and γ-processes are associated with the HNA and HBA moieties, respectively. The results of Alhaj-Mohammed et al. have been confirmed by Kalika and Yoon (1991).

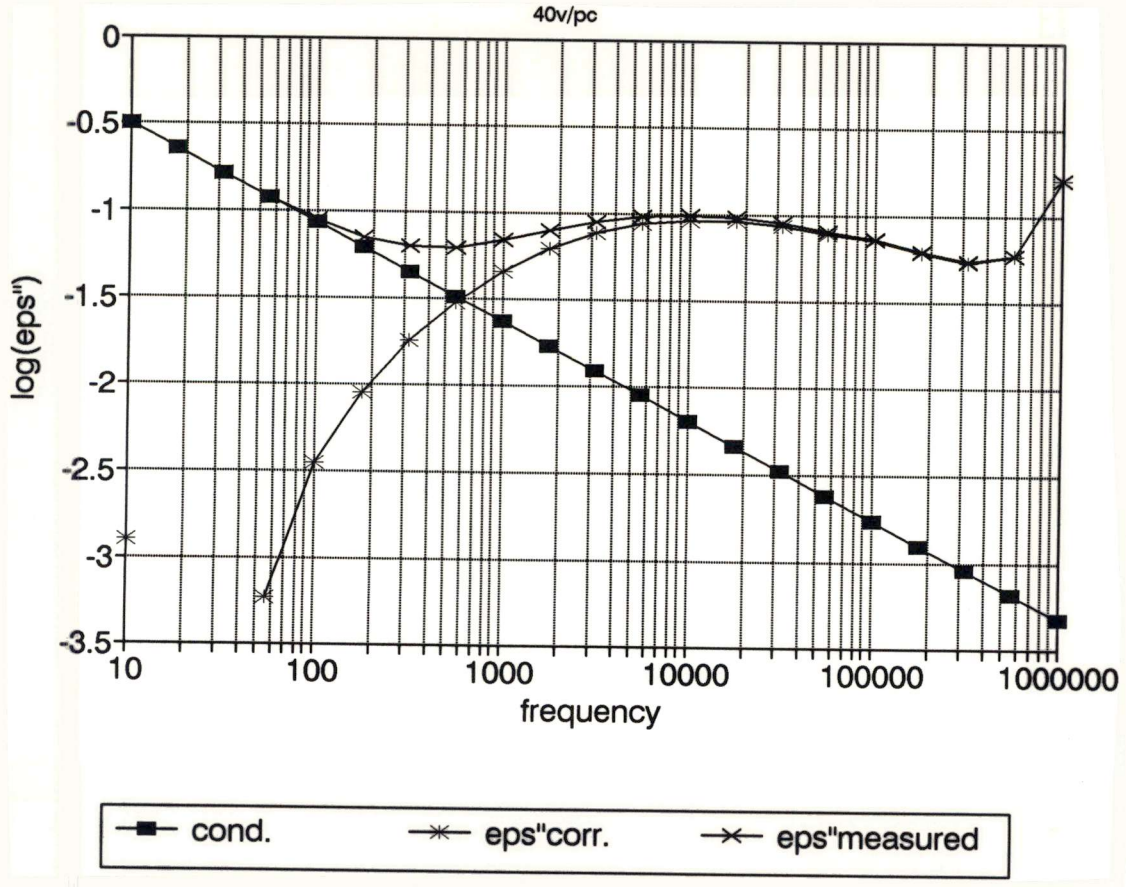


Fig. 4.18. Subtraction of the conductivity from the loss curve of 40V/PC

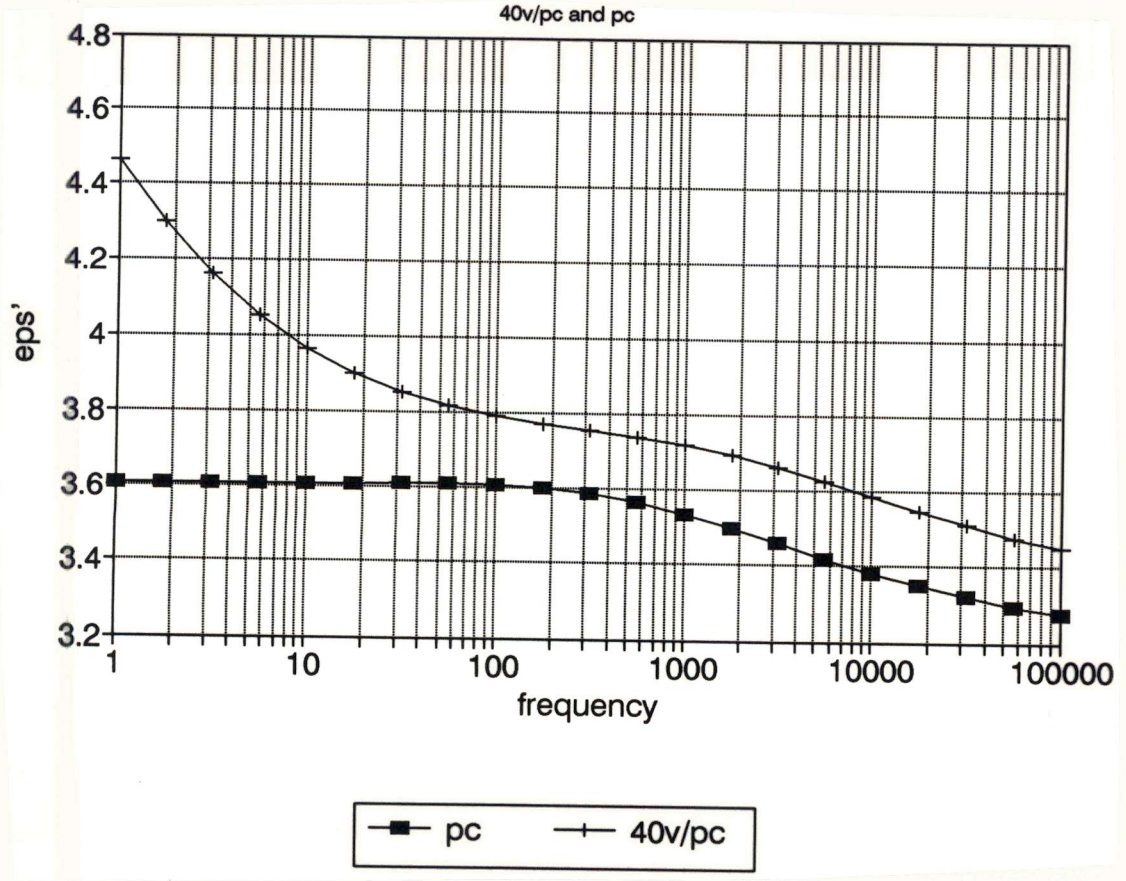


Fig. 4.18a. Dielectric storage as function of the frequency for PC and 40V/PC.

When fig. 4.2 is examined the same transitions as pointed out in Vectra can be seen. In addition the $\alpha$-peak of Noryl appears the loss of which is not as high as the $\gamma$- and $\beta$-loss of Vectra.

With regard to fig. 4.3 and 4.4 (comparison of the different compositions of V/PC) one could state that the $\beta$ relaxation peak of PC differs in temperature when different amounts of Vectra are added. There seems, however, not to exist a relation between the vol.% of Vectra added and the $\beta$-temperature. The $\beta$-relaxation of PC is attributed to the motion of the carbonyl group (McCrum et al., 1967). At the same time a relation between the amount of PC in the blend and the height of the $\beta$ relaxation of PC is expected. This relation cannot be found. This is probably due to the fact that all V/PC measurements do not start at the same loss level because of variations in thickness, sputter quality etc. In this context it is noteworthy to remark that the log($\varepsilon$") values of a material of the same composition (5V/PC say) at certain temperatures differed a value of 0.25.
When Vectra is added to PC, the dielectric loss increases strongly at temperatures above the $\alpha$-relaxation of PC. This effect is most likely due to conduction. So, it can be stated that the second component facilitates the conduction. This effect will be explained in more detail when fig. 4.13 is discussed. The effect is not so clear when the storage is taken into account. This can be explained by the fact that conduction does not lead to additional charge storage.
We also see that the $\alpha$-peak of PC shifts in temperature as function of the composition. From table 4.2 it can be seen that the $T_{\alpha}$ of V/PC blends shifts slightly towards lower temperatures with higher volume percentages of Vectra. This behaviour might indicate partial miscibility between the two components. However, the effect is hardly visible and might even be considered as coincidental when the accuracy of the measurements is taken into account.

From figs. 4.5 and 4.6 (V/N) it becomes clear that the measurements which contain higher percentages of Vectra give most

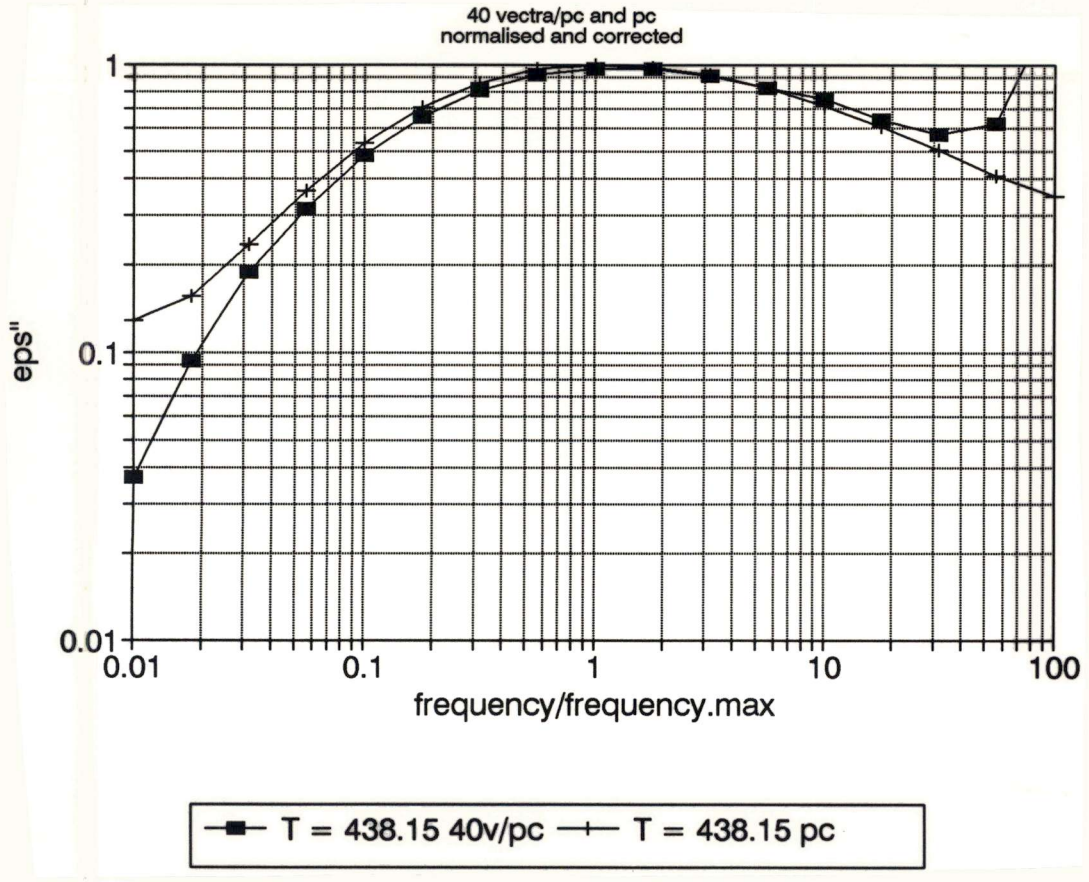


Fig. 4.19. Normalized and corrected loss curves of 40V/PC at a temperature of 165 °C.

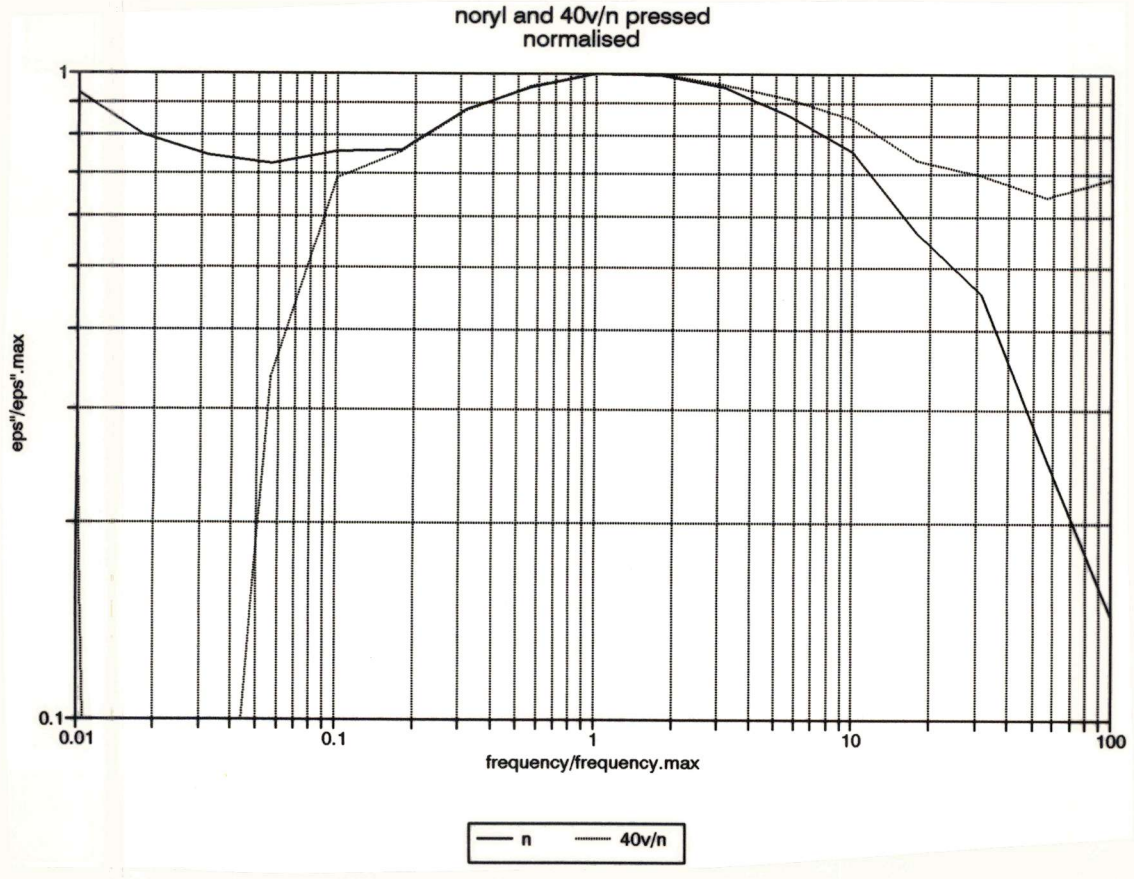


Fig. 4.20. Normalized loss curves of 40V/N and N at a temperature of 170 °C.

information because of their smoothness. One can clearly distinguish the three transitions in Vectra: even the α-transition is visible at 0.1 kHz. At 10 kHz it has been overtaken by the β-transition of Vectra. The values from table 4.3 show a strange behaviour: the α-transition does not decrease, but rather increases. The conjecture arises that the extrusion has induced a small phase separation. This would account for the relatively high α-peaks. These may be governed by the PPE moieties in the Noryl. Stoelting et al. (1970) have also found that blends of PPE and PS are not completely miscible at a molecular level.

Figs. 4.7 and 4.8 offer the possibility to compare platinum coated with gold coated samples on the one hand and pressed and extruded samples of PC on the other hand. Platinum coating shows a higher surface impedance than gold coating. Indeed this effect is more pronounced at 10 kHz than at 0.1 kHz. It causes an unwanted, uncontrolled extra loss.
The differences between pressed and extruded PC samples become visible at temperatures between 0 and 100 °C. The pressed samples show a somewhat higher loss. In fig. 4.9 (20V/PC) it can be seen that the loss of platinum coated samples is higher. This is the case around 120 °C. This observation gives reason to some prudence. McCrum et al. (1967) report on an "intermediate temperature" relaxation between the α- and β-relaxation in PC. It is not observed in well annealed specimens, but it is observed in oriented specimens. Though both samples have been pressed and cooled down in the same manner, the thermal treatment might be a critical factor. In fig. 4.9 also a shift of the β-peak can be seen. According to McCrum et al. this can also be caused by the thermal history. Figs. 4.10 and 4.11 also show higher losses when platinum electrodes have been applied. A strange inconsistency comes up here. If the higher loss using Pt electrodes is caused by a higher surface impedance, one would expect the effect to be more pronounced at the highest frequency. It is speculated that other factors account for the difference. What becomes very clear from these two figures is the loss of information when platinum electrodes are applied. In fig. 4.10 the α-peak of Vectra can not

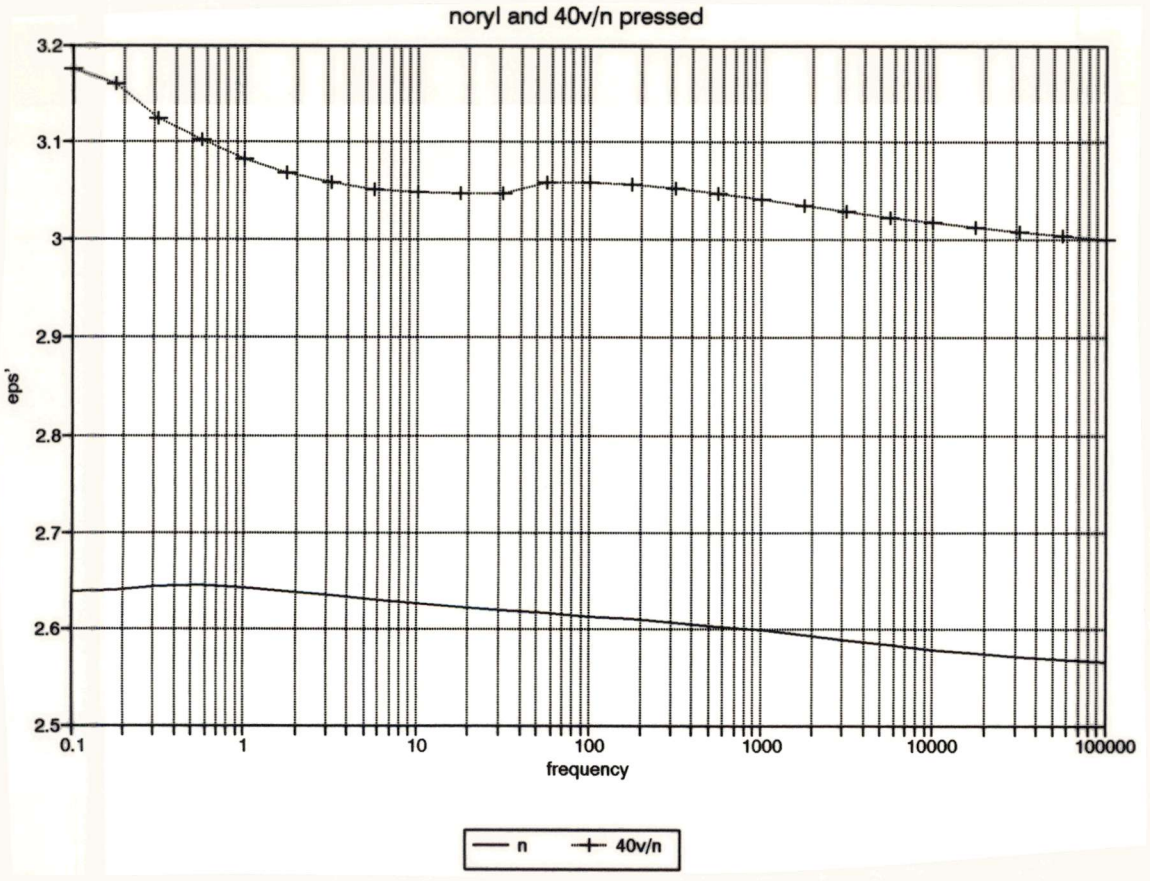


Fig. 4.20a. Dielectric storage as function of the frequency for N and 40V/N.

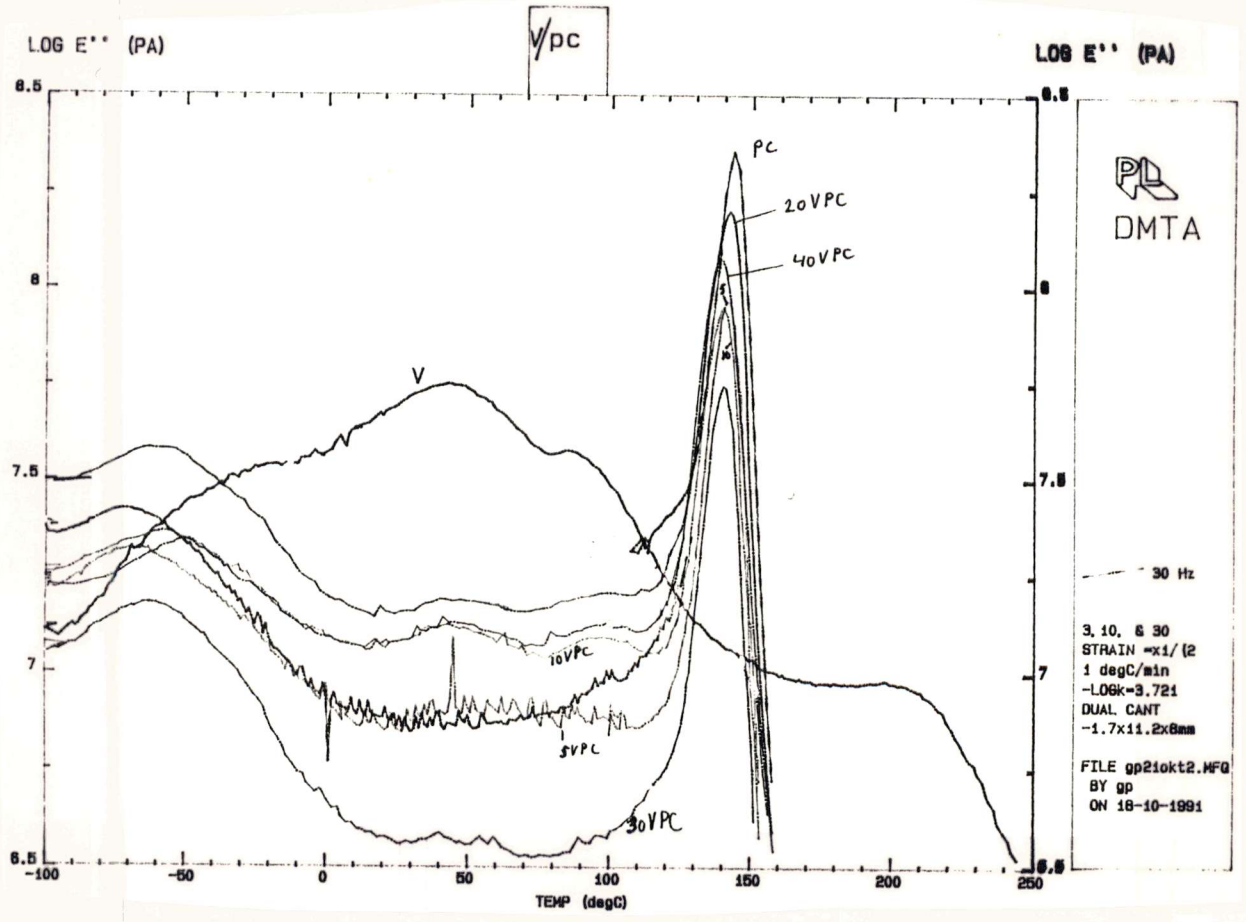


Fig. 4.22. Mechanical loss spectra of V/PC blends at different composition ratios at a frequency of 30 Hz.

be determined using platinum and similarly in fig. 4.11 the α-peak of Noryl cannot be determined (only a shoulder can be seen).

In fig. 4.12 the measured ε' values lie higher than the "calculated" ε'.It is too easy just to state that the mixing of the two polymers induces a higher storage of energy at all frequencies. It could be that ε' was determined not so well. Another difference is the clear increase in ε' at very high temperatures (above the α temperature of Noryl) in the calculated curves. In the measured curve this increase is much less. Noryl obstructs the dc conductivity of Vectra so the linear addition (2.23) cannot be applied in this case. The series model (2.24) is more alike in this situation. Using this model, the increase in ε' is less and resembles the measured curve better.

When ε" is plotted as function of the temperature (fig 4.13) some agreement between the calculated -using (2.23) and (2.26)- and measured curves can be seen. All Vectra relaxations are present in both curves. At lower relaxations the loss values of the measured data are somewhat higher. Besides the γ-peak of Vectra is more pronounced. The α-relaxation of Noryl is not visible in the calculated curves. Only a shoulder can be seen in the curve of the $\varepsilon^{1/3}$ formula. The series formula is not applicable now since the Noryl dominates here. From the measurements of the single components it can be seen that the conductivities are so high that the α-relaxation falls away completely when a curve is calculated from the data of the components by linear addition. This must mean that conduction gets less chance in the blend than in the single components.

The results for V/PC show in more than one aspect another picture. Fig. 4.14 shows that the measured ε' values lie lower than the calculated ε' values, except at high temperatures. It was seen before that this might be due to the fact that ε' was not dtermined too accurate. At temperatures above the glass transition of PC, however, the measured storage becomes higher than the calculated storage. This effect may be due to interfacial polarisation. In this case the free charges accumulate at the interfaces. This results in an increase of ε'.

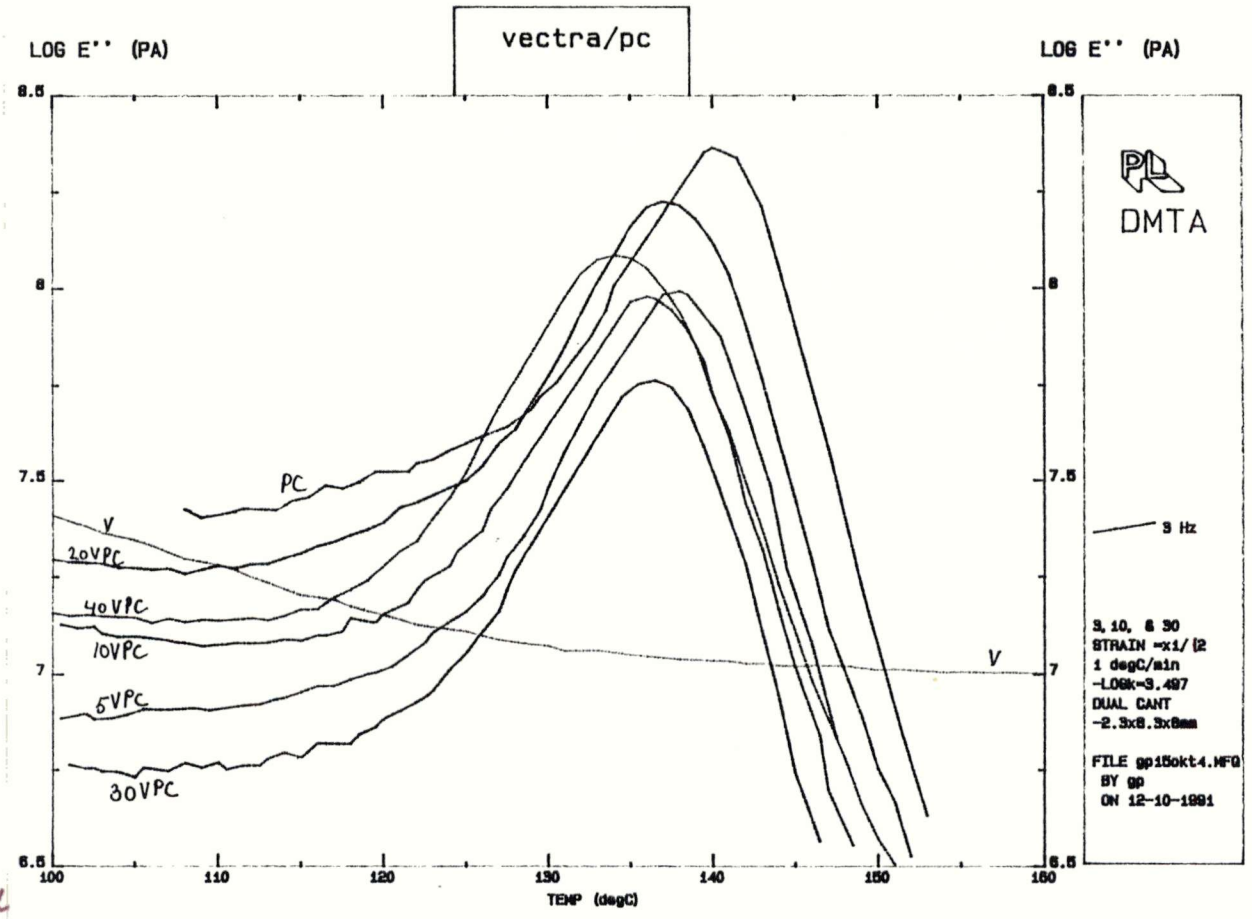


a

Fig. 4.21. Mechanical loss (a) and storage (b) spectra of V/PC blends at different composition ratios at a frequency of 3 Hz. Only the α-loss is considered.

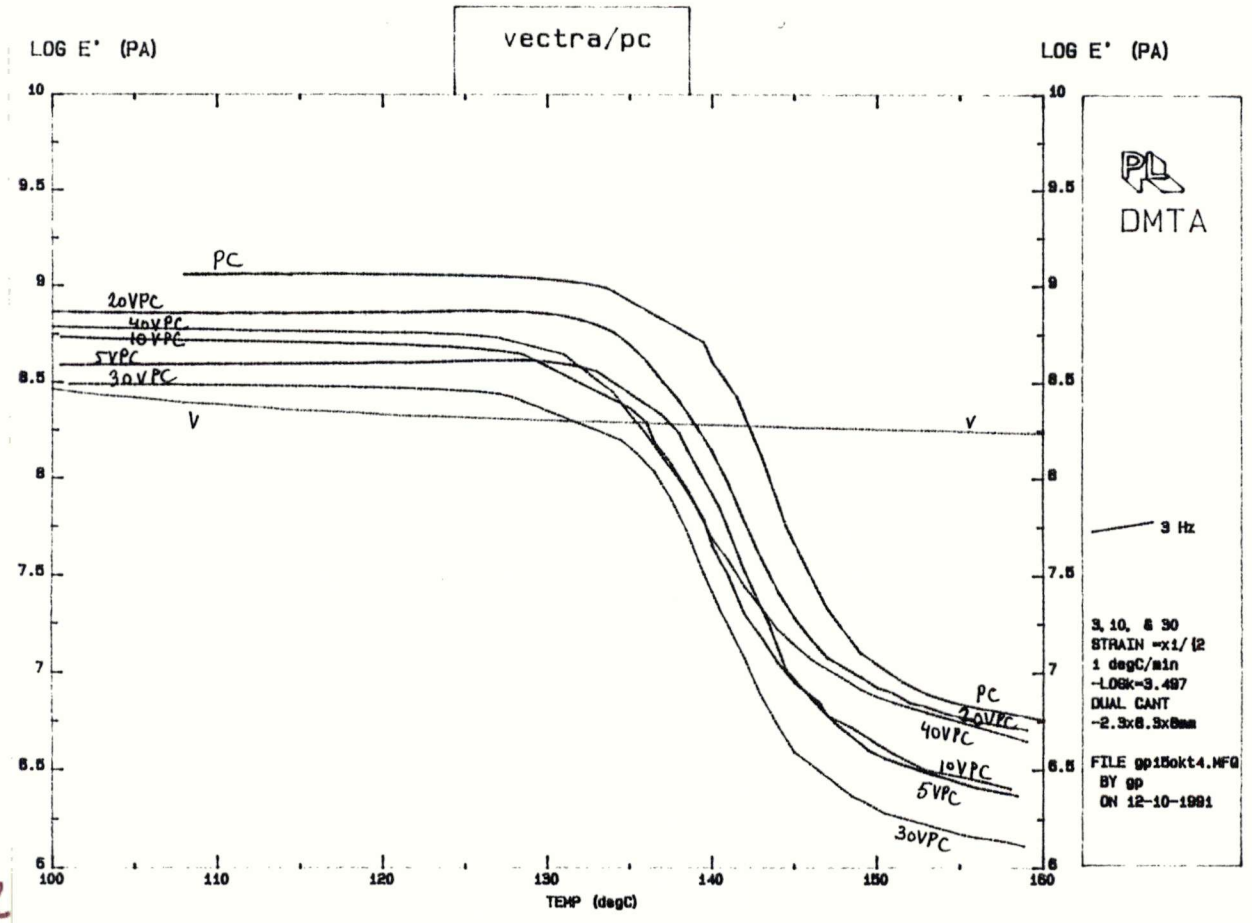


b

Fig 4.15 (ε" vs temperature of V/PC) shows also some interesting effects. At temperatures below 100 °C the measured ε" lies below the calculated ε". At higher temperatures, however, the measured ε" has a higher value, which means that the conductivity current gets more chance in the blend than in the single components. This is just the opposite behaviour to what was seen in the V/N blends. It is obvious to assume that the second phase facilitates the flow of the current. This effect was also found in figs. 4.3 and 4.4. It is speculated that specific interactions between the Vectra and the Polycarbonate facilitate the flow of the current. Those interactions are likely regarding the molecular structure of the two components. It is well known that double bonds and naphtalene groups can conduct the electrical current better (Kalika and Yoon, 1991). If interactions between the carbonyl group of the polycarbonate and the HNA moiety of the Vectra can exist - and this is likely according to Hummel and Flory (1980) -, this might be a possible explanation. Rellick and Runt (1986) put forward the possibility that one component provides charge carriers to the other component. This possibility will not further be discussed.
The additional increase of ε" may, however, also be explained by interfacial polarisation. This explanation is in accordance with the increase in ε' at elevated temperatures (fig. 4.14).
The α-transition of PC in the blend is shifted towards lower temperatures in comparison to that of pure polycarbonate. Several authors have indicated this as a very important criterion to assess the miscibility of a blend (Poolman, 1991). A shift of the α-peaks towards each other, albeit small, indicates partial miscibility in this concept. A slight shift towards lower temperatures has also been found earlier in table 4.2.
Especially the β-relaxation of polycarbonate is well detectable in the measured curve. The β- and the α-relaxation of Vectra cause more problems. As seen before this is caused by the fact that these relaxations are much smaller in comparison to PC than in comparison to Noryl.

### 5.1.2 Frequency scans

In fig. 4.16 it appears that the slopes of the measured curves at

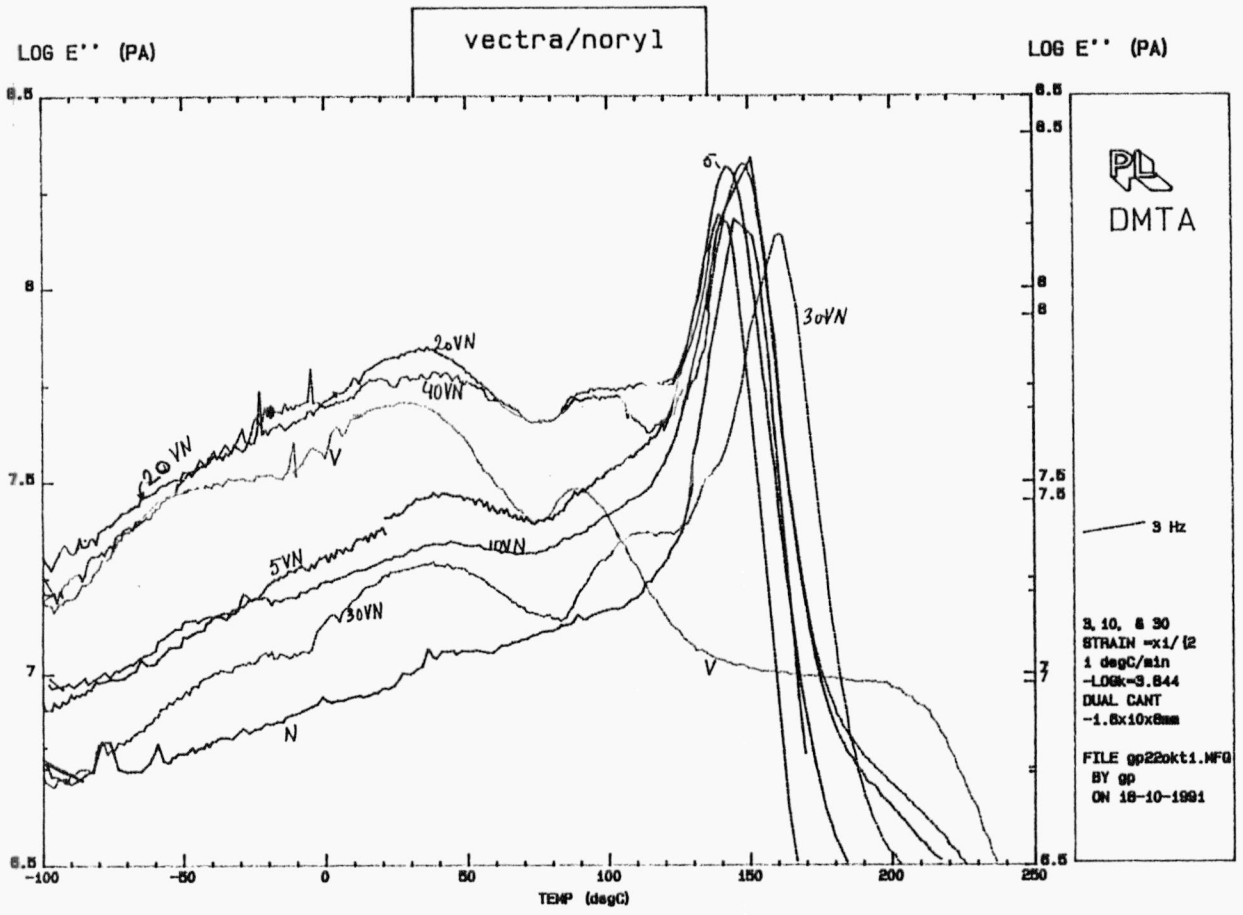


Fig. 4.23. Mechanical loss (a) and storage (b) spectra of V/N blends at different composition ratios at a frequency of 3 Hz.

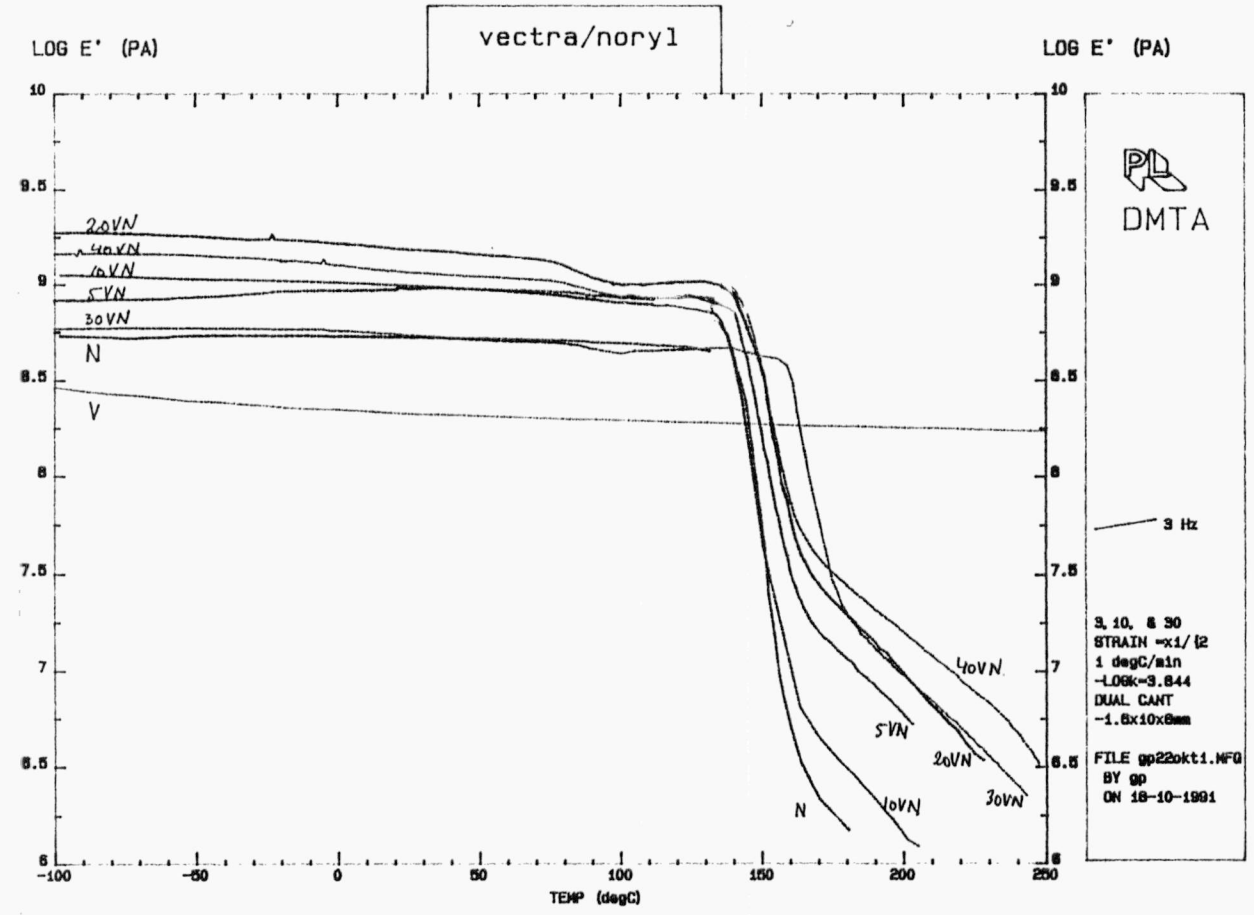

low frequencies have the value of approximately 1. Here is question of pure conduction as was discussed in chapter 2. The corresponding ε' remains at a constant level, see fig. 4.18a.
In fig. 4.17 the peak of 40V/PC seems to be broader than the peak of PC. Applying the concept Rellick and Runt (1986) use one could state that partial miscibility occurs. What is meant by partial miscibility in this case is shown in fig. 5.3. However, a few restrictions must be made. The 40V/PC peak appears to be somewhat broader on the high-frequency side but much broader on the low frequency side. What adds to this broadening is some contribution at low frequencies. Considering the slope of -0.5 and the fact that the corresponding ε' does not remain constant (fig. 4.18a), this contribution is not believed to be due to conductivity. It is supposed to stem from interfacial polarisation. The likeliness of this phenomenon to occur was discussed before. So, in fact the interfacial polarisation rather than the conductivity is subtracted in fig. 4.18. Bearing this in mind, the curve resulting after subtraction can be seen in fig. 4.19. The resulting curve of 40V/PC is even narrower now at low frequencies. Considering the restrictions made above, one has to be careful in drawing a firm conclusion in this particular case.

From fig. 4.20 it can be seen that the Noryl peak is smaller on the high frequency side. On the low frequency side the Noryl peak has the same value as the 40 V/N peak. When the contribution of the conductivity is subtracted, the Noryl peak will also be smaller on this side. Yet it is strange that the contribution of conductivity is more pronounced in Noryl. It is speculated that this effect is due to phase separation in Noryl. In fig. 4.20a there seems to be an extra increase in ε' of 40V/N at low frequencies. This effect is also attributed to interfacial polarisation in the V/N blend. Note that ε' of Noryl still increases slightly with decreasing frequency while PC (fig. 4.18a) remains constant. This could be due to some interfacial polarisation in Noryl.

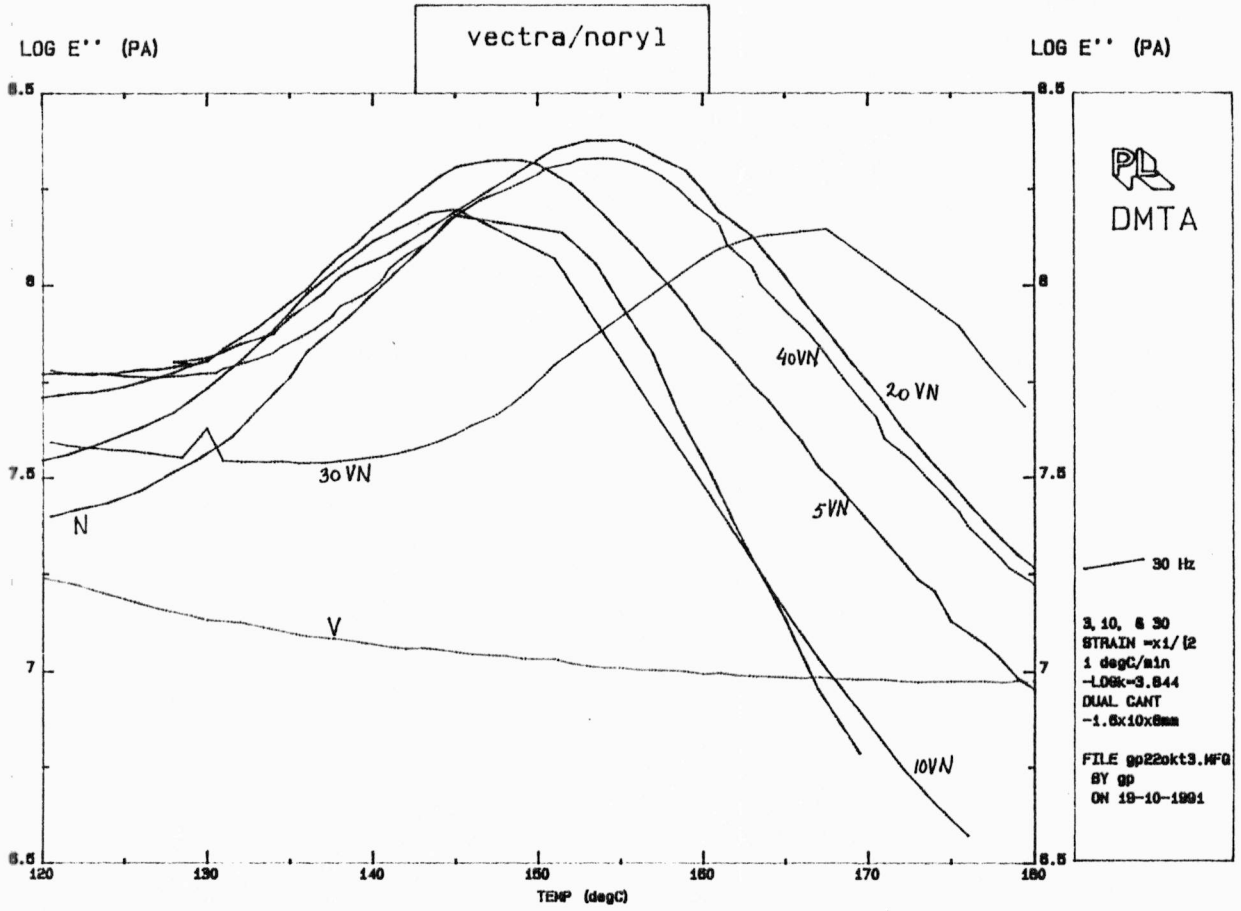


Fig. 4.24. Mechanical loss spectra of V/N blends at different composition ratios at a frequency of 30 Hz. Only the α-loss is considered

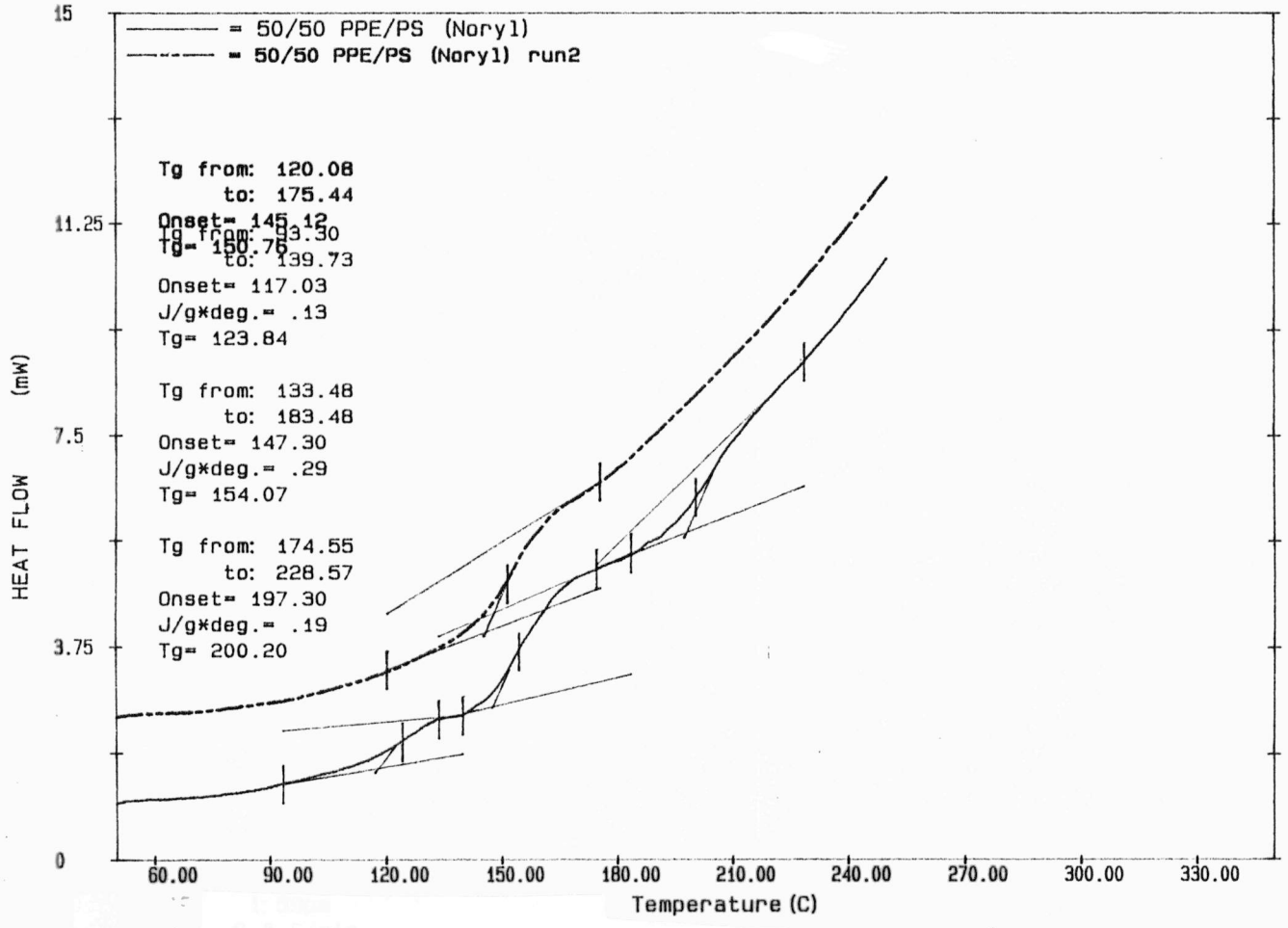


Fig. 4.25. DSC trace of two different runs of Noryl.

## 5.2 Mechanical relaxation experiments

First, some general characteristics of the DMTA scans will be discussed. It is tried not to refer to the DETA measurements because for this comparison an apart subsection is reserved.

* The DMTA measurements showed a somewhat shivery path. The reason for this behaviour may be a slight instability of the vibration which is imposed on the sample.
* The $\alpha$-peaks of the matrix polymers are equal in height at various frequencies. This agrees with the theoretical expectations.
* Sub $T_\alpha$ relaxations can be observed clearly, also at lower concentrations of the Vectra.

Fig. 4.21 and 4.22 show that the $\beta$-peak of PC and the $\beta$- and $\alpha$-peak of Vectra (the latter can hardly be discerned) remain at a fairly constant temperature at the different composition ratios. The peaks differ in height. There is no relation between the loss peak height and the composition. This holds both for the $\alpha$- and the lower relaxation peaks. The $\alpha$-transitions of PC shift a bit towards lower temperatures with increasing volume percentage Vectra. This is further visualised in table 4.5. From this table we notice that the $\alpha$-relaxation temperature of PC decreases when the volume percentage Vectra in the blend increases. (The value of 12.8 vol.% Vectra (20V/PC) is an exception.) As mentioned before, this might indicate partial miscibility of the two components. See fig. 5.4.

Table 4.5 summarises the values of the different relaxation peaks. it can be seen that the value of the $\beta$-relaxation temperature of PC increases in temperature with the Vectra content. This is a clue indicating specific interactions between Vectra and PC. Especially the value of -50 $^{o}$C seems somewhat high. This transition is suspected to be a combination of the $\beta$-peak of PC and the $\gamma$-peak of Vectra. The $\beta$-peaks of Vectra are fairly constant with temperature. The higher values of the $\alpha$-peak of Vectra are quite easy to explain. The $\alpha$-peaks of Vectra belong already to the "domain" of the sharp and high $\alpha$-peaks of PC. This

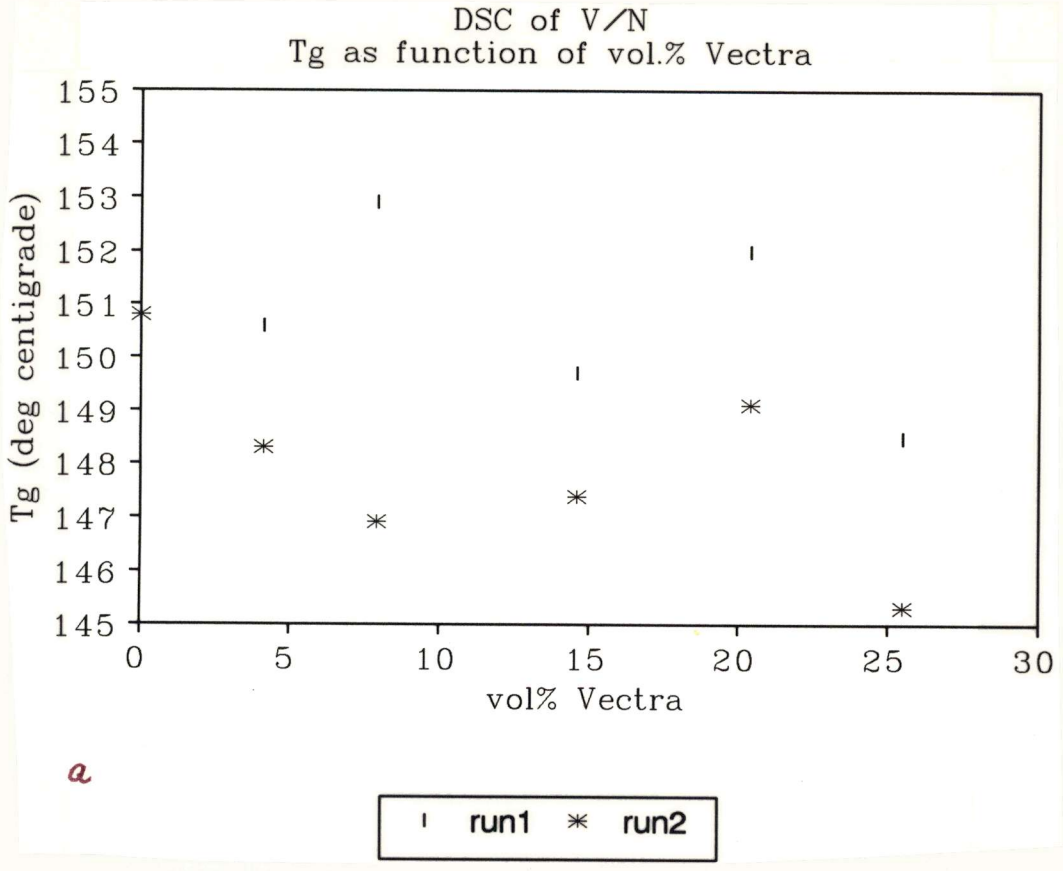


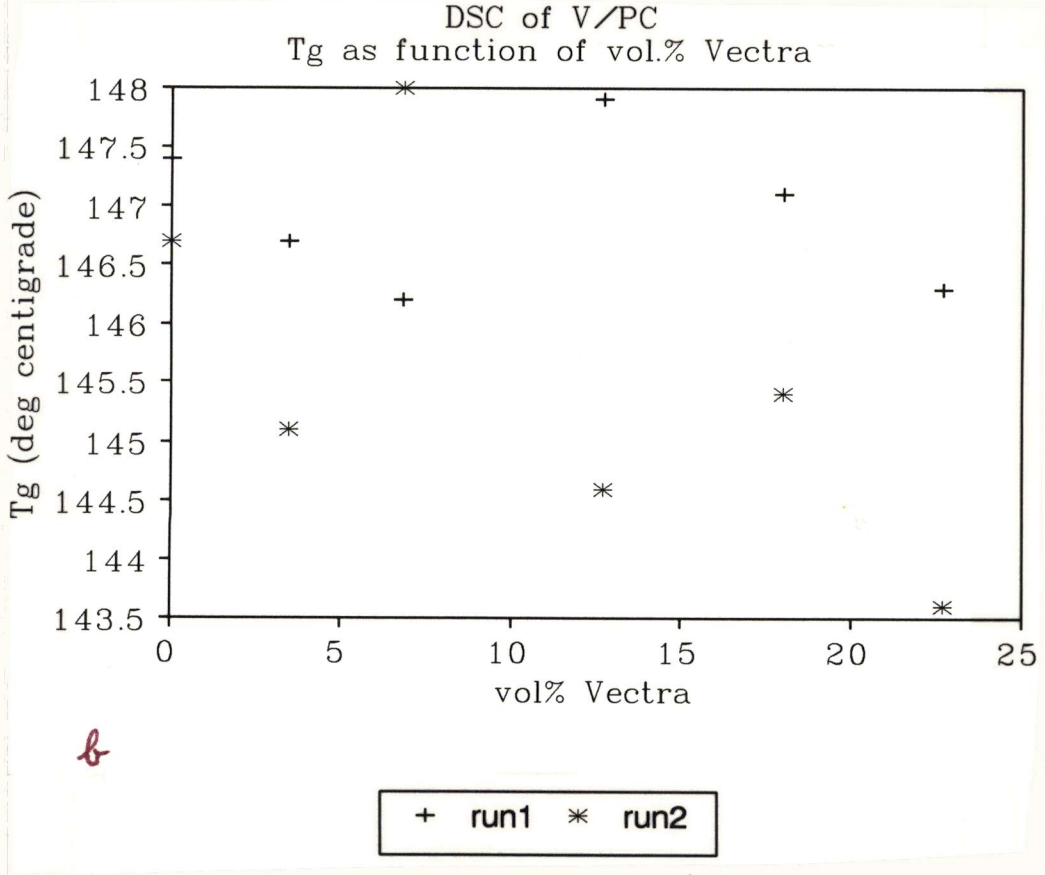


Fig. 4.26. $T_g$ as function of vol.% Vectra: (a) V/N, (b) V/PC.

means that the resulting peaks lie at a higher temperature. This behaviour was seen before in the case of the α-peak of the Vectra lying in the "domain" of the β-peak of the Vectra. In this case the resulting α-peak of Vectra shifted towards lower temperatures, see fig. 5.2.

Fig 4.23 and 4.24 show that the mechanical losses of 5V/N and 10V/N lie at a considerable lower level than the other compositions. Furthermore, the β-peaks of Vectra are rather constant in temperature, as was expected. The γ-peak of Vectra can hardly be discerned. Just as was the case with the V/PC measurements the α-peak of Vectra manifests itself at a somewhat higher temperature when Vectra is blended with Noryl. The temperature of the α-peak of Noryl as function of the composition shows a very strange behaviour (table 4.6). With increasing vol.% Vectra the α-temperature increases, but remains constant at higher volume percentages. Again, the impression forces itself that some minor phase separation has taken place in Noryl. The $T_\alpha$ of Noryl in table 4.6 shows excellent agreement with the $T_\alpha$ found by Stoelting et al. (1970).

### 5.3 Differential Scanning Calorimetry

Calorimetric measurements have been performed during two heating runs. In almost all measurements, the $T_g$ of the second run lies at a lower temperature than the $T_g$ of the first run. This can be explained as follows. The samples of the first run have been extruded which means that they contain a certain amount of stress. After having been heated and cooled down again the polymer molecules have had enough time to rearrange somewhat. They have had the opportunity to relax.

A very interesting phenomenon occurs in the Noryl and the 40V/N samples. The first run shows three $T_g$'s while the second run shows only one $T_g$. This is visualised in fig. 4.25. It could be that due to extrusion phase separation has occurred. When the Noryl is heated to 300 °C and cooled down again the phase separation has been removed.

Despite the very shivery and unpredictable path of the curve in

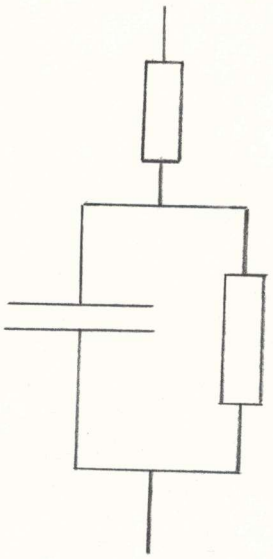

Fig. 5.1. Model of a polymer with an additional capacitive component in series.

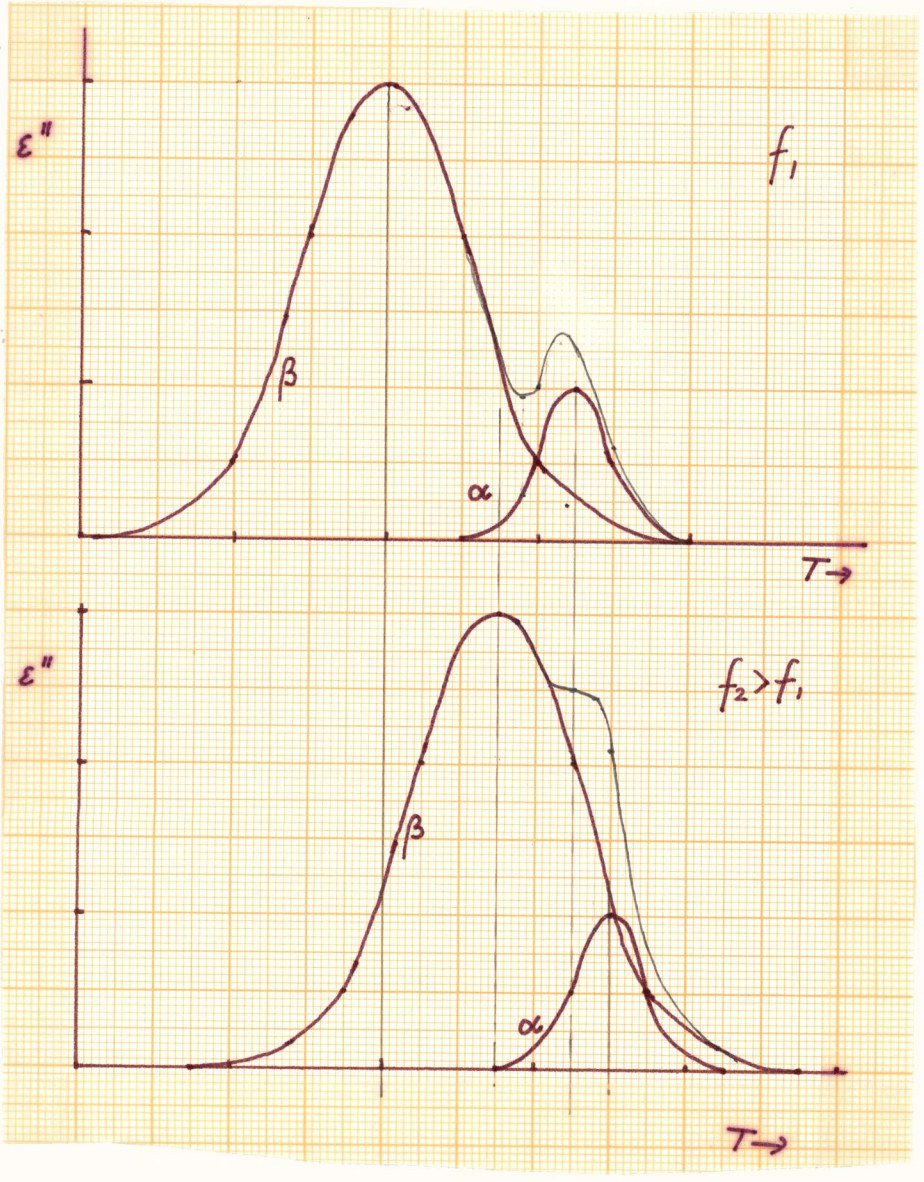


Fig. 5.2. α- and β-peak unite at higher frequencies.

fig. 4.26 it can be seen that with increasing vol.% Vectra the $T_g$ shifts towards lower temperatures. In the case of V/N the shift amounts some 5 °C in both runs. In the case of V/PC this is some 2 °C. Considering the accuracy of the measurements, it is not useful to discuss these results further. In the DSC scans no glass transitions of Vectra can be seen, except in the scan of pure Vectra.

### 5.4 Comparison of the methods used

In this subsection the DETA, DMTA and DSC measurements are compared.

Comparing table 4.2 to table 4.5 (both pressed samples) it can be seen that the $\beta$-temperature of PC is at all composition ratios lower in the dielectric case. The difference amounts some 10 °C. It is doubtful whether in table 4.5 the $\beta$-transition of PC or the $\gamma$-transition of Vectra is concerned. Probably it is a combination of both transitions. The $\beta$-peak of Vectra can be detected at more compositions in the mechanical case. The measured values do not differ much, considering the accuracy in the measurements. The $\alpha$-peaks in Vectra are not quite the same in both cases, but it should be taken into account that it is very difficult to determine the $\alpha$-peak of Vectra well. The $\alpha$-peak of PC is at all composition ratios some 8 °C higher in the dielectric case. This phenomenon can be explained by the fact that conductivity shows up in the dielectric measurements. This conductivity rises the $\alpha$-temperature.

Comparing table 4.3 and 4.6 is of hardly any use since extruded (dielectric) and pressed (mechanical) samples will be compared in this case. It has appeared at several places in the discussion that this makes a great difference. When figs. 4.5 and 4.24 are compared the plots are different in character. What is very striking, however, is that the $\alpha$-transitions of Noryl in both cases initially increase with increasing volume percentage Vectra and remain at a constant level later. It was already pointed out that phase separation could be the reason for this behaviour. From

Fig. 5.3

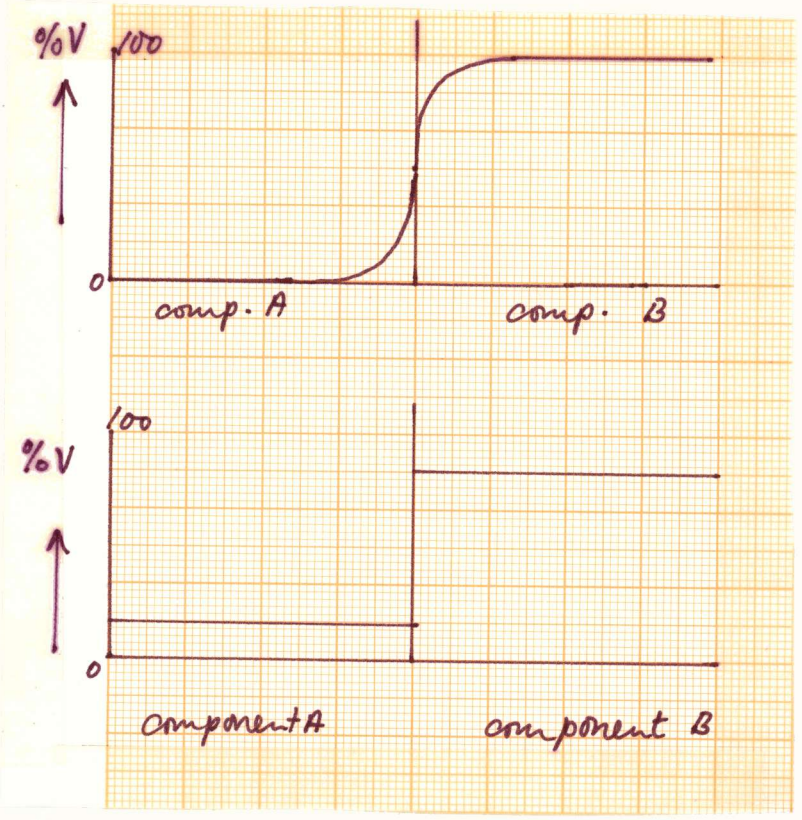


Fig. 5.4




Fig. 5.3. A possible case of partial miscibility: peak broadening does occur, peak shift does not.

Fig. 5.4. The commonly used definition of partial miscibility: peak broadening does not necessarily occur, peak shift does.

these data one might be inclined to say that phase separation can occur both in extruded and pressed samples.
Comparing table 4.2 to the proper part of table 4.7 (i.e. the upper right), it can be seen that the glass-transition and the α-transition at 33 Hz do not differ much (approximately 3 $^{0}$C) in temperature. When the frequency is low enough, the α-transition is generally considered to be identical to the glass-transition (Poolman, 1991). As the frequency is still 33 Hz the agreement is fairly good.
Comparing table 4.5 to the upper right part of table 4.7 a difference of approximately 4$^{0}$C is found. This is a fair agreement considering the remark made in the previous paragraph. In this case both in the DSC and the DMTA measurements a decreasing tendency of the α-peak of PC vs. vol.% Vectra appears.

Comparing table 4.3 to the lower left part of table 4.7 a difference of approximately 10 $^{0}$C is seen. Furthermore, table 4.3 shows an increasing tendency of the α-peak of Noryl vs. vol.% Vectra, while this tendency can not be found back in table 4.7 and fig. 4.26a. On the contrary, this figure rather shows a decreasing tendency.

When table 4.6 is compared to the lower right part of table 4.7 an average difference of some 5 $^{o}$C is seen. In addition, the increasing tendency of the α-peak of Noryl vs. vol.% Vectra, table 4.6, does not appear in table 4.7 and fig 4.26a.

## 5.5 Scanning Electron Microscopy

The surfaces of the spherical Vectra particles in V/PC are not smooth which means that the surface tension is low. This might have been caused by e.g. interactions between the two components. This becomes very clear in photo 1. The Vectra particles lie in holes and are connected with PC by small protuberances. In the case of V/PC no fibers are formed.

The surfaces of the fibers in V/N are smooth which means a high

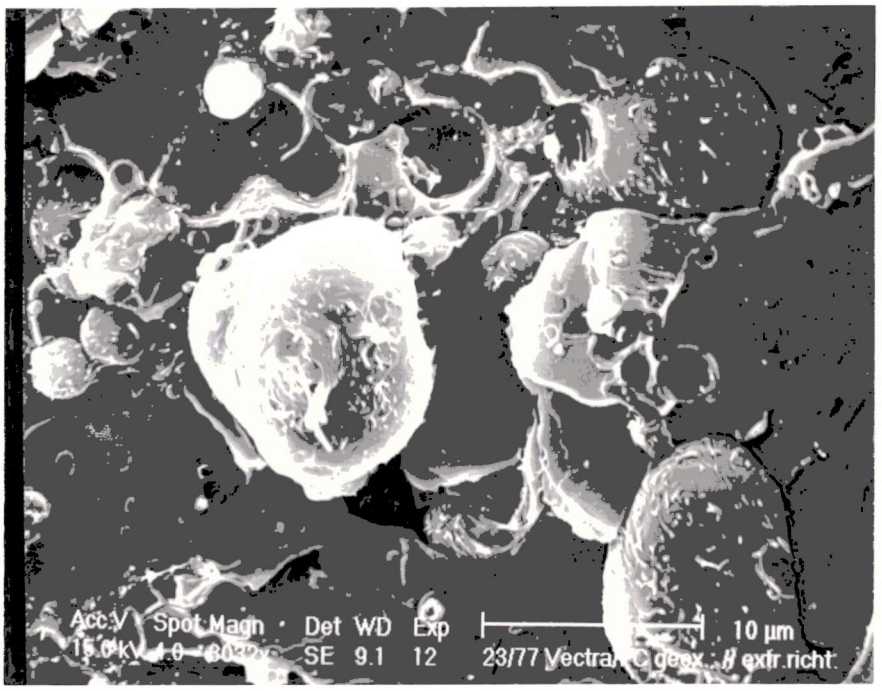


Photo 1. 40V/PC, extruded, broken // extr. direction.

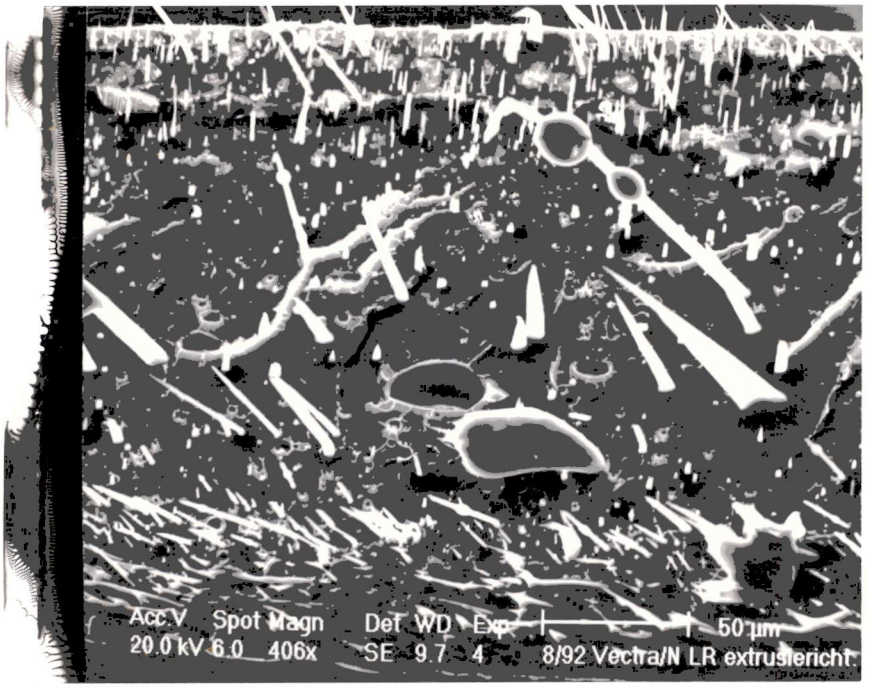


Photo 2. 10V/N, extruded, broken ⊥ extr. direction.

surface tension between the two components. The fibers are all pulled out of the matrix which indicates a poor adhesion between the two components. This is found back in other experiments as well. No evidence for specific interactions or partial miscibility between Vectra and Noryl is found.

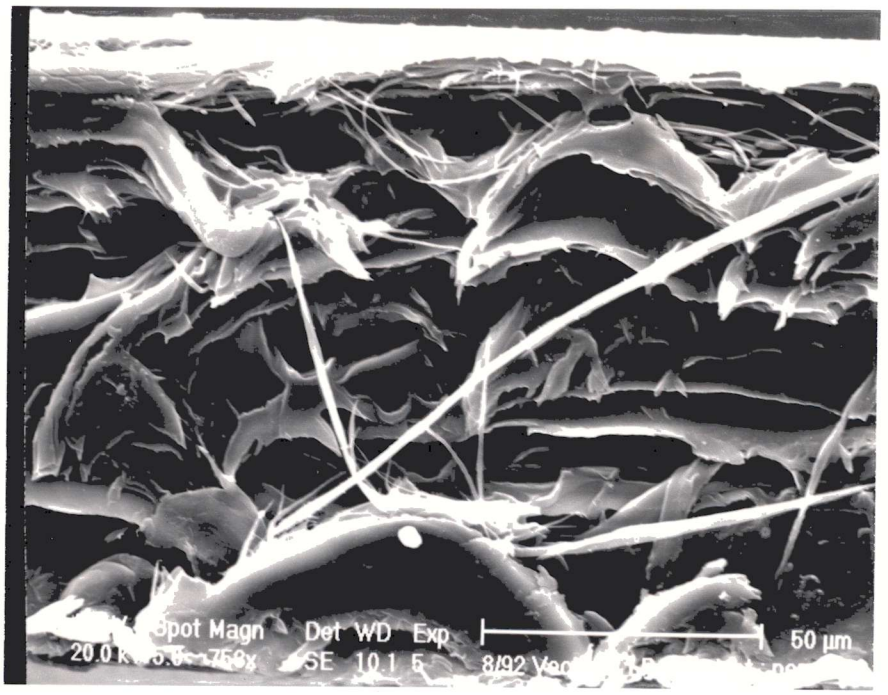


Photo 3. 10V/N, pressed, broken // extr. direction.

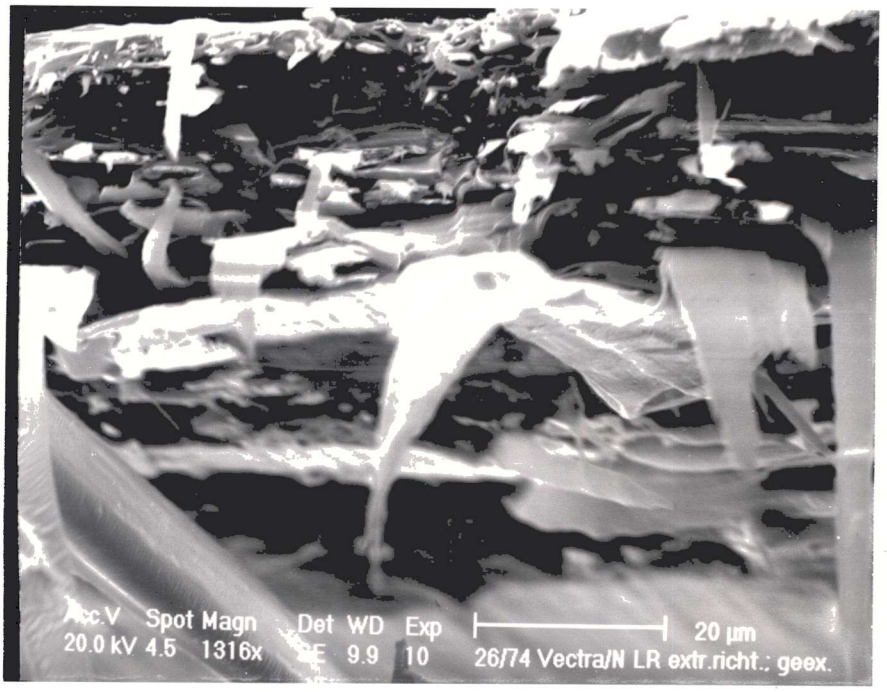


Photo 4. 40V/N, extruded, broken ⊥ extr. direction.

# 6 CONCLUSIONS

* Blending Vectra to PC leads to higher storage and loss permittivities at temperatures above the glass transition. This effect is attributed to interfacial polarisation and conductivity.

* Blending Vectra to Noryl leads to lower storage and loss permittivities at temperatures above the glass transition.

* Between Vectra and PC specific interactions occur; this is not the case between Vectra and Noryl

* In Vectra/PC blends partial miscibility between the two components occurs. In Vectra/Noryl blends phase separation of Noryl into PPE and PS takes place.

* Thermal treatment of the samples is a critical factor, especially in the case of Noryl and Vectra/Noryl blends.

* Dielectric measurements of Vectra show good agreement with literature.

* Gold coated samples provide better results than platinum coated samples when dielectric measurements are concerned.

* DMTA and DSC and measurements support dielectric measurements.

# 7 RECOMMENDATIONS FOR FURTHER RESEARCH

* The influence of thermal treatment should be investigated by subjecting the samples to well defined temperature programs.

* Accurate and reproducible measurements are necessary to evaluate phenomena as peak broadening and peak shifting.

* It would be desirable to obtain a simple program capable of subtracting the conductivity contribution from the dielectric loss. In addition this program should preferably be capable of separating the loss curve in the different relaxation peaks.

* Considering the fact that DMTA and DSC measurements merely act as a support for the DETA measurements it is wiser to concentrate the future effort solely on DETA measurements.

* It was impossible to describe most of the observed phenomena quantitatively. For future developments it seems indispensible to model the results theoretically.

## LITERATURE REFERENCES


Alhaj-Mohammed, M.H. et al., *J. Pol. Sci. Part B,* 26, 1988, 1751.

Bailey, R.T., A.M. North and R.A. Pethrick, *Molecular Motion in High Polymers,* Clarendon Press, Oxford, 1981.

Blythe, A.R., *Electrical Properties of Polymers,* Cambridge University Press, Cambridge, 1979.

Ciferri, A., ed., *Liquid Crystallinity in Polymers,* VCH, New York, 1991.

Cole, R.H. and K.S. Cole, *J. Chem. Phys.,* 9, 1941, 341.

Debije, P., *Polar molecules,* Chemical Catalog Co., New York, 1929.

Deutsch, K. et al., *J. Pol. Sci.,* 13, 1954, 365.

Elmendorp, J.J., *A study on polymer blending microrheology,* PhD thesis, Delft, 1986.

Flynn, J.H., in *Polymers: polymer characterization and analysis,* p. 849-869, ed. J.I. Kroschwitz, John Wiley and Sons, New York, 1990.

Havriliak S. and S. Negami., *J. Pol. Sci. Part C,* 14, 1966, 99.

Hedvig, P., *Dielectric Spectroscopy of Polymers,* Adam Hilger, Bristol, 1977.

Hummel, J.P. and P.J. Flory, *Macromolecules,* 13, 1980, 497.

Kalika, D.S. and D.Y. Yoon, *Macromolecules,* 24, 1991, 3404.

Kauzmann, W., *Revs. Mod. Phys.,* 14(12), 1942.

Kremer, F. et al., *Progr. Coll. Pol. Sci.*, 80, 1989, 129.

Ku, C.C. and R. Liepins, *Electrical Properties of Polymers*, Carl Hanser Verlag, Munich, 1987.

McCrum, N.G., B.E. Read and G. Williams, *Anelastic and Dielectric Effects in Polymeric Solids*, John Wiley and Sons, London, 1967.

Murayama, T., *Dynamic Mechanical Analysis of Polymeric Material*, Elsevier, Amsterdam, 1978.

Nijenhuis, K. te, *Vervormingsgedrag van macromoleculaire stoffen*, Faculteit der Scheikundige Technologie, Delft, 1986.

Operators' manual DETA, Polymer Laboratories, 1986.

Operators' manual DMTA, Polymer Laboratories, 1986.

Operators' manual DSC7, Perkin Elmer, 1991.

Operators' manual Novocontrol, 1990.

Poolman, G.C., *Diëlektrische, dynamisch-mechanische en DSC metingen aan polymeermengsels*, Faculteit der Scheikundige Technologie en der Materiaalkunde, Delft, 1991.

Rellick, G.S. and J. Runt, *J. Pol. Sci. Part B*, 24, 1986, 313.

Rellick, G.S. and J. Runt, *J. Pol. Sci. Part B*, 26, 1988, 1425.

Schlosser, E. and A. Schönhals, *Coll. Pol. Sci.*, 267, 1989, 963.

Shatzki, T.F., *J. Pol. Sci.*, 57, 1962, 496.

Stoelting, J. et al., *Pol. Eng. Sci.*, 10 (3), 1970, 133.

Turnhout, J. van, *Elektrische eigenschappen van polymeren,* Faculteit der Scheikundige Technologie en der Materiaalkunde, Delft, 1990.

Turnhout, J. van, *Internal memorandum,* Delft, 29th May, 1992.

Verbraak, C.L.J.A., *Personal communication,* Delft, 15th April 1992.

Ward, I.M., *Mechanical Properties of Solid Polymers,* John Wiley and Sons, London, 1971.

Wetton, R.E. and P.J. Corish, *Pol. Testing,* 8(5), 1989, 303.

Willems, C., *Dielectric relaxations in a self-reinforcing blend,* poster, Laboratory of Polymer Technology, Delft, 1992.

Williams, M.I. et al., *J. Am. Chem. Soc.,* 77, 1955, 3701.